

(19) **DANMARK**



Patent- og
Varemærkestyrelsen

(10) **DK/EP 2061512 T3**

(12) **Oversættelse af
europæisk patentskrift**

-
- (51) Int.Cl.: **A 61 K 47/64 (2017.01)** **C 07 K 5/103 (2006.01)** **C 07 K 7/06 (2006.01)**
C 07 K 7/08 (2006.01)
- (45) Oversættelsen bekendtgjort den: **2020-01-20**
- (80) Dato for Den Europæiske Patentmyndigheds bekendtgørelse om meddelelse af patentet: **2019-10-02**
- (86) Europæisk ansøgning nr.: **07805515.9**
- (86) Europæisk indleveringsdag: **2007-08-23**
- (87) Den europæiske ansøgnings publiceringsdag: **2009-05-27**
- (86) International ansøgning nr.: **IL2007001055**
- (87) Internationalt publikationsnr.: **WO2008023378**
- (30) Prioritet: **2006-08-23 US 839409 P**
- (84) Designerede stater: **AT BE BG CH CY CZ DE DK EE ES FI FR GB GR HU IE IS IT LI LT LU LV MC MT NL PL PT RO SE SI SK TR**
- (73) Patenthaver: **YEDA RESEARCH AND DEVELOPMENT CO. LTD., at the Weizmann Institute of Science, P.O. Box 95, 76100 Rehovot, Israel**
- (72) Opfinder: **SCHERZ, Avigdor, 4 Tor Ha'aviv Street, 76329 Rehovot, Israel**
SALOMON, Yoram, 43B Gordon Street, 76287 Rehovot, Israel
RUBINSTEIN, Efrat, 16 Mivtza Kadash Street, 75221 Rishon Letzion, Israel
BRANDIS, Alexander, 9/3 Ehad Ha'am Street, 76261 Rehovot, Israel
EREN, Doron, 121 Shikun Banim, 76870 Netaim, Israel
NEIMANN, Karin, 10 David Elazar Street, 74027 Ness Ziona, Israel
- (74) Fuldmægtig i Danmark: **Dennemeyer & Associates S.A, P.O. Box 700425, DE-81304 Munich, Tyskland**
- (54) Benævnelse: **KONJUGATER AF RGD-PEPTIDER OG (BAKTERIE)CHLOROPHYLFOTOSENSIBILISATORER SAMT ANVENDELSER DERAFF**
- (56) Fremdragne publikationer:
CHALEIX V ET AL: "RGD-porphyrin conjugates: Synthesis and potential application in photodynamic therapy" EUROPEAN JOURNAL OF ORGANIC CHEMISTRY, WILEY-VCH VERLAG, WEINHEIM, DE, vol. 8, 2003, pages 1486-1493, XP002373372 ISSN: 1434-193X
CHALEIX V ET AL: "Efficient synthesis of RGD-containing cyclic peptide-porphyrin conjugates by ring-closing metathesis on solid support" TETRAHEDRON LETTERS, ELSEVIER, AMSTERDAM, NL, vol. 45, no. 27, 28 June 2004 (2004-06-28), pages 5295-5299, XP004515132 ISSN: 0040-4039
STERNBERG E D ET AL: "Porphyrin-based Photosensitizers for Use in Photodynamic Therapy" TETRAHEDRON, ELSEVIER SCIENCE PUBLISHERS, AMSTERDAM, NL, vol. 54, no. 17, 23 April 1998 (1998-04-23), pages 4151-4202, XP004113291 ISSN: 0040-4020
FROCHOT ET AL: "Interest of RGD-containing linear or cyclic peptide targeted tetraphenylchlorin as novel photosensitizers for selective photodynamic activity" BIOORGANIC CHEMISTRY, ACADEMIC PRESS INC.,

Fortsættes ...

NEW YORK, NY, US, vol. 35, no. 3, 29 April 2007 (2007-04-29), pages 205-220, XP022057138 ISSN: 0045-2068
SOL V ET AL: "Amino porphyrins as photoinhibitors of Gram-positive and -negative bacteria" BIOORGANIC &
MEDICINAL CHEMISTRY LETTERS, OXFORD, GB, vol. 14, no. 16, 2004, pages 4207-4211, XP008087422 ISSN:
0960-894X

DESCRIPTION

FIELD OF THE INVENTION

[0001] The present invention relates to photosensitizers and in particular to novel conjugates of chlorophyll and bacteriochlorophyll derivatives with peptides containing the RGD motif or with RGD peptidomimetics, to their preparation and their use in methods of photodynamic therapy and diagnosis of tumors and different vascular diseases such as age-related macular degeneration.

DEFINITIONS AND ABBREVIATIONS

[0002] **AMD**: age-related macular degeneration; **Bchl a**: bacteriochlorophyll a: pentacyclic 7,8,17,18-tetrahydroporphyrin with a 5th isocyclic ring, a central Mg atom, a phytyl or geranylgeranyl group at position 17³, a COOCH₃ group at position 13², an H atom at position 13², methyl groups at positions 2, 7, 12, 18, an acetyl group at position 3, and an ethyl group at position 8, herein compound 1; **Bphe**: bacteriopheophytin a (Bchl in which the central Mg is replaced by two H atoms); **Bpheid**: bacteriopheophorbide a (the C-17²-free carboxylic acid derived from Bphe without the central metal atom); **Chl**: chlorophyll; **EC**: endothelial cells; **ECM**: extracellular matrix; **NIR**: near-infrared; **Pd-Bpheid**: Pd-bacteriopheophorbide a; **PDT**: photodynamic therapy; **RGD-4C**: the cyclic nonapeptide CDCRGDCFC-NH₂; **Rhodobacteriochlorin**: tetracyclic 7,8,17,18-tetrahydroporphyrin having a -CH₂CH₂COOH group at position 17, a -COOH at position 13, methyl groups at positions 2, 7, 12, 8, and ethyl groups at positions 3 and 8; **ROS**: reactive oxygen species; **VTI**: vascular-targeted imaging; **VTP**: vascular-targeted PDT.

[0003] IUPAC numbering of the bacteriochlorophyll derivatives is used throughout the specification. Using this nomenclature, the natural bacteriochlorophylls carry two carboxylic acid esters at positions 13² and 17², however they are esterified at positions 13³ and 17³.

BACKGROUND OF THE INVENTION

[0004] Photodynamic therapy (PDT) is a non-surgical treatment of tumors in which non-toxic drugs and non-hazardous photosensitizing irradiation are combined to generate cytotoxic reactive oxygen species *in situ*. This technique is more selective than the commonly used tumor chemotherapy and radiotherapy.

[0005] PDT of tumors involves the combination of administered photosensitizer and local light

delivery, both innocuous agents by themselves, but in the presence of molecular oxygen they are capable of producing cytotoxic reactive oxygen species (ROS) that can inactivate cells. Being a binary treatment modality, PDT allows for greater specificity and has the potential of being more selective, yet not less destructive, when compared with commonly used chemotherapy or radiotherapy (Dougherty et al., 1998; Bonnett et al., 1999; Kessel and Dougherty, 1999; Mazon, 1999; Hahn and Glatstein, 1999).

[0006] Porphyrins have been employed as the primary photosensitizing agents in clinics. Optimal tissue penetration by light apparently occurs between 650-800 nm. Porfimer sodium (Photofrin®, a trademark of Axcan Pharma Inc.), the world's first approved photodynamic therapy agent, which is obtained from hematoporphyrin-IX by treatment with acids and has received FDA approval for treatment of esophageal and endobronchial non-small cell lung cancers, is a complex and inseparable mixture of monomers, dimers, and higher oligomers.

[0007] Large amounts of work have been devoted to the synthesis of single pure compounds - so-called "second generation" sensitizers - which absorb at long wavelength, have well established structures and exhibit better differentiation between their retention in tumor cells and their retention in skin or other normal tissues. In order to optimize the performance of the porphyrin drugs in therapeutics and diagnostics, several porphyrin derivatives have been proposed in which, for example, there is a central metal atom (other than Mg) complexed to the four pyrrole rings, and/or the peripheral substituents of the pyrrole rings are modified and/or the macrocycle is dihydrogenated to chlorophyll derivatives (chlorins) or tetrahydrogenated to bacteriochlorophyll derivatives (bacteriochlorins).

[0008] Due to their intense absorption in favorable spectral regions (650-850 nm) and their ready degradation after treatment, chlorophyll (Chl) and bacteriochlorophyll (BChl) derivatives have been identified as excellent sensitizers for PDT of tumors and to have superior properties in comparison to porphyrins. Bacteriochlorophylls are of potential advantage compared to the chlorophylls because they show intense near-infrared bands, i.e., at considerably longer wavelengths than chlorophyll derivatives.

Tumor vascular targeting

[0009] Targeting photodynamic reagents for destruction of the tumor vasculature, as opposed to the tumor cells themselves, may offer therapeutic advantages since tumor-cell growth and development critically depend on continuous oxygen and nutrient supply (Ruoslahti, 2002). Such vascular damage may include thrombus formation and further restrict tumor blood perfusion (Huang et al., 1997). Furthermore, targeting the tumor vascular endothelial cell (EC) layer is expected to circumvent the poor penetration of tumor stroma by the therapeutic macromolecules (Huang et al., 1997; Burrows and Thorpe 1994). Although tumor blood vessels might be affected by the tumor microenvironment and acquire a tumor associated "signature", they are not malignant and less likely to develop drug resistance. Furthermore, when a targeted antivascular agent is also active against the tumor cells, additional gains in

efficacy can be expected. Thus, by combining antivasular properties with antitumor cytotoxic activities in one drug, its efficacy can be expected to increase and, consequently, decrease the required effective cytotoxic dose. In addition to ECs, tumor cells have also been shown in one case to comprise part of the luminal surface mosaic of the tumor blood vessels (Ruoslahti, 2002; Chang et al., 2000). Consequently these tumor cells are thought to be directly exposed to the blood and freely interact with therapeutic macromolecules that otherwise are unable to cross the endothelial barrier.

[0010] Selective vascular targeting can rely on the differential susceptibility and consequent response to therapeutic agents of tumor and normal blood vessels. Alternatively, differential endocytosis may promote selective uptake of cytotoxic or other therapeutic agents. Recent studies have suggested organ/tissue specific properties for vascular ECs (Ruoslahti, 2002). The blood vessels in different tissues are likely to express tissue specific endothelial markers that are mostly unknown. Pathological processes such as inflammation, ischemia and malignancy can also impose their signature on the respective vasculature (Ruoslahti, 2002; Ruoslahti and Rajotte, 2000; Ruoslahti, 2000; Rajotte et al., 1998; Arap et al., 1998). The biochemical features that characterize blood vessels in tumors may include angiogenesis-related molecules such as certain integrins. The integrins $\alpha_v\beta_3$, $\alpha_v\beta_5$ and $\alpha_5\beta_1$ have been identified in expression patterns typical for angiogenic vascular ECs associated with tumors, wounds, inflammatory tissue, and during vascular remodeling (Brooks et al., 1994a; Brooks et al., 1994b; Brooks et al., 1995; Elceiri and Cheresh, 1999). Endothelial-cell growth factor receptors, proteases, peptidases, cell surface proteoglycans and extracellular matrix (ECM) components have also been described (Ruoslahti, 2000). This rich repertoire of heterogenic molecules and processes may provide new opportunities for targeted delivery of therapies.

[0011] Different strategies have been pursued to achieve this goal. Circulating peptides, peptidomimetics or antibodies that target specific sites in the vasculature are attractive as carriers for therapeutics and diagnostic agents offering theoretical advantages over such conjugates that directly target tumor cells, mostly situated beyond physiological barriers such as the blood vessel wall.

[0012] Chaleix et al., 2003, disclose the synthesis of RGD-porphyrin conjugates as potential candidates for PDT application, in which the unmetalated porphyrin macrocycle is substituted at each of the positions 10,15,20 by 4-methylphenyl or acetylatedglucosyloxyphenyl and at position 5 by a residue of a linear RGD-containing peptide linked to the macrocycle via a spacer arm.

Selective uptake of RGD-containing peptides by endothelial and tumor cells via $\alpha_v\beta_3$ and $\alpha_v\beta_5$ integrins

[0013] The arginine-glycine-aspartic acid Arg-Gly-Asp (RGD) motif of ECM components, like fibronectin (Pierschbacher and Ruoslahti, 1984) and vitronectin, binds to integrins (Ruoslahti

and Pierschbacher, 1987; D'Souza SE et al., 1991; Joshi et al., 1993; Koivunen et al., 1994). Integrin-mediated adhesion leads to intracellular signaling events that regulate cell survival, proliferation, and migration. Some 25 integrins are known, and at least eight of them bind the RGD motif as the primary recognition sequence in their ligands.

[0014] Data obtained by phage display methods (Pasqualini and Ruoslahti, 1996) screening for RGD-containing peptides, have shown their selective binding to endothelial lining of tumor blood vessels (Ruoslahti, 1996; Pasqualini et al., 1997). Because the expression of integrins is reported to be high on activated, but more restricted on quiescent, ECs, small synthetic RGD-containing peptides have been proposed as antagonists impairing the growth of vascular endothelial and tumor cells. RGD peptides also retard signal transmission, affect cell migration and induce tumor cell regression or apoptosis (Su et al., 2002). RGD-analogues are used in tumor imaging (Haubner et al., 2001), anti-angiogenesis approaches (Kawaguchi et al., 2001; Pasqualini et al., 2000), and in tumor targeting of radionucleotides (van Hagen et al., 2000) and chemotherapeutic drugs (Arap et al., 1998; Zitzmann et al., 2002).

[0015] Integrins are also expressed on cancer cells and therefore play an important role in the invasion, metastasis, proliferation and apoptosis of cancer cells. Metastasis invasion of tumor cells into preferred organs may represent cell-homing phenomena that depend on the adhesive interaction between the tumor cells and organ-specific endothelial markers (Ruoslahti and Rajotte, 2000). By binding to integrin of either endothelial or tumor cells, RGD peptides are capable of modulating *in vivo* cell traffic by inhibition of tumor cell-ECM and tumor cell-EC attachments, which are obligatory for metastatic processes. Several studies have indicated that RGD-containing compounds can interfere with tumor cell metastatic processes *in vitro* (Goligorsky et al., 1998; Romanov and Goligorsky 1999) and *in vivo* (Saiki et al., 1989; Hardan et al., 1993).

[0016] Peptides that are specific for individual integrins are of considerable interest and of possible medical significance. The $\alpha_v\beta_3$ integrin was the first integrin shown to be associated with tumor angiogenesis. RGD peptides that specifically block the $\alpha_v\beta_3$ integrin show promise as inhibitors of tumor and retinal angiogenesis, of osteoporosis and in targeting drugs to tumor vasculature (Assa-Munt et al., 2001). Coupling of the anticancer drug doxorubicin or a pro-apoptotic peptide to an $\alpha_v\beta_3$ integrin-binding RGD peptide yields compounds that are more active and less toxic than unmodified drugs when tested against xenograft tumors in mice (Ruoslahti, 2000; Arap et al., 1998; Arap et al., 2002; Ellerby et al., 1999).

[0017] US 6,576,239, EP 0927045 B1 and WO 98/010795 (all of The Burnham Institute, Inventors: E. Ruoslahti and R. Pasqualini) disclose a conjugate comprising a tumor homing peptide comprising the amino acid sequence RGD or NGR, said tumor homing peptide linked to a therapeutic or diagnostic moiety, provided said moiety is not a phage particle. The therapeutic moiety may be a cytotoxic agent or a cancer chemotherapeutic agent such as doxorubicin. The conjugate selectively homes to angiogenic vasculature upon *in vivo* administration. The tumor homing peptide may be a peptide of up to 20 or 30 amino acids or of 50 to 100 amino acids in length, linear or cyclic. One preferred peptide is the cyclic

nonapeptide, CDCRGDCFC or H-Cys*-Asp-Cys*-**Arg-Gly-Asp**-Cys*-Phe-Cys*-NH₂.

Selective vascular response induced in tumors by photodynamic therapy (PDT)

[0018] Application of novel bacteriochlorophyll (Bchl) derivatives as sensitizers in PDT has been reported by our group in recent years in the scientific literature (Zilberstein et al., 2001; Schreiber et al., 2002; Gross et al., 1997; Zilberstein et al., 1997; Rosenbach-Belkin et al., 1996; Gross et al., 2003a; Koudinova et al., 2003; Preise et al., 2003; Gross et al., 2003b) and in the patent publications US 5,726,169 US 5,650,292, US 5,955,585, US 6,147,195, US 6,740,637, US 6,333,319, US 6,569,846, US 7,045,117, DE 41 21 876, EP 1 246 826, WO 2004/045492, WO 2005/120573. The spectra, photophysics, and photochemistry of Bchl derivatives have made them optimal light-harvesting molecules with clear advantages over other sensitizers presently used in PDT. These Bchl derivatives are mostly polar and remain in the circulation for a very short time with practically no extravasations into other tissues (Brandis et al., 2003). Therefore, these compounds are good candidates for vascular-targeted PDT that relies on short (5-10 min) temporal intravascular encounter with light and higher susceptibility of the tumor vessels to the PDT-generated cytotoxic ROS.

[0019] Recent studies performed by our group showed that primary photosensitization is intravascular with rapid development of ischemic occlusions and stasis within the illumination period. This process also induces photochemically induced lipid peroxidation (LPO) and early EC death that is primarily confined to the tumor vasculature (Gross et al., 2003a; Koudinova et al., 2003). Due to light independent progression of free radical chain reactions along with developing hypoxia, LPO and cell death spread beyond the vascular compartment to cover the entire tumor interstitium until complete necrosis of the tumor is attained around 24 hours post PDT. Hence, the primary action of PDT blocks blood supply and induces hypoxia that initiates, in a secondary manner, a series of molecular and pathophysiological events that culminate with tumor eradication.

[0020] Mitochondria, lysosomes, plasma membrane, and nuclei of cells have been evaluated as potential PDT targets. Since most PDT sensitizers do not accumulate in cell nuclei, PDT has a generally low potential of causing DNA damage, mutations, and carcinogenesis. Hydrophilic sensitizers are likely to be taken up by pinocytosis and/or endocytosis and therefore become localized in lysosomes or endosomes. Light exposure will then permeabilize the lysosomes so that sensitizers and hydrolytic enzymes are released into the cytosol (Dougherty et al., 1998).

[0021] PDT damage to plasma membrane can be observed within minutes after light exposure. This type of damage is manifested as swelling, shedding of vesicles containing plasma membrane marker enzymes, cytosolic enzymes and lysosomal enzymes, reduction of active transport, depolarization of plasma membrane, inhibition of the activities of plasma membrane enzymes, changes in intracellular Ca²⁺, up- and down-regulation of surface antigens, LPO that may lead to protein crosslinking, and damage to multidrug transporters

(Dougherty et al., 1998).

[0022] Reports that PDT could rapidly induce apoptosis, both *in vitro* and *in vivo*, have provided insight into the nature of the photokilling mechanisms. Insight into the mechanism of apoptosis after PDT has perhaps been provided by reports that indicate an association between mitochondrial photodamage and apoptotic responses. Recent studies performed by our group showed that the Bchl based photosensitizers induce the activation of the apoptotic pathway. However, apoptosis is probably not the cause for cell death, since inhibiting the apoptotic pathways did not rescue the cells (Mazor et al. 2003, unpublished).

[0023] Chaleix et al., 2003 (Eur. J. Org Chem., vol. 8:1486-1493) discloses RGD-porphyrin conjugates as potential candidates for PDT, in which the unmetalated porphyrin macrocycle is substituted at each of the positions 10,15,20 by 4-methylphenyl or acetylatedglucosyloxyphenyl and at position 5 by a residue of a linear RGD-containing peptide linked to the macrocycle via a spacer arm. Chaleix et al., 2004 (Tetrahedron Letters, vol. 45:5295-5299), discloses solid-phase synthesis of glucosylated porphyrins bearing a cyclic pseudopeptide incorporating a RGD sequence obtained by ring-closing methatesis. Sternberg et al., 1998 (Tetrahedron, vol. 54, no. 17: 4151-4202) reviews the synthesis and properties of a wide variety of porphyrin-based photosensitizers including porphyrins, chlorins and bacteriochlorins, which have been used or suggested as photosensitizers in PDT. Frochot et al., 2007 (Bioorganic Chemistry, vol. 35, no. 3:205-220) discloses RGD-containing linear or cyclic peptide targeted tetraphenylchlorin as sensitizers for selective PDT.

[0024] Reference is made to the following patents and patent applications of the applicants of the present application: US 5,726,169 US 5,650,292, US 5,955,585, US 6,147,195, US 6,740,637, US 6,333,319, US 6,569,846, US 7,045,117, DE 41 21 876, EP 1 246 826, WO 2004/045492, WO 2005/120573.

SUMMARY OF THE INVENTION

[0025] The present invention relates to a conjugate of a RGD-containing peptide or RGD peptidomimetic and a photosensitizer selected from chlorophyll and bacteriochlorophyll,

[0026] In one embodiment, the photosensitizer is a chlorophyll or bacteriochlorophyll of the formulas I, II and III herein.

[0027] The invention further provides a diagnostic, therapeutic or radiotherapeutic composition for visualization, PDT therapy or radiotherapy of tissues or organs comprising an effective amount of a photosensitizer-RGD peptide conjugate of the invention and a pharmaceutically acceptable carrier.

[0028] The conjugates of the invention can be used in methods for tumor diagnosis using different diagnostic techniques and in methods of photodynamic therapy of tumors and

vascular diseases and in tumor radiotherapy.

BRIEF DESCRIPTION OF THE FIGURES

[0029]

Figs. 1A-1C show characterization spectra of conjugate **11**. **Fig. 1A**: Mass spectrometry measurement. **Fig. 1B**: Spectrophotometry analysis. **Fig. 1C**: HPLC results after synthesis (conjugate **11** is peak number 3).

Figs. 2A-2B show characterization spectra of compound **9**. **Fig. 2A**: Electronic spectrum in acetone. **Fig. 2B**: Mass spectrum: ESI-MS (+) 679 (M), 702 (M+Na) m/z.

Figs. 3A-3B show purification and characterization of Eu-RGD-4C. **Fig. 3A**: Chromatography of Eu-RGD-4C (a single pick). **Fig. 3B**: Mass spectrometry analysis (MW of isothiocyanatophenyl-DTPA-Eu-RGD-4C=1498, arrow).

Fig. 4 shows the results of a receptor-binding assay. The specific binding activity of free Eu-RGD-4C to the integrin receptor was measured using H5V cells in the absence (total binding) or presence of 1 μ M RGD-4C (non-specific binding).

Fig. 5 shows Scatchard analysis of bound (B) and free (F) Eu-RGD-4C based on the results of the receptor-binding assay described in **Fig. 4**.

Fig. 6 shows results of a solid phase receptor assay measuring Eu-RGD-4C binding to isolated $\alpha_v\beta_3$ integrin receptor. Time-resolved fluorometry was used for fluorescence determination.

Figs. 7A-7B show the effect of RGD-4C on H5V endothelial cells detachment. The morphological changes of the cells were documented using light microscopy. 5% of rounded cells (n=200) after incubation in the absence (**Fig. 7A**) and 99% in the presence of RGD-4C (**Fig. 7B**). After replacement of the medium with a fresh one and incubation for 3 h at 37 °C, the % of rounded cells (n=200) in the absence and in the presence of RGD-4C were 6% and 8%, respectively (not shown).

Fig. 8 shows the effect of RGD-4C on HUVEC detachment. The morphological changes of the cells were documented using light microscopy. The upper panels a-e represent the phase contrast microscopy of cell detachment in the presence of increasing concentrations of RGD-4C (a: control; b: 25 μ M; c: 50 μ M; d: 100 μ M; e: 200 μ M). The lower panels represent the recovery of the cells 24 h after replacement of the medium with a fresh one.

Fig. 9 shows the cellular uptake and localization of conjugate **24** in H5V endothelial cells as depicted in a trans photograph (a), a fluorescence image (b) (excitation filter: 520 nm; emission filter: 780 nm) and a merge of the photograph and image (c).

Fig. 10 is a series of fluorescence images showing the cellular uptake and localization of conjugate **24** and compound **8** in H5V endothelial cells measured 20 min (upper panels) or 2.5

hours (lower panels) after incubation with the compounds in a medium containing 10% or 75% FCS (excitation filter: 520 nm; emission filter: 780 nm). (a) **8**, 10% FCS; (b) **24**, 10% FCS; (c) **8**, 75% FCS; (d) **24**, 75% FCS.

Figs. 11A-11D are a series of graphs showing the biodistribution of conjugate **24**, i.v. injected into CD1 nude male mice with tumor xenografts of rat C6 glioma (**11A**; each time point represents 6 mice), mouse CT26luc colon carcinoma (**11B**; each time point represents 2 mice), and mouse 4T1luc carcinoma of the breast (**11C**; each time point represents 3 mice), sacrificed at the indicated times. Pd concentrations in different organs were determined by ICP-MS. The boxes present time-windows most suitable for PDT and imaging measurements.

Fig. 12 shows biodistribution of compound **8**, i.v. injected (tail vein) into CD1-nude male mice with tumor xenografts of rat C6 glioma, sacrificed at the indicated times. Pd concentrations were determined by ICP-MS.

Fig. 13 shows the biodistribution of Cu-conjugate **15** in mice bearing MDA-MB-231 breast tumor. The animals were sacrificed at selected time points. Cu concentrations are shown at selected time point, after the subtraction of time 0, as an average value from three animals.

Figs. 14A-14B are graphs showing the biodistribution of conjugate **42** (that contains the RAD motif), i.v. injected into CD1 nude male mice with tumor grafts of mouse CT26luc colon carcinoma, sacrificed at the indicated times. Pd concentrations in different organs were determined by ICP-MS. **Fig. 14A** ICP-MS results for conjugate **42**. Each time point represents 2 mice. **Fig. 14B** shows the same results with focus on specific organs of interest (blood, tumor, liver, kidneys and muscle) compared to the results obtained for RGDconjugate **24** (see **Figs. 11A-11D**).

Fig. 15 shows a comparison of whole-body NIR fluorescence imaging after administration of the compound **8** (upper panels) or of conjugate **24**. The given images illustrate the fluorescence of a mouse bearing rat C6 glioma xenograft on the back of the right posterior limb (a) 4 hours, (b) 24 hours, (c) 48 hours and (d) 72 hours post injection of 200 nmol dose of conjugate **24** or compound **8**. Tumors are indicated by arrows and all images are normalized to the same scale.

Figs. 16A-16C are a photograph (**16A**), a fluorescence image (**16B**) and a luminescence image (luciferase+luciferin; **16C**) of a mouse bearing, on the right anterior limb, a subcutaneous xenograft of CT26luc colon cancer (transfected with luciferase) 24 hr after the injection of 200 nmol dose of conjugate **24**. The fluorescence and luminescence images were acquired using IVIS system.

Figs. 17A-17C show photographs (**17A**) and fluorescence (**17B**) and bioluminescence (**17C**) images of two mice bearing subcutaneous grafts of mouse 4T1luc mammary gland cancer (transfected with luciferase) on the right anterior limb, 24 hr after the injection of 200 nmol dose of conjugate **24**.

Fig. 18 shows the fluorescence imaging of a mouse bearing ovarian carcinoma MLS xenograft, taken 8 (left panel) and 14 (right panel) hours after i.v. injection of conjugate **31**. The

fluorescence and luminescence images were acquired using IVIS system.

Fig. 19 shows fluorescence images of two mice bearing rat C6 glioma xenograft 24 hours after the administration of 140 nmol of conjugate **24** alone (left mouse), or one hour after injection of 8.5 μ mol of cycloRGDfK peptide (right mouse). Each mouse was documented from above (upper panel, left) and from aside (upper panel, right). Zoom in photographs are also shown (lower panel). The circles on the fluorescence images indicate the location of the xenografted rat C6 glioma tumor.

Fig. 20 shows black & white photographs (upper panels) and fluorescence images (lower panels) of CD-1 nude male mice bearing CT26luc xenografts on the back of the posterior limb, 24 hours after the administration of RGD conjugate **24** (panels a,c) or RAD conjugate **42** (panels b,d). Tumors are indicated by arrows and all images are normalized to the same scale. The fluorescence images were acquired using IVIS system.

Fig. 21 shows black & white photographs (upper panels) and fluorescence images (lower panels) of mice bearing (a) OVCAR 8, (b) CT26luc, (c) MLS, and (d) 4T1luc xenografts on the back of the posterior limb, 24 hours after the administration of conjugate **24**. Tumors are indicated by arrows and all images are normalized to the same scale.

Fig. 22 shows a photograph (upper image, taken using digital camera) and a fluorescence image (lower image) from conjugate **24** localization in lung metastasis of 4T1luc breast cancer tumor in BALB/c female mouse, 24 hr after i.v. injection of conjugate **24** (15 mg/kg). The NIR fluorescence signal originated from localization of conjugate **24** taken using Imaging System Xenogen IVIS® 100.

Figs. 23A-23I are a series of photographs (a), bioluminescence (b) and fluorescence (c) images of CT26luc lung metastases in CD-1 nude male mice 24 hours (**A,B**), 9 hours (**C,D**), 4 hours (**E,F**) after the i.v. injection of conjugate **24** (15 mg/kg). Images **G,H** are of CT26luc lung metastases in CD-1 nude male mice that were not injected with the conjugate. Image **I** is of CD-1 nude male mouse without lung metastases 24 hours after the i.v. injection of conjugate **24**. The middle image is the bioluminescence signal originated from the reaction of luciferin with the luciferase transfected tumor cells. The right image is the NIR fluorescence signal originated from **24** taken using Xenogen IVIS® Imaging System 100. The arrows indicate the lung metastases.

Fig 24 shows black & white photographs (a), bioluminescence (b) and fluorescence (c) images of CD-1 nude male mouse bearing CT26luc primary tumor on the back of its left leg and metastases in the near lymph node, 24 hours after the i.v. injection of conjugate **24** (15 mg/kg). The middle image is the bioluminescence signal originated from the reaction of luciferin with the luciferase transfected tumor cells. The right image is the NIR fluorescence signal originated from conjugate **24** taken using Xenogen IVIS® Imaging System 100. The arrows indicate the lymph node metastases.

Figs. 25A-25C show dose-response survival curve of H5V cells incubated for 90 min at 37 °C with 0-25 μ M conjugate **23** or compound **10** in different media conditions: 10% FCS in medium

(Fig. 25A), culture medium DMEM/F12 (Fig. 25B) or 10 μ M BSA in medium (Fig. 25C). Cell survival was determined using Neutral Red viability assay. The points represent average results of triplicates.

Figs. 26A-26D show dose-response survival curves of H5V cells incubated for 90 min at 37 °C with 0-25 μ M compound 10 (Figs. 16A, 16B) or conjugate 23 (Figs. 26C, 26D) in the absence or presence of free cycloRGDfK in excess (100-fold up to 1 mM), in different media conditions (10% FCS in medium (Figs. 26A, 27C) or 10 μ M BSA in medium (Figs. 26B, 26D)). Cell survival was determined using Neutral Red viability assay. The points represent average results of triplicates.

Figs. 27A-27B show dose-response survival curves of H5V cells incubated for 15 min at 37°C (Fig. 27A) or 4°C (Fig. 27B) with 0-20 μ M conjugate 23 in 10% FCS in medium in the absence or presence of excess free cycloRGDfK (100 fold up to 1mM). Cell survival was determined using Neutral Red viability assay. The points represent average results of triplicates.

Fig. 28 shows dose-response survival curve of H5V cells incubated for 2 hours at 37°C with 0-25 μ M conjugate 24 in culture medium DMEM/F12 with 10% FCS. Cell survival was determined using Neutral Red viability assay. The points represent average results of triplicates.

Fig. 29 shows dose-response survival curve of H5V cells incubated 90 min at 37°C with 0-20 μ M conjugate 11 or compound 8 (Pd-MLT) in 10 μ M BSA in medium. Cell survival was determined using Neutral Red viability assay. The points represent average results of triplicates.

Figs. 30A-30B show dose-response survival curves of H5V cells incubated for 90 min at 37°C with 0-10 μ M conjugate 11 (Fig. 30A) or compound 8 (Fig. 30B) in 10 μ M BSA in medium in the absence or presence of excess RGD-4C (1 mM). Cell survival was determined using Neutral Red viability assay. The points represent average results of triplicates.

Figs. 31A-31E are pictures of C6 glioma tumor xenografts treated with conjugate 24 or compound 8. CD-1 nude male mice bearing C6 glioma xenografts were treated as follows: **31A.** conjugate 24 was i.v. injected 15 mg/kg, 15-min illumination (90 J/cm²) 8 hours post injection; upper panels: (a) pre PDT; (b) 2 days post PDT; (c) 3 days post PDT; (d) 4 days post PDT; lower panels: (a) 7 days post PDT; (b) 9 days post PDT; (c) 14 days post PDT; (d) 18 days post PDT. **31B.** conjugate 24 was i.v. injected 24 mg/kg, 10-min illumination (60 J/cm²) 8 hours post injection; a, b, c and d in upper and lower panels as for 31A. **31C.** Dark control - conjugate 24 was i.v. injected without illumination; a) pre PDT, b) 5 days post PDT. **31D.** Light control - illumination without injection of photosensitizer; a) pre PDT, b) 5 days post PDT. **31E.** Unconjugated photosensitizer control - compound 8 was i.v. injected 9 mg/kg, 10 min illumination (60 J/cm²) 8 hours post injection, a) pre PDT, b) 11 days post PDT. Images were taken at indicated time post PDT.

Figs. 32A-E show the therapeutic results of applying 15 mg/kg, 10 min illumination (60 J/cm²), 8 hours post injection of conjugate 24 to mice bearing CT26luc tumors. **32A** - conjugate 24

was i.v. injected 15 mg/kg, 10 min illumination (60 J/cm^2) 8 hours post injection; (a) pre PDT, (b) 1 day post PDT; (c) 4 days post PDT; (d) 8 days post PDT; (e) 12 days post PDT; (f) 19 days post PDT. **32B** - overlaid images taken after i.p. injection of luciferin to the mouse described in **32A**, using the IVIS system. The first image is black and white, which gives the photograph of the animal. The second image is color overlay of the emitted photon data. All images are normalized to the same scale; (a) pre PDT; (b) 1 day post PDT; (c) 4 days post PDT; (d) 8 days post PDT. **32C** - Bioluminescence signal quantification (photon/sec/cm^2) of the data shown in **32B**. **32D** - control with compound **8** alone: the mice were i.v. injected with compound **8** and illuminated after 8 hours; (a) pre PDT; (b) 2 days post PDT. **32E** - control with mixture of compound **8** and cycloRGDfK: the mice were i.v. injected with mixture of compound **8** with cycloRGDfK and illuminated after 8 hours; (a) pre PDT; (b) 2 days post PDT. **32F** - control with cycloRGDfK alone: the mice were i.v. injected with cycloRGDfK and illuminated after 8 hours; (a) pre PDT; (b) 2 days post PDT. Images were taken at indicated time post PDT.

Fig. 33 shows the Kaplan-Mayer curve for the protocols indicated in the Table 5 with asterisk.

Figs. 34A-34B show the fluorescent mammary cancer MDA-MB-231 RFP clone 3 (resistant to hygromycin) after 1 sec and 3 sec exposure, respectively.

Figs. 35A-35B show two representative examples to local response of human mammary cancer MDA-MB-231-RFP to PDT. Mice with MDA-MB-231-RFP xenografts ($\sim 0.5 \text{ cm}^3$) on their backs were i.v. injected with 7.5 mg/kg of conjugate **13** and illuminated 8 h later through the mouse skin. **35A** - Photographs taken from (a) day 0 (before treatment) and after treatment at (b) 1, (c) 4, (d) 7, (e) 12 and (f) 90 days. By day 4 partial necrosis was seen, by day 7 tumor flattening was observed, after 90 days the wound healed and the animal was cured. At the right, photographs of the mouse at day 0 and after 90 days. **35B** - In vivo whole-body red fluorescence imaging of CD-1 nude male mice bearing MDA-MB-231-RFP orthotopic tumor. The photos were taken at the times like in **35A**. No signal was detected 90 days after treatment.

Fig. 36 shows accumulation of conjugate **13** in orthotopic human breast MDA-MB-231-RFP primary tumor (tumor size $\sim 1 \text{ cm}^3$). Images were taken from 15 min to 24 hr post drug injection. Upper panels - In vivo whole-body red fluorescence imaging of CD-1 nude female mice bearing MDA-MB-231-RFP orthotopic tumor. Lower panels - In vivo whole-body NIR fluorescence imaging of conjugate **13** accumulation. The drug shows no specific accumulation in the tumor during the first 24 hours. a to i - 15 min, 1h, 2h, 3h, 4.5h, 6h, 7.5h, 9h, 24h

Fig. 37 shows accumulation of conjugate **13** in orthotopic human breast MDA-MB-231-RFP primary tumor (tumor size $\sim 1 \text{ cm}^3$). Images were taken from day 1 to 6 post drug injection. Top panel - In vivo whole-body red fluorescence imaging of CD-1 nude female mice bearing MDA-MB-231-RFP orthotopic tumor. Bottom panel - In vivo whole-body NIR fluorescence imaging of conjugate **13** accumulation. The drug shows accumulation in the tumor, reaching peak concentration specifically in the tumor from day 2 post injection a to i - 1h, 9h, 1 day, 2 days, 3 days, 4 days, 5 days, 6 days, 7 days.

DETAILED DESCRIPTION OF THE INVENTION

[0030] In a broad aspect, the present invention relates to a conjugate of a photosensitizer selected from chlorophyll (Chl) and bacteriochlorophyll (BChl) and an RGD-containing peptide or an RGD peptidomimetic

[0031] It is one object of the present invention to provide conjugates of photosensitizers that specifically target the sensitizer to the tumor vasculature. There are some advantages for vascular photosensitizer targeting over vascular targeting with conventional chemotherapy. First, during accumulation of a targeted conventional drug, it is often active, unless it is a prodrug, while the targeted photosensitizer is not active until locally illuminated. Second, a targeted conventional drug will bind and act also at undesirable targets presenting the homing address whereas the targeted photosensitizer will be activated only at the relevant illuminated site. Furthermore, PDT with photosensitizers targeted to the neovascular endothelial signatures in tumor may be remarkably selective in inducing photodynamic EC injury.

[0032] The integrin $\alpha_v\beta_3$ has been reported to play an important role in tumor metastasis and angiogenesis, which involves growth of new blood vessels from preexisting vasculatures during tumor growth. This integrin may be a viable marker for tumor growth and spread. Therefore, noninvasive imaging methods for visual monitoring of integrin $\alpha_v\beta_3$ expression in real-time provides opportunities for assessing therapeutic intervention as well as for detection of metastasis.

[0033] Integrins link the intracellular cytoskeleton of cells with the extracellular matrix by recognizing the RGD. RGD peptides interact with the integrin receptor sites, which can initiate cell-signaling processes and influence many different diseases. Thus, the integrin RGD binding site is an attractive pharmaceutical target. The integrin $\alpha_v\beta_3$ has an RGD binding site and peptides containing the sequence RGD home to, and act as antagonists of, $\alpha_v\beta_3$ integrin. Thus, in one preferred embodiment of the invention, the RGD-containing peptide is an antagonist of an integrin receptor.

[0034] In the bifunctional conjugates of the invention, the homing property is provided by the RGD-containing peptide while the PDT effect is provided by the photosensitizer. These conjugates should be able to target the sensitizer to neovessels of primary solid tumors and possibly respective metastases for the purpose of diagnosis and for photodynamic destruction. They can further act as antiangiogenic agents and initiate apoptotic destruction of neo-endothelial and blood exposed tumor cells.

[0035] The terms "RGD-containing peptide" or "RGD peptide" are used herein interchangeably and mean a peptide containing the RGD sequence, also referred to as RGD motif. The term "RGD peptidomimetic" as used herein refers to compounds, particularly, non-peptidic

compounds, that mimic peptides having the RGD motif.

[0036] The RGD-containing peptide may be an all-L, all-D or an L,D linear or cyclic peptide composed of 4-100, preferably 5-50, 5-30, 5-20 or, more preferably, 5-10, amino acid residues. In preferred embodiments, the RGD peptide is composed of 4, 5, 6, 7, 9 or 25, most preferably 5 amino acid residues that may be optionally modified natural or non-natural amino acid.

[0037] As used herein, the term "amino acid" includes the 20 naturally occurring amino acids as well as non-natural amino acids.

[0038] Examples of natural amino acids suitable for the invention include, but are not limited to, Ala, Arg, Asp, Cys, Gln, Glu, Gly, Ile, Leu, Lys, Met, Phe, Pro, Ser, Thr, Tyr, and Val.

[0039] Examples of non-natural amino acids include, but are not limited to, 4-aminobutyric acid (Abu), 2-amino adipic acid, diaminopropionic (Dap) acid, hydroxylysine, homoserine, homovaline, homoleucine, norleucine (Nle), norvaline (Nva), ornithine (Orn), TIC, naphthylalanine (Nal), ring-methylated derivatives of Phe, halogenated derivatives of Phe or o-methyl-Tyr.

[0040] The term "amino acid" herein includes also modified amino acids such as modifications that occur post-translationally *in vivo*, for example, hydroxyproline, phosphoserine and phosphothreonine; D-modification; N-alkylation, preferably N-methylation, of the peptide bond; acylation or alkylation of the amino terminal group or of the free amino group of Lys; esterification or amidation of the carboxy terminal group or of a free carboxy group of Asp or Glu; and esterification or etherification of the hydroxyl group of Ser or Tyr.

[0041] The term "amino acid" includes both D- and L-amino acids. Thus, the peptides used in the conjugates of the invention can be all-D (except for glycine), all-L or L,D-amino acids. D-modifications as well as N-alkylation of the peptide bond are most beneficial to prevent peptide cleavage by enzymes in the organism. In the present invention, a D-amino acid is indicated by a small letter as for the D-phenylalanine 'f' residue in the peptide cycloRGDfK of SEQ ID NO:1 used herein.

[0042] The present invention includes also cyclic peptides. Peptides can be cyclized by a variety of methods such as formation of disulfides, sulfides and, especially, lactam formation between carboxyl and amino functions of the N- and C-termini or amino acid side chains. Cyclization can be obtained by any method known in the art, for example, through amide bond formation, e.g., by incorporating Glu, Asp, Lys, Orn, diamino butyric (Dab) acid, diaminopropionic (Dap) acid at various positions in the chain (-CO-NH or -NH-CO bonds). Backbone to backbone cyclization can also be obtained through incorporation of modified amino acids of the formulas $H-N(CH_2)_n-COOH-C(R)H-COOH$ or $H-N((CH_2)_n-NH_2)-C(R)H-COOH$, wherein $n = 1-4$, and further wherein R is any natural or non-natural side chain of an amino acid.

[0043] Cyclization can also be obtained via formation of S-S bonds through incorporation of two Cys residues. Additional side-chain to side chain cyclization can be obtained via formation of an interaction bond of the formula $-(\text{CH}_2)_n-\text{S}-\text{CH}_2-\text{CO}-$, wherein $n = 1$ or 2 , which is possible, for example, through incorporation of Cys or homoCys and reaction of its free SH group with, e.g., bromoacetylated Lys, Orn, Dab or Dap.

[0044] In some embodiments, the RGD peptides may be those described in US 6,576,239 and EP 0927045.

[0045] In one preferred embodiment, the peptide used according to the invention is the cyclic pentapeptide RGDfK of SEQ ID NO: 1, wherein 'f' indicates a D-Phe residue.

[0046] In another preferred embodiment, the peptide is the cyclic nonapeptide CDCRGDCGC of SEQ ID NO:2, herein designated 'RGD-4C', which contains four cysteine residues forming two disulfide bonds in the molecule, and is one of the promising peptides with integrin specificity. This peptide was shown to be a selective and potent ligand (affinity constant of ~ 100 nM) of the $\alpha_v\beta_5$ and $\alpha_v\beta_3$ integrins (Ruoslahti, 2002; Elceiri and Cheresh, 1999).

[0047] The aspartic acid residue of the RGD motif is highly susceptible to chemical degradation, leading to the loss of biological activity, and this degradation could be prevented by cyclization via disulfide linkage (Bogdanowich-Knipp et al., 1999). Along with improving stability, double cyclic peptides show higher potency compared to single disulphide-bridge and linear peptides in inhibiting the attachment of vitronectin to cells. The high activity of double cyclic RGD peptide is likely to be due to an appropriately restrained conformation not only of the RGD motif but also of the flanking amino acids. The number and nature of residues flanking the RGD sequence in synthetic peptides have a significant influence on how that sequence is recognized by individual integrin receptors (Koivunen et al., 1995; Pierschbacher and Ruoslahti, 1987). An aromatic residue may be particularly significant in making favorable contacts in the binding site of integrin (Koivunen et al., 1995). Cyclic RGD peptides targeted for $\alpha_v\beta_3$ internalize by an integrin independent fluid-phase endocytosis pathway that does not alter the number of functional integrin receptors on the cell surface. Additionally, cyclic RGD peptides remain or degrade in the lysosome, in a process that reaches saturation after 15 minutes, and only a small portion can leave the lysosome and reach the cell cytoplasm. This explains why cyclic RGD peptides are found in the cell cytoplasm only after a certain period of time (48 to 72 hours) (Hart et al., 1994; Castel et al., 2001).

[0048] In other preferred embodiments, the RGD peptide is selected from the cyclic peptides: (i) tetrapeptide cycloRGDK (SEQ ID NO:4), pentapeptide cycloRGDf-n(Me)K (SEQ ID NO:7), wherein f indicates D-Phe and the peptide bond between f and K is methylated; and pentapeptide cycloRGDyK (SEQ ID NO:8), wherein y indicates D-Tyr.

[0049] In another embodiment, the RGD-containing peptide is linear and may be selected from the hexapeptide GRGDSP (SEQ ID NO:3), the heptapeptide GRGDSPK (SEQ ID NO:5), and

the 25-mer (GRGDSP)₄K (SEQ ID NO:7)

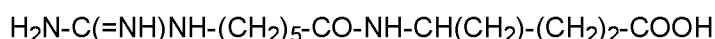
[0050] In one embodiment of the invention, the RGD peptide is linked directly to the photosensitizer chlorophyll or bacteriochlorophyll macrocycle via a functional group in its periphery, for example, COOH, forming an amide CO- NH₂ group with the amino terminal group or a free amino group of the RGD peptide.

[0051] In another embodiment, the RGD peptide is linked to the photosensitizer macrocycle via a spacer arm/bridging group such as, but not limited to, a C₁-C₂₅ hydrocarbylene, preferably a C₁-C₁₀ alkylene or phenylene, substituted by an end functional group such as OH, COOH, SO₃H, COSH or NH₂, thus forming an ether, ester, amide, thioamide or sulfonamide group.

[0052] In some embodiments, the photosensitizer is conjugated to a RGD peptidomimetic.

[0053] In one preferred embodiment the RGD peptidomimetic is a non-peptidic compound comprising a guanidine and a carboxyl terminal groups spaced by a chain of 11 atoms, at least 5 of said atoms being carbon atoms, and said chain comprises one or more O, S or N atoms and may optionally be substituted by oxo, thioxo, halogen, amino, C1-C6 alkyl, hydroxyl, or carboxy or one or more atoms of said chain may form a 3-6 membered carbocyclic or heterocyclic ring. Compounds of this type are described in WO 93/09795 of the same applicant.

[0054] In preferred embodiments, the RGD peptidomimetic above comprises in the chain N atoms and is substituted by an oxo group. In a more preferred embodiment, the RGD peptidomimetic has the formula shown in conjugate **40** herein:

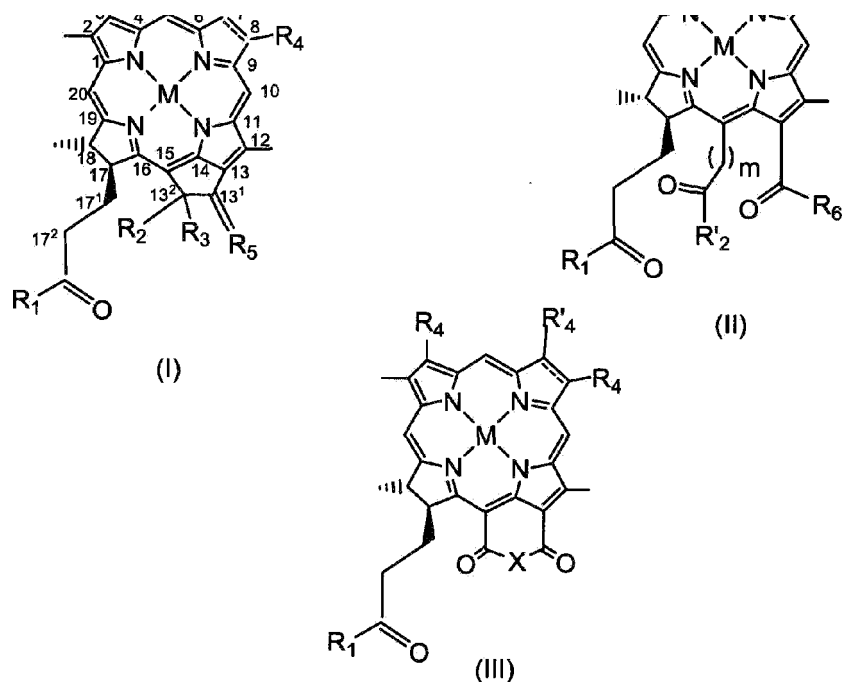


[0055] In another embodiment, the RGD peptidomimetic has the formula shown in conjugate **41** herein.

[0056] In one embodiment, the photosensitizer is a chlorophyll or bacteriochlorophyll derivative that may be a natural or a synthetic non-natural derivative of chlorophyll or bacteriochlorophyll, including compounds in which modifications have been made in the macrocycle, and/or in the periphery and/or the central Mg atom may be absent or it is replaced by other metal atom suitable for the purpose of diagnosis and/or for the purpose of PDT.

[0057] In preferred embodiments, the invention relates to a conjugate wherein the photosensitizer is a chlorophyll or bacteriochlorophyll of the formula I, II or III:





wherein

M represents 2H or an atom selected from the group consisting of Mg, Pd, Pt, Co, Ni, Sn, Cu, Zn, Mn, In, Eu, Fe, Au, Al, Gd, Er, Yb, Lu, Ga, Y, Rh, Ru, Si, Ge, Cr, Mo, P, Re and Tc and isotopes thereof;

X is O or N-R₇;

R₁, R₂ and R₆ each independently is Y-R₈, -NR₉R'₉ or -N⁺R₉R'₉R''₉ A⁻

or R₁ and R₆ in formula II together with the carbon atoms to which they are attached form a ring comprising an RGD peptide or RGD peptidomimetic;

Y is O or S;

R₂ is H, OH or COOR₉;

R₃ is H, OH, C₁-C₁₂ alkyl or C₁-C₁₂ alkoxy;

R₄ is -CH=CR₉R'₉, -CH=CR₉Hal, -CH=CH-CH₂-NR₉R'₉, -CH=CH-CH₂-N⁺R₉R'₉R''₉ A⁻, -CHO, -CH=NR₉, -CH=N⁺R₉R'₉ A⁻, -CH₂-OR₉, -CH₂-SR₉, -CH₂-Hal, -CH₂-R₉, -CH₂-NR₉R'₉, -CH₂-N⁺R₉R'₉R''₉ A⁻, -CH₂-CH₂R₉, -CH₂-CH₂Hal, -CH₂-CH₂OR₉, -CH₂-CH₂SR₉, -CH₂-CH₂-NR₉R'₉, -CH₂-CH₂-N⁺R₉R'₉R''₉ A⁻, -COCH₃, C(CH₃)=CR₉R'₉, -C(CH₃)=CR₉Hal, -C(CH₃)=NR₉, -CH(CH₃)=N⁺R₉R'₉ A⁻, -CH(CH₃)-Hal, -CH(CH₃)-OR₉, -CH(CH₃)-SR₉, -CH(CH₃)-NR₉R'₉, -CH(CH₃)-N⁺R₉R'₉ R'₉A⁻, or -C≡CR₉;

R'₄ is methyl or formyl;

R_5 is =O, =S, =N- R_9 , =N⁺ $R_9R'_9A^-$, =CR₉R'₉, or =CR₉-Hal;

R_7 , R_8 , R_9 , R'_9 and R''_9 each independently is:

1. (a) H;
2. (b) C₁-C₂₅ hydrocarbyl;
3. (c) C₁-C₂₅ hydrocarbyl, preferably C₁-C₂₅ alkyl, alkenyl or alkynyl, more preferably C₁-C₁₀ or C₁-C₆ alkyl, substituted by one or more functional groups selected from the group consisting of halogen, nitro, oxo, OR, SR, epoxy, epithio, -NRR', -CONRR', -CONR-NRR', -NHCONRR', -NHCONRNR', -COR, COOR'', -OSO₃R, -SO₃R'', -SO₂R, -NHSO₂R, -SO₂NRR', =N-OR, -(CH₂)_n-CO-NRR' -O-(CH₂)_n-OR, -O-(CH₂)_n-O-(CH₂)_n-R, -OPO₃RR', -PO₂HR, and -PO₃R''R'', wherein R and R' each independently is H, hydrocarbyl or heterocyclyl and R'' is hydrocarbyl or heterocyclyl;
4. (d) C₁-C₂₅ hydrocarbyl, preferably C₁-C₂₅ alkyl, more preferably C₁-C₁₀ or C₁-C₆ alkyl, substituted by one or more functional groups selected from the group consisting of positively charged groups, negatively charged groups, basic groups that are converted to positively charged groups under physiological conditions, and acidic groups that are converted to negatively charged groups under physiological conditions;
5. (e) C₁-C₂₅ hydrocarbyl, preferably C₁-C₂₅ alkyl, more preferably C₁-C₁₀ or C₁-C₆ alkyl, containing one or more heteroatoms and/or one or more carbocyclic or heterocyclic moieties;
6. (f) C₁-C₂₅ hydrocarbyl, preferably C₁-C₂₅ alkyl, more preferably C₁-C₁₀ or C₁-C₆ alkyl, containing one or more heteroatoms and/or one or more carbocyclic or heterocyclic moieties and substituted by one or more functional groups as defined in (c) and (d) above;
7. (g) C₁-C₂₅ hydrocarbyl, preferably C₁-C₂₅ alkyl, more preferably C₁-C₁₀, or C₁-C₆ alkyl substituted by a residue of an amino acid, a peptide, a protein, a monosaccharide, an oligosaccharide, a polysaccharide, or a polydentate ligand and its chelating complex with metals; or
8. (h) a residue of an amino acid, a peptide, a protein, a monosaccharide, an oligosaccharide, a polysaccharide, or a polydentate ligand and its chelating complex with metals;

R_7 may further be -NRR', wherein R and R' each is H or C₁-C₂₅ hydrocarbyl, preferably C₁-C₂₅ alkyl, more preferably C₁-C₁₀ or C₁-C₆ alkyl, optionally substituted by a negatively charged group, preferably SO₃⁻;

R_8 may further be H⁺ or a cation R⁺₁₀ when R_1 , R'_2 and R_6 each independently is Y- R_8 ;

R⁺₁₀ is a metal, an ammonium group or an organic cation;

A⁻ is a physiologically acceptable anion;

m is 0 or 1;

the dotted line at positions 7-8 represents an optional double bond; and

pharmaceutically acceptable salts and optical isomers thereof;

and said chlorophyll or bacteriochlorophyll derivative of formula I, II or III contains at least one RGD-containing peptide residue or RGD peptidomimetic residue, wherein said RGD-containing peptide is an all-L, all-D or an L,D linear or cyclic peptide composed of 4-100, preferably 5-50, 5-30, 5-20, more preferably 4, 5, 6, 7, 9 or 25 amino acid residues that may be optionally modified natural or non-natural amino acids, and said RGD-peptidomimetic is a non-peptidic compound comprising a guanidine and a carboxyl terminal group spaced by a chain of 11 atoms, at least 5 of said atoms being carbon atoms, said chain comprises one or more O, S or N atoms and may optionally be substituted by oxo, thioxo, halogen, amino, Ci-C₆ alkyl, hydroxyl, or carboxy or one or more atoms of said chain may form a 3-6 membered carbocyclic or heterocyclic ring.

[0058] In one embodiment, the dotted line at positions 7-8 represents a double bond and the photosensitizer is a chlorophyll of the formula I, II or III. The compounds of formula I wherein M is Mg, R₁ at position 17³ is phytyloxy, R₂ at position 13² is COOCH₃, R₃ at position 13² is an H atom, R₅ is O, R₄ at position 3 is vinyl, the dotted line at positions 7-8 represents a double bond, and either R'₄ is methyl at position 7 and R₄ is ethyl at position 8 or R'₄ is formyl at position 7 and R₄ is ethyl at position 8, are chlorophyll a and b, respectively, and their derivatives will have different metal atom and/or different substituents R₁, R₂, R₃, R₄, R'₄ and/or R₅.

[0059] In another embodiment, the positions 7-8 are hydrogenated and the photosensitizer is a bacteriochlorophyll of the formula I, II or III. The compounds of formula I wherein M is Mg, R₁ at position 17³ is phytyloxy or geranylgeranyloxy, R₂ at position 13² is COOCH₃, R₃ at position 13² is an H atom, R₅ is O, R₄ at position 3 is acetyl and at position 8 is ethyl, and the dotted line at positions 7-8 is absent are bacteriochlorophyll a, and their derivatives will have different metal atom and/or different substituents R₁, R₂, R₃, R₄, and/or R₅.

[0060] As used herein, the term "hydrocarbyl" means any straight or branched, saturated or unsaturated, acyclic or cyclic, including aromatic, hydrocarbyl radicals, of 1-25 carbon atoms, preferably of 1 to 20, more preferably 1 to 6, most preferably 2-3 carbon atoms. The hydrocarbyl may be an alkyl radical, preferably of 1-4 carbon atoms, e.g. methyl, ethyl, propyl, butyl, or alkenyl, alkynyl, cycloalkyl, aryl such as phenyl or an aralkyl group such as benzyl, or at the position 17 it is a radical derived from natural Chl and Bchl compounds, e.g. geranylgeranyl (2,6-dimethyl-2,6-octadienyl) or phytyl (2,6,10,14-tetramethyl-hexadec-14-en-16-yl).

[0061] As used herein, the term "carbocyclic moiety" refers to a monocyclic or polycyclic

compound containing only carbon atoms in the ring(s). The carbocyclic moiety may be saturated, i.e. cycloalkyl, or unsaturated, i.e. cycloalkenyl, or aromatic, i.e. aryl.

[0062] The term "alkoxy" as used herein refers to a group (C₁-C₂₅)alkyl-O-, wherein C₁-C₂₅ alkyl is as defined above. Examples of alkoxy are methoxy, ethoxy, n-propoxy, isopropoxy, butoxy, isobutoxy, tert-butoxy, pentoxy, hexoxy, -OC₁₅H₃₁, -OC₁₆H₃₃, -OC₁₇H₃₅, -OC₁₈H₃₇, and the like. The term "aryloxy" as used herein refers to a group (C₆-C₁₈)aryl-O-, wherein C₆-C₁₈ aryl is as defined above, for example, phenoxy and naphthoxy.

[0063] The terms "heteroaryl" or "heterocyclic moiety" or "heteroaromatic" or "heterocyclyl", as used herein, mean a radical derived from a mono- or poly-cyclic heteroaromatic ring containing one to three heteroatoms selected from the group consisting of O, S and N. Particular examples are pyrrolyl, furyl, thienyl, pyrazolyl, imidazolyl, oxazolyl, thiazolyl, pyridyl, quinoliny, pyrimidinyl, 1,3,4-triazinyl, 1,2,3-triazinyl, 1,3,5-triazinyl, benzofuryl, isobenzofuryl, indolyl, imidazo[1,2-a]pyridyl, benzimidazolyl, benzthiazolyl and benzoxazolyl.

[0064] Any "carbocyclic", "aryl" or "heteroaryl" may be substituted by one or more radicals such as halogen, C₆-C₁₄ aryl, C₁-C₂₅ alkyl, nitro, OR, SR, -COR, -COOR, -SO₃R, -SO₂R, -NHSO₂R, -NRR', -(CH₂)_n-NR-COR', and -(CH₂)_n-CO-NRR'. It is to be understood that when a polycyclic heteroaromatic ring is substituted, the substitutions may be in any of the carbocyclic and/or heterocyclic rings.

[0065] The term "halogen", as used herein, refers to fluoro, chloro, bromo or iodo.

[0066] In one embodiment of the invention, the photosensitizer of the conjugate is a chlorophyll or bacteriochlorophyll of the formula I, II or III containing at least one negatively charged group and/or at least one acidic group that is converted to a negatively charged group at the physiological pH.

[0067] As defined herein, "a negatively charged group" is an anion derived from an acid and includes carboxylate (COO⁻), thiocarboxylate (COS⁻), sulfonate (SO₃⁻), and phosphonate (PO₃²⁻), and the "acidic group that is converted to a negatively charged group under physiological conditions" include the carboxylic (-COOH), thiocarboxylic (-COSH), sulfonic (-SO₃H) and phosphonic (-PO₃H₂) acid groups. BChl derivatives with negatively charged groups or groups converted thereto under physiological conditions have been described in WO 2004/045492 of the same applicant. In another embodiment of the invention, the photosensitizer of the conjugate is a chlorophyll or bacteriochlorophyll of the formula I, II or III containing at least one positively charged group and/or at least one basic group that is converted to a positively charged group at the physiological pH.

[0068] As defined herein, "a positively charged group" denotes a cation derived from a N-containing group or from an onium group not containing N. Since tumor endothelium is

characterized by an increased number of anionic sites, positively charged groups or basic groups that are converted to positively charged groups under physiological conditions, may enhance the targeting efficiency of the conjugates of the present invention.

[0069] A "cation derived from a N-containing group" as used herein denotes, for example, but is not limited to, an ammonium $-N^+(RR'R'')$, hydrazinium $-(R)N-N^+(R'R'')$, ammoniumoxy $O\leftarrow N^+(RR')$, iminium $>C=N^+(RR')$, amidinium $-C(=RN)-N^+R'R''$ or guanidinium $-(R)N-C(=NR)-N^+R'R''$ group, wherein R, R' and R'' each independently is H, hydrocarbyl, preferably C_1-C_6 alkyl as defined herein, phenyl or benzyl, or heterocyclyl, or in the ammonium group one of R, R' and R'' may be OH, or two of R, R' and R'' in the ammonium group or R and R' in the hydrazinium, ammoniumoxy, iminium, amidinium or guanidinium groups, together with the N atom to which they are attached, form a 3-7 membered saturated ring, optionally containing one or more heteroatoms selected from the group consisting of O, S or N and optionally further substituted at the additional N atom, or said cation is derived from a compound containing one or more N atoms in a heteroaromatic ring.

[0070] In one more preferred embodiment, the conjugate of the present invention contains an ammonium group of the formula $-N^+(RR'R'')$, wherein each of R, R' and R'' independently is H or optionally substituted hydrocarbyl or heterocyclyl, as defined herein, or one of them may be OH. The $-N^+(RR'R'')$ ammonium group may be a secondary ammonium, wherein any two of the radicals R, R' or R'' are H; a tertiary ammonium, wherein only one of R, R' or R'' is H; or a quaternary ammonium, wherein each of R, R' or R'' is an optionally substituted hydrocarbyl or heterocyclyl group as defined herein. When one of R, R' or R'' is OH, the group is a hydroxylammonium group. Preferably, the ammonium group is a quaternary ammonium group wherein R, R' and R'' each is C_1-C_6 alkyl such as methyl, ethyl, propyl, butyl, hexyl. As mentioned hereinabove, the ammonium group may be an end group in the molecule or it may be found within an alkyl chain in the molecule.

[0071] In the hydrazinium $-(R)N-N^+(R'R'')$, amidinium $-C(=NR)-N^+R'R''$ and guanidinium $-(R)N-C(=NR)-N^+R'R''$ groups, R, R' and R'' may each independently be H or hydrocarbyl or heterocyclyl, or R' and R'' together with the N atom to which they are attached form a 3-7 membered saturated ring, as defined herein. Examples of such groups include those wherein R is H, and R' and R'' each is C_1-C_6 alkyl such as methyl, ethyl, propyl, butyl, hexyl.

[0072] In the ammoniumoxy $O\leftarrow N^+(RR')$ and iminium $>C=N^+(RR')$ groups, R and R' may each independently be H or hydrocarbyl, preferably C_1-C_6 alkyl, or heterocyclyl, or R and R' together with the N atom to which they are attached form a 3-7 membered saturated ring, as defined herein.

[0073] In another preferred embodiment, the bacteriochlorophyll derivative contains a cyclic ammonium group of the formula $-N^+(RR'R'')$, wherein two of R, R' and R'' together with the N atom form a 3-7 membered saturated ring defined hereinbelow.

[0074] As defined herein, "a 3-7 membered saturated ring" formed by two of R, R' and R" together with the N atom to which they are attached may be a ring containing only N such as aziridine, pyrrolidine, piperidine, piperazine or azepine, or it may contain a further heteroatom selected from O and S such as morpholine or thiomorpholine. The further N atom in the piperazine ring may be optionally substituted by alkyl, e.g. C₁-C₆ alkyl, that may be substituted by halo, OH or amino. The onium groups derived from said saturated rings include aziridinium, pyrrolidinium, piperidinium, piperazinium, morpholinium, thiomorpholinium and azepinium.

[0075] As defined herein "a cation derived from a N-containing heteroaromatic radical" denotes a cation derived from a N-heteroaromatic compound that may be a mono- or polycyclic compound optionally containing O, S or additional N atoms. The ring from which the cation is derived should contain at least one N atom and be aromatic, but the other ring(s), if any, can be partially saturated. Examples of N-heteroaromatic cations include pyrazolium, imidazolium, oxazolium, thiazolium, pyridinium, pyrimidinium, quinolinium, isoquinolinium, 1,2,4-triazinium, 1,3,5-triazinium and purinium.

[0076] The at least one positively charged group may also be an onium group not containing nitrogen such as but not limited to, phosphonium [-P⁺(RR'R")], arsonium [-As⁺(RR'R")], oxonium [-O⁺(RR')], sulfonium [-S⁺(RR')], selenonium [-Se⁺(RR')], telluronium [-Te⁺(RR')], stibonium [-Sb⁺(RR'R")], or bismuthonium [-Bi⁺(RR'R")] group, wherein each of R, R' and R", independently, is H, hydrocarbyl or heterocyclyl, preferably C₁-C₆ alkyl such as methyl, ethyl, propyl, butyl, pentyl or hexyl, or aryl, preferably, phenyl.

[0077] Examples of phosphonium groups of the formula -P⁺(RR'R") include groups wherein R, R' and R" each is methyl, ethyl, propyl, butyl or phenyl, or R is methyl, ethyl, propyl, butyl or hexyl and R' and R" both are phenyl. Examples of arsonium groups of the formula -As⁺(RR'R") include groups wherein R, R' and R" each is methyl, ethyl, propyl, butyl or phenyl. Examples of sulfonium groups of the formula -S⁺(RR') include groups wherein R and R' each is methyl, ethyl, propyl, butyl, phenyl, benzyl, phenethyl, or a substituted hydrocarbyl group.

[0078] As defined herein, "a basic group that is converted to a positively charged group under physiological conditions" is, at least theoretically, any basic group that will generate under physiological conditions a positively charged group as defined herein. It is to be noted that the physiological conditions, as used herein, do not refer solely to the serum, but to different tissues and cell compartments in the body.

[0079] Examples of such N-containing basic groups include, without being limited to, any amino group that will generate an ammonium group, any imine group that will generate an iminium group, any hydrazine group that will generate a hydrazinium group, any aminoxy group that will generate an ammoniumoxy group, any amidine group that will generate an amidinium group, any guanidine group that will generate a guanidinium group, all as defined

herein. Other examples include phosphino and mercapto groups.

[0080] Thus, the conjugates of the present invention may contain at least one basic group that is converted to a positively charged group under physiological conditions such as $-NRR'$, $-C(=NR)-NR'R''$, $-NR-NR'R''$, $-(R)N-C(=NR)-NR'R''$, $O\leftarrow NR-$, or $>C=NR$, wherein each of R, R' and R'' independently is H, hydrocarbyl, preferably C_1-C_{25} alkyl, more preferably C_1-C_{10} or C_1-C_6 alkyl, or heterocyclyl, or two of R, R' and R'' together with the N atom form a 3-7 membered saturated ring, optionally containing an O, S or N atom and optionally further substituted at the additional N atom, or the basic group is a N-containing heteroaromatic radical.

[0081] The 3-7 membered saturated ring may be aziridine, pyrrolidine, piperidine, morpholine, thiomorpholine, azepine or piperazine optionally substituted at the additional N atom by C_1-C_6 alkyl optionally substituted by halo, hydroxyl or amino, and the N-containing heteroaromatic radical may be pyrazolyl, imidazolyl, oxazolyl, thiazolyl, pyridyl, quinolinyl, isoquinolinyl, pyrimidyl, 1,2,4-triazinyl, 1,3,5-triazinyl or purinyl.

[0082] BChl derivatives with positively charged groups or groups converted thereto under physiological conditions have been described in WO 2005/120573 of the same applicant.

[0083] In one embodiment, the photosensitizer is a chlorophyll or bacteriochlorophyll of formula II and R₆ is a basic group $-NR_9R'_9$ wherein R₉ is H and R'₉ is C_1-C_6 alkyl substituted by a basic group $-NH-(CH_2)_{2-6}-NRR'$ wherein each of R and R' independently is H, C_1-C_6 alkyl optionally substituted by NH_2 or R and R' together with the N atom form a 5-6 membered saturated ring, optionally containing an O or N atom and optionally further substituted at the additional N atom by $-(CH_2)_{2-6}-NH_2$.

[0084] In another embodiment, the photosensitizer is a bacteriochlorophyll of formula II and R₆ is $-NH-(CH_2)_3-NH-(CH_2)_3-NH_2$, $-NH-(CH_2)_{2-1}$ -morpholino, or $-NH-(CH_2)_3$ -piperazino- $(CH_2)_3-NH_2$ or R₁ and R₆ together form a cyclic ring comprising an RGD peptide or RGD peptidomimetic.

[0085] In another embodiment, the photosensitizer is a chlorophyll or bacteriochlorophyll of formula III, X is $-NR_7$, R₇ is $-NRR'$, R is H and R' is C_{2-6} -alkyl substituted by SO_3^- or an alkaline salt thereof, preferably the photosensitizer is a bacteriochlorophyll and X is $-NR_7$ and R₇ is $-NH-(CH_2)_3-SO_3K$.

[0086] In another embodiment, R₇, R₈, R₉ or R'₉ each is a C_{1-6} -alkyl substituted by one or more $-OH$ groups. For example, the photosensitizer is a chlorophyll or bacteriochlorophyll of formula II and R₆ is $-NR_9R'_9$, R₉ is H and R'₉ is $HOCH_2-CH(OH)-CH_2-$.

[0087] In another embodiment, the photosensitizer is a chlorophyll or bacteriochlorophyll of formula II and R₆ is $-NR_9R'_9$, R₉ is H and R'₉ is C_{1-6} -alkyl substituted by a polydentate ligand or its chelating complexes with metals. Examples of polydentate ligands include, without being

limited to, EDTA (ethylenediamine tetraacetic acid), DTPA (diethylene triamine pentaacetic acid) or the macrocyclic ligand DOTA. In one preferred embodiment the polydentate ligand is DTPA, R_6 is $-\text{NH}-(\text{CH}_2)_3-\text{NH}-\text{DTPA}$, and the metal is Gd.

[0088] The cation R_8^+ may be a monovalent or divalent cation derived from an alkaline or alkaline earth metal such as K^+ , Na^+ , Li^+ , NH_4^+ , Ca^{2+} , more preferably K^+ ; or R_8^+ is an organic cation derived from an amine or from a N-containing group

[0089] As defined herein, the $\text{C}_1\text{-C}_{25}$ hydrocarbonyl defined for R_7 , R_8 , R_9 and R'_9 may optionally be substituted by one or more functional groups selected from halogen, nitro, oxo, OR, SR, epoxy, epithio, aziridine, $-\text{CONRR}'$, $-\text{COR}$, COOR , $-\text{OSO}_3\text{R}$, $-\text{SO}_3\text{R}$, $-\text{SO}_2\text{R}$, $-\text{NHSO}_2\text{R}$, $-\text{SO}_2\text{NRR}'$, $-\text{NRR}'$, $=\text{N}-\text{OR}$, $=\text{N}-\text{NRR}'$, $-\text{C}(=\text{NR})-\text{NRR}'$, $-\text{NR}-\text{NRR}'$, $-(\text{R})\text{N}-\text{C}(=\text{NR})-\text{NRR}'$, $\text{O}\leftarrow\text{NR}-$, $>\text{C}=\text{NR}$, $-(\text{CH}_2)_n-\text{NR}-\text{COR}'$, $-(\text{CH}_2)_n-\text{CO}-\text{NRR}'$, $-\text{O}-(\text{CH}_2)_n-\text{OR}$, $-\text{O}-(\text{CH}_2)_n-\text{O}-(\text{CH}_2)_n-\text{R}$, $-\text{PRR}'$, $-\text{OPO}_3\text{RR}'$, $-\text{PO}_2\text{HR}$, $-\text{PO}_3\text{RR}'$; one or more negatively charged groups such as COO^- , COS^- , $-\text{OSO}_3^-$, $-\text{SO}_3^-$, $-\text{OPO}_3\text{R}^-$, $-\text{PO}_2\text{H}^-$, $-\text{PO}_3^{2-}$ and $-\text{PO}_3\text{R}^-$; and/or one or more positively charged groups such as $-\text{P}^+(\text{RR}'\text{R}'')$, $-\text{As}^+(\text{RR}'\text{R}'')$, $-\text{O}^+(\text{RR}')$, $-\text{S}^+(\text{RR}')$, $-\text{Se}^+(\text{RR}')$, $-\text{Te}^+(\text{RR}')$, $-\text{Sb}^+(\text{RR}'\text{R}'')$, $-\text{Bi}^+(\text{RR}'\text{R}'')$, $\text{O}\leftarrow\text{N}^+(\text{RR}'>$, $>\text{C}=\text{N}^+(\text{RR}')$, $-\text{N}^+(\text{RR}'\text{R}'')$, $-(\text{R})\text{N}-\text{N}^+(\text{RR}'\text{R}'')$, $-(\text{R})\text{N}-\text{C}(=\text{HN})-\text{N}^+(\text{RR}'\text{R}'')$, $-\text{C}(=\text{NH})-\text{N}^+(\text{RR}'\text{R}'')$, or a N-heteroaromatic cation such as pyrazolium, imidazolium, oxazolium, thiazolium, pyridinium, quinolinium, pyrimidinium, 1,2,4-triazinium, 1,3,5-triazinium and purinium; wherein n is an integer from 1 to 6, R , R' and R'' each independently is H, hydrocarbonyl or heterocyclyl, or two of R , R' and R'' together with the N atom to which they are attached form a 3-7 membered saturated ring, optionally containing one or more heteroatoms selected from the group consisting of O, S or N and optionally further substituted at the additional N atom. The $\text{C}_1\text{-C}_{25}$ hydrocarbonyl defined for R_7 , R_8 , R_9 and R'_9 may also be substituted by the residue of a mono-, oligo- or polysaccharide such as glycosyl, or of an amino acid, peptide or protein. In addition, R_8 , R_9 and R'_9 each may independently be a residue of a mono-, oligo- or polysaccharide such as glycosyl, or of an amino acid, peptide or protein, or a polydentate ligand such as DTPA, DOTA, EDTA and the like and their chelating complexes with metals.

[0090] In the groups OR and SR, when R is H, the groups hydroxy and mercapto are represented, respectively, and when R is other than H, ethers and sulfides are represented. In the group $-\text{PRR}'$, the phosphino group is represented when R and R' are H. In the group $-\text{COR}$, when R is H, the formyl group $-\text{CHO}$ of an aldehyde is represented, while when R is other than H, this is the residue of a ketone such as alkylcarbonyl and arylcarbonyl groups. In the group COOR , when R is not H, this is a carboxylic acid ester group such as the alkoxy carbonyl and aryloxy carbonyl groups. Similarly, esters are represented in the groups $-\text{OSO}_3\text{R}$, $-\text{SO}_3\text{R}$, $-\text{SO}_2\text{R}$, $-\text{OPO}_3\text{RR}'$, $-\text{PO}_2\text{HR}$ and $-\text{PO}_3\text{RR}'$ when R and R' are other than H.

[0091] In one preferred embodiment of the invention, the photosensitizer is unmetalated, namely, M is 2H. In other preferred embodiments, the photosensitizer is metalated as defined

hereinabove, more preferably M is Pd, Cu or Mn, most preferably Pd.

[0092] In some preferred embodiments of the invention, the photosensitizer is a bacteriochlorophyll of the formula I, II or III, more preferably formula II, and M is 2H, Cu, Mn, more preferably Pd. In other embodiments, the photosensitizer is a chlorophyll of the formula I, II or III, more preferably formula II, and M is 2H, Cu or Mn.

[0093] In some preferred embodiments, the conjugate comprises a photosensitizer bacteriochlorophyll of the formula II wherein M is Pd, Mn, Cu or 2H; m is 1; R₁ is NH-P, wherein P is the residue of an RGD-containing peptide or RGD peptidomimetic linked directly to the NH- or via a spacer; R'₂ is methoxy; R₄ at position 3 is acetyl and at position 8 is ethyl; R'₄ is methyl; and R₆ is -NH-(CH₂)₂-SO₃⁻ Me⁺, wherein Me⁺ is Na⁺ or K⁺.

[0094] In other preferred embodiments, the conjugate comprises a photosensitizer bacteriochlorophyll of the formula II wherein M is Pd or 2H; m is 1; R₁ is NH-P, wherein P is the residue of an RGD-containing peptide or RGD peptidomimetic linked directly to the NH- or via a spacer; R'₂ is methoxy; R₄ at position 3 is acetyl and at position 8 is ethyl; R'₄ is methyl; and R₆ is -NH-CH₂-CH(OH)-CH₂-OH.

[0095] In another embodiment, the conjugate comprises a bacteriochlorophyll of the formula III wherein M is Pd; R₁ is NH-P, wherein P is the residue of an RGD-containing peptide or RGD peptidomimetic linked directly to the NH- or via a spacer; R₄ at position 3 is acetyl and at position 8 is ethyl; R'₄ is methyl; X is N-R₇ and R₇ is -NH-(CH₂)₃-SO₃⁻ Me⁺, wherein Me⁺ is Na⁺ or K⁺.

[0096] In another embodiment, the conjugate comprises a bacteriochlorophyll of the formula I wherein M is Mn; R₁ is NH-P, wherein P is the residue of an RGD-containing peptide or RGD peptidomimetic linked directly to the NH- or via a spacer; R₂ is OH; R₃ is COOCH₃; R₄ at position 3 is acetyl and at position 8 is ethyl; R'₄ is methyl; and R₅ is O.

[0097] In another embodiment, the conjugate comprises a chlorophyll of the formula II wherein M is selected from Mn, Cu or 2H; m is 1; R₁ is NH-P, wherein P is the residue of an RGD-containing peptide or RGD peptidomimetic linked directly to the NH- or via a spacer; R₄ at position 3 is vinyl and at position 8 is ethyl; R'₄ is methyl; and R₆ is -NH-(CH₂)₂-SO₃⁻ Me⁺, wherein Me⁺ is Na⁺ or K⁺.

[0098] In another embodiment, the conjugate comprises a bacteriochlorophyll of the formula II wherein M is 2H; m is 1; R₁ is NH-P, wherein P is the residue of an RGD-containing peptide or RGD peptidomimetic linked directly to the NH- or via a spacer; R'₂ is methoxy; R₄ at position 3 is acetyl and at position 8 is ethyl; R'₄ is methyl; and R₆ is -NH-(CH₂)₃-NH-(CH₂)₃-NH₂.

[0099] In another embodiment, the conjugate comprises a bacteriochlorophyll of the formula II wherein M is 2H; m is 1; R₁ is NH-P, wherein P is the residue of an RGD-containing peptide or RGD peptidomimetic linked directly to the NH- or via a spacer; R'₂ is methoxy; R₄ at position 3 is acetyl and at position 8 is ethyl; R'₄ is methyl; and R₆ is -NH-(CH₂)₂-morpholino.

[0100] In another embodiment, the conjugate comprises a bacteriochlorophyll of the formula II wherein M is 2H; m is 1; R₁ is NH-P, wherein P is the residue of an RGD-containing peptide or RGD peptidomimetic linked directly to the NH- or via a spacer; R'₂ is methoxy; R₄ at position 3 is acetyl and at position 8 is ethyl; R'₄ is methyl; and R₆ is -NH-(CH₂)₃-piperazino-(CH₂)₃-NH₂.

[0101] In another embodiment, the conjugate comprises a bacteriochlorophyll of the formula II wherein M is Pd; m is 1; R₁ is NH-P, wherein P is the residue of the RGD-peptidomimetic; R'₂ is methoxy; R₄ at position 3 is acetyl and at position 8 is ethyl; R'₄ is methyl; and R₆ is -NH-(CH₂)₂-SO₃K (conjugate **40**).

[0102] In another embodiment, the conjugate comprises a bacteriochlorophyll of the formula II wherein M is Pd; m is 1; R₁ is NH-P, wherein P is the residue of the RGD-peptidomimetic; R'₂ is methoxy; R₄ at position 3 is acetyl and at position 8 is ethyl; R'₄ is methyl; and R₆ is -NH-(CH₂)₂-SO₃K (conjugate **41**).

[0103] In another embodiment, R₁ and R₆ together form a cyclic ring comprising-NH-RGD-CO-NH-(CH₂)₂-NH- or -NH-RGD-CO-NH-(CH₂)₃-piperazino-(CH₂)₃-NH-. In one embodiment, the conjugate comprises a bacteriochlorophyll of the formula II wherein m is 1; R'₂ is methoxy; R₄ at position 3 is acetyl and at position 8 is ethyl; R'₄ is methyl; and either R₁ and R₆ together form a cyclic ring comprising -NH-RGD-CO-NH-(CH₂)₂-NH- and M is Pd (Conjugate **37**) or M is 2H (Conjugate **38**) or R₁ and R₆ together form a cyclic ring comprising -NH-RGD-CO-NH-(CH₂)₃-piperazino-(CH₂)₃-NH- and M is Pd (Conjugate **39**).

[0104] In another embodiment, the conjugate comprises a chlorophyll of the formula II wherein M is 2H; m is 1; R'₂ is methoxy; R₁ is NH-P, wherein P is the residue of the RGD-containing peptide of SEQ ID NO:1; R₄ at position 3 is vinyl and at position 8 is ethyl; R'₄ is methyl; and R₆ is -NH-(CH₂)₂-SO₃ K (Conjugate **16**).

[0105] In another embodiment, the conjugate comprises a chlorophyll of the formula II wherein M is Mn; m is 1; R'₂ is methoxy; R₁ is NH-P, wherein P is the residue of the RGD-containing peptide of SEQ ID NO:1; R₄ at position 3 is vinyl and at position 8 is ethyl; R'₄ is methyl; and R₆ is -NH-(CH₂)₂-SO₃ K (Conjugate **17**).

[0106] In another embodiment, the conjugate comprises a chlorophyll of the formula II wherein M is Cu; m is 1; R'₂ is methoxy; R₁ is NH-P, wherein P is the residue of the RGD-containing

peptide of SEQ ID NO:1; R₄ at position 3 is vinyl and at position 8 is ethyl; R'₄ is methyl; and R₆ is -NH-(CH₂)₂-SO₃ K (Conjugate 18).

[0107] In another embodiment, the conjugate comprises a bacteriochlorophyll of the formula I wherein M is Mn; R₁ is NH-P, wherein P is the residue of the RGD-containing peptide of SEQ ID NO:1; R₂ is OH; R₃ is COOCH₃; R₄ at position 3 is acetyl and at position 8 is ethyl; R'₄ is methyl; and R₅ is O (Conjugate 12).

[0108] In another embodiment, the conjugate comprises a bacteriochlorophyll of the formula I wherein M is 2H; R₁ is NH-P, wherein P is the residue of the RGD-containing peptide of SEQ ID NO:1; R₂ is H; R₃ is COOCH₃; R₄ at position 3 is acetyl and at position 8 is ethyl; R'₄ is methyl; and R₅ is O (Conjugate 27).

[0109] In another embodiment, the conjugate comprises a bacteriochlorophyll of the formula I wherein M is 2H; R₁ is NH-(CH₂)₂-NH-CO-P, wherein P is the residue of the RGD-containing peptide of SEQ ID NO:4; R₂ is H; R₃ is COOCH₃; R₄ at position 3 is acetyl and at position 8 is ethyl; R'₄ is methyl; and R₅ is O (Conjugate 32).

[0110] In another embodiment, the conjugate comprises a bacteriochlorophyll of the formula II wherein M is Pd; m is 1; R₁ is NH-P, wherein P is the residue of the RGD-containing peptide of SEQ ID NO:2; R'₂ is methoxy; R₄ at position 3 is acetyl and at position 8 is ethyl; R'₄ is methyl; and R₆ is -NH-(CH₂)₂-SO₃K (Conjugate 11).

[0111] In another embodiment, the conjugate comprises a bacteriochlorophyll of the formula II wherein M is 2H; m is 1; R₁ is NH-P, wherein P is the residue of the RGD-containing peptide of SEQ ID NO:1; R'₂ is methoxy; R₄ at position 3 is acetyl and at position 8 is ethyl; R'₄ is methyl; and R₆ is -NH-(CH₂)₂-SO₃K (Conjugate 13).

[0112] In another embodiment, the conjugate comprises a bacteriochlorophyll of the formula II wherein M is Mn; m is 1; R₁ is NH-P, wherein P is the residue of the RGD-containing peptide of SEQ ID NO:1; R'₂ is methoxy; R₄ at position 3 is acetyl and at position 8 is ethyl; R'₄ is methyl; and R₆ is -NH-(CH₂)₂-SO₃K (Conjugate 14).

[0113] In another embodiment, the conjugate comprises a bacteriochlorophyll of the formula II wherein M is Cu; m is 1; R₁ is NH-P, wherein P is the residue of the RGD-containing peptide of SEQ ID NO:1; R'₂ is methoxy; R₄ at position 3 is acetyl and at position 8 is ethyl; R'₄ is methyl; and R₆ is -NH-(CH₂)₂-SO₃K (Conjugate 15).

[0114] In another embodiment, the conjugate comprises a bacteriochlorophyll of the formula II wherein M is Pd; m is 1; R₁ is NH-P, wherein P is the residue of the RGD-containing peptide of SEQ ID NO:1; R'₂ is methoxy; R₄ at position 3 is acetyl and at position 8 is ethyl; R'₄ is methyl;

and R₆ is -NH-(CH₂)₂-SO₃K (Conjugate 24).

[0115] In another embodiment, the conjugate comprises a bacteriochlorophyll of the formula III wherein M is Pd; R₁ is NH-P, wherein P is the residue of of the RGD-containing peptide of SEQ ID NO:1; R₄ at position 3 is acetyl and at position 8 is ethyl; R'₄ is methyl; X is N-R₇ and R₇ is -NH-(CH₂)₃-SO₃K (Conjugate 19).

[0116] In another embodiment, the conjugate comprises a bacteriochlorophyll of the formula II wherein M is 2H; m is 1; R₁ is NH-P, wherein P is the residue of the RGD-containing peptide of SEQ ID NO:3; R'₂ is methoxy; R₄ at position 3 is acetyl and at position 8 is ethyl; R'₄ is methyl; and R₆ is -NH-(CH₂)₂-SO₃K (Conjugate 26).

[0117] In another embodiment, the conjugate comprises a bacteriochlorophyll of the formula II wherein M is Pd; m is 1; R₁ is NH-P, wherein P is the residue of the RGD-containing peptide of SEQ ID NO:5; R'₂ is methoxy; R₄ at position 3 is acetyl and at position 8 is ethyl; R'₄ is methyl; and R₆ is -NH-(CH₂)₂-SO₃K (Conjugate 33).

[0118] In another embodiment, the conjugate comprises a bacteriochlorophyll of the formula II wherein M is Pd; m is 1; R₁ is NH-P, wherein P is the residue of the RGD-containing peptide of SEQ ID NO:6; R'₂ is methoxy; R₄ at position 3 is acetyl and at position 8 is ethyl; R'₄ is methyl; and R₆ is -NH-(CH₂)₂-SO₃K (Conjugate 34).

[0119] In another embodiment, the conjugate comprises a bacteriochlorophyll of the formula II wherein M is Pd; m is 1; R₁ is NH-P, wherein P is the residue of the RGD-containing peptide of SEQ ID NO:7; R'₂ is methoxy; R₄ at position 3 is acetyl and at position 8 is ethyl; R'₄ is methyl; and R₆ is -NH-(CH₂)₂-SO₃K (Conjugate 35).

[0120] In another embodiment, the conjugate comprises a bacteriochlorophyll of the formula II wherein M is Pd; m is 1; R₁ is NH-CH[(-(CH₂)₂-CO-NH-P)]₂, wherein P is the residue of the RGD-containing peptide of SEQ ID NO:8; R'₂ is methoxy; R₄ at position 3 is acetyl and at position 8 is ethyl; R'₄ is methyl; and R₆ is -NH-(CH₂)₂-SO₃K (Conjugate 36).

[0121] In another embodiment, the conjugate comprises a bacteriochlorophyll of the formula II wherein M is Pd; m is 1; R₁ is NH-P, wherein P is the residue of of the RGD-containing peptide of SEQ ID NO:1; R'₂ is methoxy; R₄ at position 3 is acetyl and at position 8 is ethyl; R'₄ is methyl; and R₆ is -NH-CH₂-CH(OH)-CH₂OH. (Conjugate 23).

[0122] In another embodiment, the conjugate comprises a bacteriochlorophyll of the formula II wherein M is 2H; m is 1; R₁ is NH-P, wherein P is the residue of the RGD-containing peptide of SEQ ID NO:1; R'₂ is methoxy; R₄ at position 3 is acetyl and at position 8 is ethyl; R'₄ is methyl;

and R₆ is -NH-(CH₂)₃-NH-CO-DTPA (Conjugate **43**) or its chelate complex with Gd (Conjugate **44**).

[0123] The invention further provides the novel bacteriochlorophyll of the formula II, wherein M is Pd; R₁ is COOH; R₂ is methoxy; R₄ at position 3 is acetyl and at position 8 is ethyl; R₄' is methyl; and R₆ is -NH-CH₂-CH(OH)-CH₂-OH (compound **10**).

[0124] In another aspect, the present invention provides a pharmaceutical composition comprising a conjugate of an RGD-containing peptide or an RGD peptidomimetic and a photosensitizer selected from a chlorophyll or a bacteriochlorophyll as defined herein and a pharmaceutically acceptable carrier.

[0125] In one embodiment, the pharmaceutical composition comprises a conjugate comprising a chlorophyll or a bacteriochlorophyll photosensitizer of formula I, II or III as defined herein or a pharmaceutically acceptable salt thereof.

[0126] In one preferred embodiment the pharmaceutical composition comprises a conjugate in which the chlorophyll has formula II, more preferably selected from the conjugates **16**, **17** and **18**.

[0127] In another preferred embodiment the pharmaceutical composition comprises a conjugate in which the bacteriochlorophyll has the formula I, more preferably selected from the conjugates **12**, **27** and **32**.

[0128] In another preferred embodiment the pharmaceutical composition comprises a conjugate in which the bacteriochlorophyll has the formula III, more preferably the conjugate **19**.

[0129] In another more preferred embodiment the pharmaceutical composition comprises a conjugate in which the bacteriochlorophyll has the formula II conjugated with an RGD peptide, more preferably with the RGD peptide of SEQ ID NO:1, more preferably selected from the conjugates **13**, **15**, **23**, **28**, **29**, **30**, **31**, **43**, and **44**, and more preferably the conjugate **24**.

[0130] In another embodiment the pharmaceutical composition comprises a conjugate in which the bacteriochlorophyll has the formula II conjugated with an RGD peptide of any of SEQ ID NO:2 - 8, more preferably the conjugates **11**, **26**, **33**, **34**, **35**, and **36**.

[0131] In another embodiment the pharmaceutical composition comprises a conjugate in which the bacteriochlorophyll has the formula II conjugated with an RGD peptidomimetic, more preferably the conjugates **40** and **41**.

[0132] In one embodiment, the pharmaceutical composition is for use in photodynamic therapy (PDT), more particularly for vascular-targeted PDT (VTP).

[0133] In one embodiment, the pharmaceutical composition is for use in oncology, particularly for VTP of tumors. Any suitable solid tumor is encompassed by the invention, both primary tumors and metastasis, of tumors selected from, but not limited to, from melanoma, colon, breast, lung, prostate, brain or head and neck cancer.

[0134] In another embodiment, the pharmaceutical composition is for use in non-oncologic diseases, for VTP of non-neoplastic tissue or organ. In one embodiment, the pharmaceutical composition is used for treatment of vascular diseases such as age-related macular degeneration (AMD) or disorders such as obesity by limiting vascular supply to adipose tissue and thus inhibiting its growth.

[0135] The pharmaceutical composition of the invention is also used for diagnostic purposes, for visualization of organs and tissues. It can be used in methods of vascular-targeted imaging (VTI).

[0136] In one embodiment, the pharmaceutical composition is used for diagnosis of tumors using several techniques. Several diagnostic techniques can be applied in accordance with the invention, by adapting the central metal atom to the particular technique.

[0137] For tumor diagnosis by dynamic fluorescence imaging, M in the photosensitizer is 2H or a metal selected from Cu, Pd Gd, Pt, Zn, Al, Eu, Er, Yb or isotopes thereof.

[0138] For tumor diagnosis by radiodiagnostic technique, M in the photosensitizer is a radioisotope selected from ^{64}Cu , ^{67}Cu , $^{99\text{m}}\text{Tc}$, ^{67}Ga , ^{201}Tl , ^{195}Pt , ^{60}Co , ^{111}In and ^{51}Cr . In one embodiment, the radiodiagnostic technique is positron emission tomography (PET) and M is ^{64}Cu or ^{67}Cu . In another embodiment, the radiodiagnostic technique is single photon emission tomography (SPET) and M is a radioisotope selected from $^{99\text{m}}\text{Tc}$, ^{67}Ga , ^{195}Pt , ^{111}In ^{51}Cr and ^{60}Co .

[0139] For tumor diagnosis by molecular magnetic resonance imaging (MRI), M is a paramagnetic metal selected from Mn^{3+} , Cu^{2+} , Fe^{3+} , Eu^{3+} , Gd^{3+} and Dy^{3+} , or the photosensitizer is substituted by a metal chelate complex of a polydentate ligand and the metal is as defined hereinbefore.

[0140] The present invention also provides a pharmaceutical composition for use in tumor radiotherapy, wherein M is a radioisotope selected from ^{103}Pd , ^{195}Pt , ^{105}Rh , ^{106}Rh , ^{188}Re , ^{177}Lu , ^{164}Er , $^{117\text{m}}\text{Sn}$, ^{153}Sm , ^{90}Y , ^{67}Cu and ^{32}P .

[0141] The present invention further provides the novel bacteriochlorophyll of the formula II, wherein M is Pd; R_1 is COOH; R'_2 is methoxy; R_4 at position 3 is acetyl and at position 8 is ethyl; R'_4 is methyl; and R_6 is -NH-CH(OH)-CH₂-OH herein identified as compound **10**.

[0142] According to one embodiment, the invention relates to the pharmaceutical composition for use in tumor diagnosis by dynamic fluorescence imaging, wherein M in the photosensitizer is 2H or a metal selected from Cu, Pd, Gd, Pt, Zn, Al, Eu, Er, Yb or isotopes thereof.

[0143] In another embodiment, the invention provides the pharmaceutical composition for use in tumor diagnosis by radiodiagnostic technique, wherein M in the photosensitizer is a radioisotope selected from ^{64}Cu , ^{67}Cu , $^{99\text{m}}\text{Tc}$, ^{67}Ga , ^{195}Pt , ^{201}Tl , ^{60}Co , ^{111}In or ^{51}Cr . In a preferred embodiment, the radiodiagnostic technique is positron emission tomography (PET) and M is ^{64}Cu or ^{67}Cu . In another preferred embodiment, the radiodiagnostic technique is single photon emission tomography (SPET) and M is a radioisotope selected from the group consisting of $^{99\text{m}}\text{Tc}$, ^{67}Ga , ^{195}Pt , ^{111}In , ^{51}Cr and ^{60}Co .

[0144] In a further embodiment, the invention provides the pharmaceutical composition for use in tumor diagnosis by molecular magnetic resonance imaging (MRI), wherein M is a paramagnetic metal selected from Mn^{3+} , Cu^{2+} , Fe^{3+} , Eu^{3+} , or Dy^{3+} and, preferably, Gd^{3+} .

[0145] The RGD peptide-photosensitizer conjugates of the invention are particularly suitable for vascular-targeting PDT (VTP) and are useful for treatment of diseases associated with angiogenesis/neovascularization and new blood vessel growth such as cancer, diabetic retinopathy, macular degeneration and arthritis. In one most preferred embodiment of the present invention, the target for treatment with the sensitizers of the invention are abnormal blood vessels, particularly blood vessels of solid tumors, age-related macular degeneration, restenosis, acute inflammation or atherosclerosis (Dougherty and Levy, 2003), due to the inherent difference of sensitivity of normal and abnormal blood vessels to the suggested PDT protocols described herein.

[0146] Thus, in one embodiment, the conjugates of the invention are useful in the oncological field for treatment by PDT of precancerous states and several cancer types such as, but not limited to, melanoma, prostate, brain, colon, ovarian, breast, head and neck, chest wall tumors arising from breast cancer, skin, lung, esophagus and bladder cancers and tumors. The compounds are useful for treatment of primary as well as metastatic tumors.

[0147] The invention further relates to tumor therapy without PDT, namely, to the pharmaceutical composition comprising a RGD peptide-photosensitizer conjugate according to the invention for use in tumor radiotherapy wherein M is a radioisotope selected from ^{103}Pd , ^{195}Pt , ^{105}Rh , ^{106}Rh , ^{188}Re , ^{177}Lu , ^{164}Er , $^{117\text{m}}\text{Sn}$, ^{153}Sm , ^{90}Y , ^{67}Cu , or ^{32}P .

[0148] In another embodiment, the compounds of the invention are useful in non-oncological areas. Besides the efficient destruction of unwanted cells, like neoplasms and tumors, by PDT, the compounds of the invention can also be used against proliferating cells and blood vessels, which are the main cause of arteriosclerosis, arthritis, psoriasis, obesity and macular degeneration. In addition, the compounds can be used in the treatment of non-malignant tumors such as benign prostate hypertrophy.

[0149] In one preferred embodiment, the conjugates of the invention can be used in PDT for treatment of cardiovascular diseases mainly for vessel occlusion and thrombosis in coronary artery diseases, intimal hyperplasia, restenosis, and atherosclerotic plaques. In a more preferred embodiment, the compounds of the invention are used for preventing or reducing in-stent restenosis in an individual suffering from a cardiovascular disease that underwent coronary angiography. In another preferred embodiment, the compounds of the invention can be used for the treatment of atherosclerosis by destruction of atheromatous plaque in a diseased blood vessel.

[0150] In another preferred embodiment, the compounds of the invention can be used in PDT for treatment of dermatological diseases, disorders and conditions such as acne, acne scarring, psoriasis, athlete's foot, warts, actinic keratosis, and port-wine stains (malformations of tiny blood vessels that connect the veins to the arteries (capillaries) located in the upper levels of the skin).

[0151] In another preferred embodiment, the conjugates of the invention can be used in PDT for treatment of ophthalmic diseases, disorders and conditions such as corneal and choroidal neovascularization and, more preferably, age-related macular degeneration (AMD).

[0152] The amount of the conjugate to be administered for PDT therapy will be established by the skilled physician according to the experience accumulated with porphyrin, ChI and BChI derivatives used in PDT, and will vary depending on the choice of the derivative used as active ingredient, the condition to be treated, the mode of administration, the age and condition of the patient, and the judgement of the physician.

[0153] The wavelength of the irradiating light is preferably chosen to match the maximum absorbance of the photosensitizer. The suitable wavelength for any of the compounds can be readily determined from its absorption spectrum. In a preferred embodiment, a strong light source is used, more preferably lasers at 720-790 nm when the photosensitizer is a BChI derivative.

[0154] The conjugates of the invention may be further used in photodynamic therapy as an adjuvant to another current therapy used for the treatment of a disease, disorder or condition, to make it more effective. For example, they may be used intraoperatively in combination with surgery, to help prevent the recurrence of cancer on large surface areas such as the pleura (lining of the lung) and the peritoneum (lining of the abdomen), common sites of spread for some types of cancer, in intraoperative treatment of recurrent head and neck carcinomas, or following femoral artery angioplasty to prevent restenosis. The conjugates may be also used in intraoperative PDT tumor diagnosis, for example, of brain tumors.

[0155] Another possibility according to the invention is to use the conjugates of the invention in PDT of large solid tumors by interstitial therapy, a technique that involves feeding optic fibers directly into tumors using needles guided by computed tomography (CT). This may be

especially useful in areas that require extensive surgery such as in head and neck tumors.

[0156] The amount of conjugate to be administered and the route of administration will be determined according to the kind of disease, stage of the disease, age and health conditions of the patient, but will be much lower than the currently used dosage of Photofrin II® (about 5-40 mg HpD/kg body weight) or Tookad® (about 2-10 mg/kg body weight).

[0157] The pharmaceutical compositions of the invention can be administered to the patient by standard procedures used in PDT, for example, systemically, particularly by injection, more preferably by intravenous injection, locally by direct injection into the solid tumor, or topically for treatment of skin diseases and conditions.

[0158] The invention will now be illustrated by the following Examples.

EXAMPLES

I CHEMICAL SECTION

[0159] In the Examples herein, the intermediates and compounds **1-10** and the conjugates of the invention (**11-24**) will be presented by their respective Arabic numbers in bold and underlined according to the following List of Compounds and the Appendix. The formulas of all the compounds and conjugates are presented in the Appendix at the end of the description, just before the References.

List of Compounds

[0160]

- 1.** Bacteriochlorophyll a (Bchl a)
- 2.** 13²-OH-Bacteriochlorophyll a (13²-OH-Bchl a)
- 3.** Bacteriopheophorbide a (Bpheid a)
- 4.** 13²-OH-Bacteriopheophorbide a (13²-OH-Bpheid a)
- 4a.** Bacteriopurpurin 18 (BPP 18)
- 5.** Chlorophyll a (Chl a)
- 6.** Pheophorbide a (Pheid a)

- 7.** Palladium Bacteriopheophorbide a (Pd-Bpheid)
- 8.** Palladium 3¹-oxo-15-methoxycarbonylmethyl-Rhodobacteriochlorin 13¹-(2-sulfoethyl)amide potassium salt
- 9.** Manganese(III) 13²-OH-Bacteriopheophorbide a (Mn(III) 13²-OH-Bpheid a)
- 10.** Palladium 3¹-oxo-15-methoxycarbonylmethyl-Rhodobacteriochlorin-13¹-(2,3-dihydroxypropyl)amide potassium salt
- 11.** Palladium 3¹-oxo-15-methoxycarbonylmethyl-Rhodobacteriochlorin 13¹-(2-sulfoethyl)amide-17³-(RGD-4C)amide potassium salt
- 12.** Manganese(III) 13²-OH-Bacteriopheophorbide-17³-(cycloRGDfK)amide
- 13.** 3¹-oxo-15-methoxycarbonylmethyl-Rhodobacteriochlorin 13¹-(2-sulfoethyl) amide-17³-(cycloRGDfK)amide potassium salt
- 14.** Manganese(III) 3¹-oxo-15-methoxycarbonylmethyl-Rhodobacteriochlorin 13¹-(2-sulfoethyl)amide-17³-(cycloRGDfK)amide potassium salt
- 15.** Copper(II) 3¹-oxo-15-methoxycarbonylmethyl-Rhodobacteriochlorin 13¹-(2-sulfoethyl)amide-17³-(cycloRGDfK)amide potassium salt
- 16.** 3¹,3²-Didehydrorhodochlorin 13¹-(2-sulfoethyl)amide-17³-(cycloRGDfK) amide potassium salt
- 17.** Manganese(III) 3¹,3²-Didehydrorhodochlorin 13¹-(2-sulfoethyl)amide-17³-(cycloRGDfK)amide potassium salt
- 18.** Copper(II) 3¹,3²-Didehydrorhodochlorin 13¹-(2-sulfoethyl)amide-17³-(cycloRGDfK)amide potassium salt
- 19.** Palladium Bacteriopurpurin N-(3-sulfopropylamino)imide-17³-(cycloRGDfK) amide potassium salt
- 20.** Meso-5-(4-cycloRGDfK-benzamido)-10,15,20-tris(4-carboxyphenyl)porphine
- 21.** Copper(II) meso-5-(4-cycloRGDfK-benzamido)-10,15,20-tris(4-carboxyphenyl) porphine
- 22.** Gadolinium(III) meso-5-(4-cycloRGDfK-benzamido)-10,15,20-tris(4-carboxyphenyl)porphine
- 23.** Palladium 3¹-oxo-15-methoxycarbonylmethyl-Rhodobacteriochlorin-13¹-(2,3-dihydroxypropyl)amide-17³-(cycloRGDfK)amide

- 24.** Palladium 3¹-oxo-15-methoxycarbonylmethyl-Rhodobacteriochlorin 13¹-(2-sulfoethyl)amide-17³-(cycloRGDfK)amide potassium salt.
- 25.** 3¹-oxo-15-methoxycarbonylmethyl-Rhodobacteriochlorin 13¹-(2-sulfoethyl) amide potassium salt.
- 26.** 3¹-oxo-15-methoxycarbonylmethyl-Rhodobacteriochlorin 13¹-(2-sulfoethyl)amide-17³-(GRGDSP)amide potassium salt
- 27.** Bacteriopheophorbide-17³-(cycloRGDfK)amide
- 28.** 3¹-oxo-15-methoxycarbonylmethyl-Rhodobacteriochlorin 13¹-(3-[(3-aminopropyl)amino]propyl)amide-17³-(cycloRGDfK)amide
- 29.** 3¹-oxo-15-methoxycarbonylmethyl-Rhodobacteriochlorin 13¹-(2,3-dihydroxypropyl)amide-17³-(cycloRGDfK)amide
- 30.** 3¹-oxo-15-methoxycarbonylmethyl-Rhodobacteriochlorin 13¹-(2-morpholino-N-ethyl)amide-17³-(cycloRGDfK)amide
- 31.** 3¹-oxo-15-methoxycarbonylmethyl-Rhodobacteriochlorin 13¹-{3-[4-(3-aminopropyl)-piperazin-1-yl]-propyl}amide-17³-(cycloRGDfK)amide
- 32.** Bacteriopheophorbide-17³-(2-cycloRGDK-amido-N-ethyl)amide
- 33.** Palladium 3¹-oxo-15-methoxycarbonylmethyl-Rhodobacteriochlorin 13¹-(2-sulfoethyl)amide-17³-(GRGDSPK)amide potassium salt
- 34.** Palladium 3¹-oxo-15-methoxycarbonylmethyl-Rhodobacteriochlorin 13¹-(2-sulfoethyl)amide-17³-[(GRGDSP)₄K]amide potassium salt
- 35.** Palladium 3¹-oxo-15-methoxycarbonylmethyl-Rhodobacteriochlorin 13¹-(2-sulfoethyl)amide-17³-(cycloRGDf-N(Me)K)amide potassium salt
- 36.** Palladium 3¹-oxo-15-methoxycarbonylmethyl-Rhodobacteriochlorin 13¹-(2-sulfoethyl)-17³-N-[4-heptanedioic acid bis-(cycloRGDyK-amido)]amide potassium salt
- 37.** Palladium 3¹-oxo-15-methoxycarbonylmethyl-Rhodobacteriochlorin 13¹,17³-cyclo(2-RGD-amido-N-ethyl)diamide
- 38.** 3¹-oxo-15-methoxycarbonylmethyl-Rhodobacteriochlorin 13¹,17³-cyclo(2-RGD-amido-N-ethyl)diamide

39. Palladium 3¹-oxo-15-methoxycarbonylmethyl-Rhodobacteriochlorin 13¹,17³-cyclo {3-[4-(3-aminopropyl-DGR-amido)-piperazin-1-yl]-propyl} diamide

40. Palladium 3¹-oxo-15-methoxycarbonylmethyl-Rhodobacteriochlorin 13¹-(2-sulfoethyl)amide-17³-[4-(methyl-5-(6-guanidino-hexanoylamino)-pentanoic acid)]amide potassium salt

41. Palladium 3¹-oxo-15-methoxycarbonylmethyl-Rhodobacteriochlorin 13¹-(2-sulfoethyl)amide-17³-[7-amido-3-[[1-(4-guanidino-butyryl)-piperidine-3-carbonyl]-amino]-heptanoic acid] potassium salt

42. Palladium 3¹-oxo-15-methoxycarbonylmethyl-Rhodobacteriochlorin 13¹-(2-sulfoethyl)amide-17³-(cycloRADfK)amide potassium salt

43. 3¹-oxo-15-methoxycarbonylmethyl-Rhodobacteriochlorin 13¹-(3-DTPA-amido-N-propyl)amide-17³-(cycloRGDfK)amide

44. 3¹-oxo-15-methoxycarbonylmethyl-Rhodobacteriochlorin 13¹-(3-Gd-DTPA-amido-N-propyl)amide-17³-(cycloRGDfK)amide

Materials and Methods

[0161]

(i) Bacteriochlorophyll a (Bchl a), 1, was obtained as described by Scherz and Parson, 1984. The procedure started from extraction of pigments from dry (lyophilized) cells of the photosynthetic bacteria *Rhodovulum sulfidophilum*. Purification of the crude pigment extract was carried out by DEAE-Sepharose column chromatography according to Omata and Murata, 1983. Briefly, DEAE-Sepharose was washed with distilled water and then converted to an acetate form by suspending it in a 1M sodium acetate buffer (pH = 7). The slurry was washed 3 times with acetone and finally suspended in methanol-acetone (1:3, v:v) for storage at 5°C. The purity was checked by thin layer chromatography (TLC). Detailed description of TLC conditions can be found in Fiedor et al., 1992.

(ii) 13²-OH-Bacteriochlorophyll a (13²-OH-Bchl), 2, was produced by allomerization of Bchl a by stirring a methanol solution of Bchl a (1 g/ml) in the dark, in contact with air, as described in Struck et al., 1992.

(iii) Bacteriopheophorbide (Bpheid), 3, and 13²-OH-Bacteriopheophorbide (13²-OH-Bpheid) 4, were synthesized following Wasielewski and Svec, 1980, by demetallation-

deesterification of the corresponding Bchl a or 13²-OH-Bchl a with 80% aqueous trifluoroacetic acid. Purification of synthesized Bpheid or 13²-OH-Bpheid is carried out on Silica ("Kieselgel 60", Merck, Germany) column with gradient of methanol in chloroform (0 to 15/25% vol.) as eluent.

(iv) Chlorophyll a (Chl), 5, and (v) Pheophorbide a (Pheid), 6. Chl was obtained from cyanobacteria *Spirulina platensis* following the same routine for obtaining Bchl (see above). Further, Chl is converted into Pheid following the same procedure as described for Bpheid above.

(vi) Palladium Bacteriopheophorbide a (Pd-Bpheid a), 7, was synthesized as described in WO 2000/033833 (Example 2 therein)

(vii) Palladium 3¹-oxo-15-methoxycarbonylmethyl-Rhodobacteriochlorin 13¹-(2-sulfoethyl)amide potassium salt, 8, was synthesized as described in WO 2004/045492 (Example 1, synthesis of compound 4).

(viii) 3¹-oxo-15-methoxycarbonylmethyl-Rhodobacteriochlorin 13¹-(2-sulfoethyl)amide dipotassium salt, 25, was synthesized by reaction of Bpheid with taurine as described in WO 2004/045492 (Example 2, synthesis of compound 5).

(ix) Bacteriopurpurin 18 (BPP18), 4a was synthesized as described by Mironov et al., 1992.

(x) The resin, the amino acid derivatives, N-hydroxybenzotriazole (HOBt) and benzotriazole-1-yl-oxy-tris-pyrrolidino-phosphonium hexafluorophosphate (PyBOP) were purchased from Novabiochem; N,N-Diisopropylethylamine (DIEA), N,N'-diisopropylcarbodiimide (DIC) ethylenediamine, 1,4-bis(3-aminopropyl)-piperazine, 1,3-dimethylbarbituric acid (DMBA), diethyldithiocarbamic acid, sodium salt (DEDTC), 2,2,2-trifluoroethanol (TFE), triisopropylsilane (TIS), 1,2-ethanedithiol (EDT), trifluoroacetic acid (TFA), meso-tetra(4-carboxyphenyl)porphine, sodium L-ascorbate and 4-oxoheptanedioic acid, were purchased from Aldrich (USA); N-hydroxysuccinimide (NHS) was purchased from Sigma (USA); N-hydroxysulfosuccinimide (sulfo-NHS), 1,3-dicyclohexylcarbodiimide (DCC), N-(3-dimethylaminopropyl)-N'-ethylcarbodiimide (EDC), N-Fmoc-6-aminohexanoic acid, N(^β-Fmoc-N^ω-Boc-β-L-homolysine, and N-Fmoc-piperidine-3-carboxylic acid were purchased from Fluka (Switzerland); cadmium acetate, copper acetate and manganese(II) chloride were from Merck (Germany); and tetrakis (triphenylphosphine) palladium was obtained from Acros.

[0162] Chemicals and solvents of analytical grade were generally used except when performing HPLC, where HPLC-grade solvents are applied.

(x) Peptide synthesis - Peptides were synthesized by solid phase methods via Fmoc chemistry using protected amino acids and cyclicized according to procedures common in the art. Removal of Fmoc-group and completion of couplings were monitored by the ninhydrin

(Kaiser) test. TFA or a cocktail solution of TFA/thioanisole/H₂O/ triisopropylsilane (TIS) was used for peptide removal from the resin simultaneously with deprotection (Arg-pentamethylchroman-6-ylsulfonyl (Pmc) or 2,2,4,6,7-pentamethyldihydro benzofuran-5-sulfonyl (Pbf); Asp-OtBu; Ser-*tert*-butyl (tBu); Lys-*tert*-butyloxycarbonyl (Boc), allyloxycarbonyl (Alloc) or Dde).

1. (i) Linear peptides GRGDSPK, (GRGDSP)₄K or GRGDSP were obtained using Fmoc-Lys(Boc)-Wang resin or 2-chlorotrityl chloride resin, respectively.
2. (ii) Cyclic peptides (cycloRGDfK), (cycloRGDyK), (cycloRADfK) and (cycloRGDf-N(Me)K) were prepared by synthesis of pentapeptides on 2-chlorotrityl chloride resin and their subsequent cyclization in solution as described in Haubner et al., 1999. N^α-methyl protected lysine was prepared from 2-aminoheptanedioic acid as described previously (Freidinger et al., 1983). Another method of synthesis of cycloRGDfK by cyclization on the resin is described in Example 13 herein.
3. (iii) Cyclic peptide RGD-4C was prepared by synthesis of CDCRGDCFCG by standard solid phase synthesis protocol and its cyclization by spontaneous oxidative formation of disulfide bonds (Koivunen et al. 1995).
4. (iv) Cyclic peptidyl-amine cycloRGDK-NH₂ was synthesized on chlorotrityl-resin (protections: Arg-Pbf; Asp-OtBu; N^ε-Lys-Alloc). Then, N-terminal Fmoc group and the Alloc protecting group on the ε-amino of the lysine residue were cleaved, and the cyclization between the two aminos through an urea bond using *N,N*-carbonyldiimidazole (CDI) was allowed for 12-16 h. The cyclic peptide was cleaved from the support and the lysine carboxylate was reacted with 1,2-diaminoethane (DCC activation) to obtain the required peptidylamine.
5. (v) Cyclopeptide dimer (cycloRGDyK)₂. 4-Oxoheptanedioic acid was converted into 4-aminoheptanedioic acid according to Wanunu et al., 2005. Then the amino group was Boc-protected and carboxylic moieties were activated with NHS/DCC in DMF. The diester was purified on silica column with chloroform-methanol, and then reacted with cycloRGDyK in DMF containing DIEA overnight. The Boc protection was cleaved with TFA-water-dichloromethane (DCM) (90:5:5). The desired compound was purified by HPLC.
6. (vi) RGD-Peptidomimetics (RGD-PM1, RGD-PM2) were obtained according to WO 93/09795. Namely, one amino group of ethyl 5-amino-4-aminomethyl)pentanoic acid (Vaillancourt et al. 2001 and refs therein) was protected with equimolar amount of Boc anhydride and the carboxylic group was protected with *tert*-butyl alcohol. The product was purified on silica column, and coupled with N-Fmoc-6-aminohexanoic acid followed by Fmoc-deprotection and conversion of the amine to guanidinium with 3,5-dimethylpyrazole 1-carboxamide nitrate (pH 9.5; 50°C). Finally, the N-Boc and O-*t*Bu were removed with TFA, and the product RGD-PM1 was purified by HPLC. The synthesis of RDG-PM1 is depicted in **Scheme 3**. For the synthesis of RGD-PM2 (see **Scheme 3**), N^β-Fmoc-N^ω-Boc-β-L-homolysine was attached to Wang-resin. Next, couplings with N-Fmoc-piperidine-3-carboxylic acid and N-Fmoc-4-aminobutyric acid were performed using solid phase methods. After guanidinium formation (as described

above), the resulting material was deprotected and removed from the resin with TFA, and the product RGD-PM2 was purified by HPLC.

(ix) TLC: silica plates (Kieselgel-60, Merck, Germany); chloroform-methanol (4:1, v/v).

(x) The extinction coefficients of the metallocomplexes were determined by correlating the central metal concentration (using flame photometry with metal salt as a standard) with the optical density of the examined solution at the particular wavelength.

(xi) Mass spectra. Electrospray ionization mass spectra (ESI-MS) were recorded on a platform LCZ spectrometer (Micromass, England). The Matrix-assisted laser desorption/ionization mass spectra (MALDI-TOF-MS) measurements were performed on Bruker REFLEX time-of-flight instrument (Bruker Daltonics, USA).

(xii) Optical absorption (UV-VIS) spectra of the different complexes were recorded with either Genesis-2 (Milton Roy, England), V-570 (JASCO, Japan) or Shimadzu UV-1650PC (Japan) spectrophotometers.

(xiii) HPLC was performed using an LC-900 instrument (JASCO, Japan) equipped with a UV-915 diode-array detector, or a Waters Delta Prep 4000 system equipped with a Waters 486 UV-VIS tunable absorbance detector and a Waters fraction collector, controlled by Millennium v3.05 program. The flow rate was set to 75 ml/min, using a preparative column (Vydac C18, 218TP101550, 50 x 250 mm, 10-15 μ m), the detector was set at wavelength 380 nm and the fraction collector was set at a time mode of 6 s/fraction. Solvents used in the HPLC purification were as follows: solvent A: 50 mM solution of ammonium acetate in H₂O; solvent B: acetonitrile.

(ivx) LC-MS API 150EX (Applied Biosystems/MDS SCIEX), was performed using YMS-Pack Pro C18 column. Mobile phase: solvent A: 0.2% AcOH/0.12% NH₄OH/H₂O; solvent B: 4.75% A/0.2% AcOH/acetonitrile. Flow rate: 200 μ l/min. Gradient: 20% B(0-2min) to 95% B(25-30 min).

Example 1. Synthesis of conjugate 11

[0163] Compound 8, obtained as described in Material and Methods, was directly conjugated to the cyclic peptide RGD-4C as described in **Scheme 1** as follows: compound 8 (10 mg) was reacted overnight with NHS (20 mg) in the presence of EDC (20 mg) in DMSO (3 ml). The obtained activated succinimide ester (Bauminger and Wilchek, 1980) was purified on a silica column using CHCl₃:MeOH (6:1, vol.), dried and kept under argon in the dark until further use. RGD-4C (2 mg, 1.97 μ moles) was dissolved in 800 μ l DMSO and added to the activated ester (4.8 mg, 5.13 μ moles in 800 μ l DMSO and 400 μ l NaHCO₃ buffer 0.1 M pH 8.5). The reaction mixture was incubated at room temperature for 24 hours, and stirred under argon. The obtained conjugate 11 was purified using HPLC and identified by mass spectroscopy (1837

m/z) (Figs. 1A-1C). Yield: 18%.

Example 2. Synthesis of conjugate 12

[0164] Conjugate 12 was prepared starting from the synthesis of compound 9.

(i) Synthesis of compound 9

[0165] Compound 4 (20 mg), obtained as described in Materials and Methods, was dissolved in DMF (8 ml) that was previously passed through Alumina B column (1x5cm), and bubbled with Argon for 5-10 minutes. Cadmium acetate (85 mg, 10 eq. to 4) was added and the reaction mixture heated to 110°C. The reaction progress was monitored spectrally (in acetone). Metalation occurred within 5 minutes. MnCl₂·2H₂O (55 mg, 10 eq.) was added while stirring until the reaction was completed (within additional 5-10 minutes). To remove inorganic salts, the reaction solution was evaporated; the solid was re-dissolved in acetonitrile, the solution was filtered through Whatman paper on Buchner funnel and evaporated. Finally, HPLC of the crude product re-dissolved in water was performed (LC-900 instrument, JASCO, Japan; column S10P- μ m ODS-A 250x20 mm, YMC, Japan) with 50% aqueous acetonitrile as a mobile phase at a flow of 8 ml/min, and the pure product 9 was eluted at 10.5 - 13.5 min., providing a full separation of the product from chlorin admixtures and by-products. Yield: 88%.

[0166] The structure of compound 9 was confirmed spectrally (see electronic spectrum depicted in Fig 2A) and by mass spectrum (Fig. 2B, ESI-MS, positive mode and also negative mode to check for the absence of MnCl₂; 679 m/z).

(ii) Synthesis of conjugate 12

[0167] Compound 9 (15 mg) was dissolved in DMSO with sulfo-NHS (30 mg) and DCC (24 mg), the reaction mixture was stirred at room temperature under argon atmosphere overnight, evaporated, re-dissolved in 5 mM phosphate buffer pH 8.0 (1.5 ml) and filtered. CycloRGDfK (30 mg) in DMSO (2.5 ml) was added to the filtrate, the mixture was stirred under argon atmosphere for 6 hrs, evaporated, re-dissolved in water (2 ml), and purified on HPLC on preparative C₁₈ column using a gradient elution of acetonitrile in water, 10-40%, during 15 min., flow 7 ml/min. The purified conjugate 12 was dried under reduced pressure and stored at -20°C under argon atmosphere till application.

Example 3. Synthesis of conjugate 14

[0168] The title compound was prepared starting from the synthesis of the unmetalated conjugate 13, as follows.

(i) Synthesis of conjugate 13

[0169] Bpheid (compound 3) (40 mg), prepared as described in Materials and Methods above, was activated with NHS (80 mg) and DCC (60 mg) in chloroform (5 ml) under stirring, at room temperature overnight. The obtained activated ester was purified on silica column using chloroform as eluent, and then reacted with cycloRGDfK (40 mg) in DMSO (5 ml) under stirring and argon atmosphere overnight. Then, taurine (50 mg) dissolved in 1M dipotassium hydrogen phosphate (1.5 ml, pH adjusted to 8.2) was added to the reaction, and the mixture was evaporated, leading to the putative compound 13. The product was purified by HPLC on reversed phase using gradient elution with 5 mM phosphate buffer, pH 8.0, and methanol, as described previously (Brandis et al., 2005). Yield: 52%.

(ii) Synthesis of conjugate 14

[0170] Manganese was inserted into compound 13 using the procedure employed in Example 2. The product, conjugate 14, was purified by HPLC using gradient elution with acetonitrile and water as described previously (Brandis et al., 2005).

Example 4. Synthesis of conjugate 15

[0171] An aqueous solution of copper acetate (2 mg) was added to a mixture of conjugate 13 (3 mg) (prepared in Example 3 (i)) and sodium ascorbate (2 mg) in water. The reaction was immediately monitored by spectrophotometry. After copper insertion into the macrocycle, the product was purified on a RP-18 cartridge (Lichrolut, Merck), first using water to wash out non-reacted copper acetate and ascorbates, and then methanol for the elution of the main compound, conjugate 15, which was collected and evaporated. Yield: 86%.

[0172] For the preparation of radioactive conjugates, the same procedure is used with water-soluble salts other than acetate of freshly-prepared radioactive isotope ^{64}Cu or ^{67}Cu ($t_{1/2}$ is 12.70 h and 2.58 d, respectively).

Example 5. Synthesis of conjugate 17

[0173] The title compound was prepared starting from the preparation of the unmetalated conjugate 16.

(i) Synthesis of conjugate 16

[0174] Conjugate 16 was prepared as in Example 3(i), but using Pheid (compound 6) as the starting material instead of Bpheid.

(ii) Synthesis of conjugate 17

[0175] Conjugate 17 was synthesized according to the procedure described in Example 3(ii), using conjugate 16 obtained above as the starting material.

Example 6. Synthesis of conjugate 18

[0176] The title compound was synthesized following the procedure of Example 5 above, using compound 16 as the starting material.

Example 7. Synthesis of conjugate 19

[0177] The preparation of conjugate 19 is schematically described in **Scheme 2** hereinafter.

[0178] Bacteriopurpurin 18 (BPP 18), 4a (20 mg) obtained as described in Materials and Methods, and palladium acetate (10 mg) in chloroform (8 ml) were mixed with palmitoyl ascorbate (25 mg) in methanol (12 ml). After 20 min. of stirring, the reaction was completed (monitoring was carried out by spectrophotometry), and the mixture was shaken with chloroform/water. The organic layer was collected, dried over sodium sulfate, evaporated, and purified on silica column with chloroform-acetone elution, to obtain Pd-BPP 18. UV-VIS Spectrum: 342, 414, 534 and 810 nm in chloroform.

[0179] Pd-BPP 18 (18 mg) was stirred with hydrazine hydrate (12 μ l) in pyridine (8 ml) for 35 min, the reaction mixture was poured into chloroform (30 ml) and 1N HCl (30 ml), and stirred for additional 2 hrs. Then, the organic layer was dried over sodium sulfate, propane sultone (50 mg) was added, and the mixture stirred for 10 min. and evaporated. The residue was treated with aqueous ammonia (28%, 3 ml) for 30 min. to eliminate unreacted sultone by conversion into sulfopropylamine, and the mixture was evaporated again. Water (3 ml) was added to dissolve the residue and the product was purified on a RP-18 cartridge (Lichrolut, Merck), first using water to wash out sulfopropylamine, and then methanol for the elution of the main compound, thus obtaining Pd-Bacteriopurpurin-N-(3-sulfopropylamino)imide (UV-VIS Spectrum: 344, 417, 528 and 822 nm in water).

[0180] Pd-Bacteriopurpurin-N-(3-sulfopropylamino)imide (10 mg) was reacted overnight with NHS (20 mg), in the presence of EDC (20 mg) in DMSO (3 ml). The obtained activated ester was purified on a silica column using CHCl₃:MeOH (5:1), dried and kept under argon in the dark until further use.

[0181] CycloRGDfK (5 mg) was dissolved in 1 ml of DMSO, added to the activated complex (5 mg) in 1 ml of DMSO, and the reaction mixture was incubated at room temperature for 24 hours, and stirred under argon. The obtained conjugate **19** was purified using HPLC, and identified by mass spectroscopy (ESI-MS positive mode, 1415 m/z).

Example 8. [Reference compound] Synthesis of conjugate **21**

[0182] The title compound was prepared starting from the synthesis of conjugate **20** as follows.

(i) Synthesis of conjugate **20**

[0183] Meso-tetra(4-carboxyphenyl)porphine (20 mg, 25 µmol), was mixed with sulfo-NHS (4 mg, 36 µmol) and EDC (6 mg, 30 µmol) in DMSO (6 ml), and stirred at room temperature for 24 hr. Then, cycloRGDfK (20 mg, 33 µmol) was added, the reaction mixture was stirred for further 24 hr, and then evaporated to dryness, re-dissolved in water and purified on HPLC on preparative C₁₈ column, using a gradient elution of acetonitrile in 0.2% acetic acid 30-50% during 15 min., flow 6 ml/min. The purified conjugate **20** was dried under reduced pressure and stored at - 20°C.

(ii) Synthesis of conjugate **21**

[0184] Conjugate **20** (4 mg) was dissolved in 50%-aqueous methanol and aqueous solutions of copper acetate (2 mg) and sodium ascorbate (2 mg) were added. The reaction was completed in 2 min. (monitored by spectrophotometry). The product was purified on RP-18 cartridge (Lichrolut, Merck), first, using water to wash out unreacted copper acetate and ascorbate, and then methanol for the elution of the main compound, conjugate **21**, which is collected and evaporated (UV-VIS Spectrum: 418 and 538 nm in water).

Example 9. [Reference compound] Synthesis of conjugate **22**

[0185] Conjugate **20** (4 mg), obtained in Example 8(i) above, and gadolinium acetylacetonate (10 mg) were heated in imidazole (0.3 g) at 210°C, as previously described (Horrocks et al.,

1978). The reaction was completed in 50 min. (monitored by spectrophotometry). After sublimation of imidazole, the product was re-dissolved in water and purified on HPLC, as described in Example 8(i).

Example 10. Synthesis of conjugate 23

[0186] Conjugate 23 was prepared starting from the synthesis of compound 10.

(i) Synthesis of compound 10

[0187] Pd-Bpheid a (compound 7) (100 mg) was dissolved in N-methylpyrrolidone (1 ml) and 3-amino-2-propanediol (405 mg) and the solution was mixed during 3 hours at room temperature under argon atmosphere. The product 10 was purified on HPLC using YMC-C18 preparative column with 0.2% acetic acid/acetonitrile. Yield: 86%. Analysis was performed on LC-MS using YMC-C18 analytical column with ammonium acetate, pH 4.5/acetonitrile. ESI-MS positive mode, 805 m/z.

(ii) Synthesis of conjugate 23

[0188] Compound 10 (50 mg), NHS (80 mg) and DCC (216 mg) were dissolved in dry N,N-dimethylformamide (8 ml). The solution was stirred for 90 min at room temperature under argon atmosphere. The active ester formed was purified on HPLC using YMC-C18 preparative column with 0.2% acetic acid/acetonitrile, analyzed on LC-MS using YMC-C18 analytical column with ammonium acetate, pH 4.5/acetonitrile, and identified by mass spectroscopy: ESI-MS positive mode, 902 m/z.

[0189] The active ester (10 mg) was dissolved in dry N-methylpyrrolidone (1 ml). CycloRGDfK (8 mg) and triethylamine (10 μ l) were added and the solution was stirred for 75 min. The product was purified on HPLC using YMC-C18 preparative column with 0.2% acetic acid/acetonitrile. Yield: 50%. Analysis was performed on LC-MS using YMC-C18 analytical column with ammonium acetate pH 4.5/acetonitrile: ESI-MS positive mode, 1393 m/z.

Example 11. Synthesis of conjugate 24

[0190] Compound 8 (100 mg) was activated with NHS (70 mg) and N-cyclohexylcarbodiimide-N'-methyl polystyrene (120 mg) in DMF (5 ml). The solution was stirred at 50°C during 15 hours and filtered through a sinter glass. CycloRGDfK (100 mg) was dissolved in DMF (5 ml) containing N-methylmorpholine (100 μ l) and added to the filtrate. The mixture was stirred under argon atmosphere at room temperature for 24 hours, the solvent was evaporated in

vacuum, and the product **24** was purified on HPLC using YMC-C18 preparative column with ammonium acetate pH 4.5/acetonitrile. Yield: 23%. Analysis was performed on LC-MS with YMC-C18 analytical column under the same conditions. UV-VIS spectrum (HPLC): 332, 386, 516, and 750 nm. ESI-MS positive mode, 1425 m/z.

Example 12. Synthesis of conjugate **26**

[0191] To the Fmoc-protected GRGDSP-resin (0.35 mmol), a mixture of compound **25** (530 mg, 0.7 mmol), HOBT, PyBOP (both 0.7 mmol) and DIEA (2.1 mmol) in 6 ml of DMF was added, and the reaction was agitated during 2 h under argon atmosphere. After washings with DMF (10 x 5 ml) and DCM (5 x 5 ml), the resin was dried in vacuum for at least 3h. The peptide-conjugate was then cleaved from the resin and deprotected (Arg, Pbf; Asp, OtBu) using a cocktail solution of 85:5:5:5 TFA/thioanisole/H₂O/triisopropylsilane (TIS) (10 ml) for 10 min at 0°C and then 1h at room temperature under Ar atmosphere. The resin was filtered and washed with the cocktail solution (4 ml) and the combined filtrate was evaporated by a stream of N₂ to about half of its volume. Upon addition of cold Et₂O (30 ml), a dark precipitate appeared. Centrifugation and decantation of the Et₂O layer and additional treatment with cold Et₂O (2 x 30 ml) afforded the crude dark solid, which was further purified by RP-HPLC (264 mg; 58%). Analysis was performed on LC-MS using YMC-C18 analytical column with ammonium acetate pH 4.5/acetonitrile: ESI-MS positive mode, 1306 m/z.

Example 13. Synthesis of conjugates **28-31**

[0192] The title compounds were prepared starting from the synthesis of the unmetalated Bpheid-cycloRGDfK conjugate **27**, as follows.

(i) Solid phase synthesis of cycloRGDfK

[0193] Fmoc-C^α-allyl protected aspartic acid was attached on 2-chlorotrityl chloride resin. Next, glycine, N^G-Pbf arginine, N^ε-Dde lysine, and phenylalanine were attached on the resin by usual Fmoc chemistry, forming fKRGD peptidyl-resin. Then, the N-terminal Fmoc group was removed with 2%-piperidine/DMF, and the C^α-allyl group on aspartic acid residue was removed with tetrakis(triphenylphosphine) palladium and 1,3-dimethylbarbituric acid (DMBA) in DCM. The peptide was cyclized in the presence of HOBT/PyBOP and DIEA. The ε-amine of the lysine residue was cleaved with 4%-hydrazine/DMF.

*(ii) Synthesis of conjugate **27***

[0194] Bpheid (**3**, 0.6 mmol) was bound to ϵ -NH₂-Lys on the fKRGD peptidyl-resin (0.3 mmol) in DMF using PyBOP/HOBt (0.6 mmol) as coupling agents and DIEA (1.8 mmol) as a base, thus obtaining conjugate **27**.

(iii) Synthesis of conjugates 28-31

[0195] Conjugate **27** (0.1 mmol) was treated on the resin with the appropriate amine in Table 1 (5-6 mmol) in DMF at room temperature during 2 h. Then, the amine excess was washed off, the product was disconnected from the resin, deprotected with the TFA-containing cocktail, and finally purified by RP-HPLC. Analysis was performed on LC-MS using YMC-C18 analytical column with ammonium acetate pH 4.5/acetonitrile. The results are shown in Table 1.

Table 1. Yield and ESI-MS of Conjugates 28-31

Conjugate	Amine	Yield, mg (%)	ESI-MS (+), m/z
28	bis(3-aminopropyl)amine	71 (53)	1327
29	3-amino-1,2-propanediol	63 (49)	1287
30	N-(2-aminoethyl)morpholine	75 (56)	1326
31	1,4-bis(3-aminopropyl)piperazine	75 (54)	1396

Example 14. Synthesis of conjugate 32

[0196] Conjugate **32** was obtained by coupling peptidylamine cycloRGDK-NH₂ (obtained as described in Material and Methods) and Bpheid a (**3**) in DMF solution in the presence of DCC, followed by Pbf and O-tBu deprotection with TFA. The product was purified by RP-HPLC. Yield: 53%. Analysis was performed on LC-MS using YMC-C18 analytical column with ammonium acetate pH 4.5/acetonitrile: ESI-MS positive mode, 1135 m/z.

Example 15. Synthesis of conjugate 33

[0197] Conjugate **33** was obtained by conjugating compound **8** with the linear peptide GRGDSPK (obtained as described in Material and Methods) similarly to the method described for conjugate **24** in Example 11. Yield: 55%. Analysis was performed on LC-MS using YMC-C18 analytical column with ammonium acetate pH 4.5/acetonitrile: ESI-MS positive mode, 1537 m/z.

Example 16. Synthesis of conjugate 34

[0198] Conjugate **34** was obtained by conjugating compound **8** with the linear peptide (GRGDSP)₄K (obtained as described in Material and Methods) similarly to the method described for conjugate **24** in Example 11. Yield: 41%. Analysis was performed on LC-MS using YMC-C18 analytical column with ammonium acetate pH 4.5/acetonitrile. MALDI-MS positive mode, 3291 (M+2Na) m/z.

Example 17. Synthesis of conjugate **35**

[0199] Conjugate **35** was obtained by conjugating compound **8** with cycloRGDf-N(Me)K (obtained as described in Material and Methods) similarly to the method described for conjugate **24** in Example 11. Yield: 58%. Analysis was performed on LC-MS using YMC-C18 analytical column with ammonium acetate pH 4.5/acetonitrile: ESI-MS positive mode, 1439 m/z.

Example 18. Synthesis of conjugate **36**

[0200] Conjugate **36** was obtained by conjugating compound **8** with the cyclic dimer peptide (cycloRGDyK)₂ (obtained as described in Material and Methods) similarly to the method described for conjugate **24** in Example 11. Yield: 27%. Analysis was performed on LC-MS using YMC-C18 analytical column with ammonium acetate pH 4.5/acetonitrile. MALDI-MS positive mode, 2245 (M+2Na) m/z.

Example 19. Synthesis of conjugate **37**

[0201] The conjugate **37** was synthesized from Pd-Bpheid (compound **7**) and the peptide RGD. The peptide was prepared by the solid phase procedure by coupling of Fmoc-Arg (Pbf)-Gly-OH to a resin bound H-Asp-O-Allyl residue.

(i) Preparation of protected dipeptide Arg-Gly

[0202] A solution of Fmoc-Gly-OH (4.162 g; 14 mmol) and DIEA (9.755 g; 56 mmol) in 100 ml of dry DCM was stirred with 10 g of 2-chlorotriyl chloride resin (1.4 mmol/g) for 1h at room temperature (rt). The Fmoc group was removed by treatment with 5% piperidine in DMF/DCM (1:1), followed by 20% piperidine in DMF. Then, Fmoc-Arg (Pbf)-OH (18.17 g; 28 mmol) in DMF (130 ml) was activated with HOBt (4.29 g; 28 mmol) and DIC (4.34 ml; 28 mmol) for 15 min at rt and added to the reaction vessel. The mixture was stirred for 2h at rt. The peptidyl-resin was washed and dried in vacuum for 3h. The protected dipeptide was cleaved from the resin by stirring with a cocktail solution of AcOH/2,2,2-trifluoroethanol (TFE)/DCM (1:1:3) for 1h

at rt. Upon treatment with cold Et₂O (1 l), the oily residue solidified. Filtration and washings with cold Et₂O afforded the white precipitate (8.64 g; 87.5%) with homogeneity of about 99% (HPLC).

(ii) Synthesis of the tripeptide RGD

[0203] Attachment of the third amino acid to the dipeptide obtained in step (i) above started by stirring 2-chlorotrityl chloride resin (0.5 g; 1.4 mmol/g) with a solution of Fmoc-Asp-O-Allyl (138.4 mg; 0.35 mmol) and DIEA (244 μ l; 1.4 mmol) in DCM during 1h at rt to give a loading of about 0.7 mmol/g. Then, the resin was washed and Fmoc was removed as described above. Fmoc-Arg (Pbf)-Gly-OH (371 mg; 0.525 mmol), HOBt (80.4 mg; 0.525 mmol) and DIC (81 μ l; 0.525 mmol) were dissolved in 2.5 ml DMF and stirred at rt for 20 min. The resulting solution was added to the washed H-Asp-O-Allyl-resin, and the mixture was agitated for 2h at rt. The peptidyl-resin was washed, and Fmoc was removed.

(iii) Synthesis of conjugate 37

[0204] A mixture of compound 7 (268 mg; 0.375 mmol), HOBt (57.4 mg; 0.375 mmol) and DIC (58 μ l; 0.375 mmol) in 3 ml of DMF was stirred for 30 min at rt and added to an aliquot of Fmoc-deprotected tripeptidyl-resin obtained in (ii) above (about 0.125 mmol). The mixture was agitated for 2h at rt, and the conjugate of 7 with the linear tripeptide RGD was obtained. This reaction and all following operations with modified peptidyl-resin were performed in Argon atmosphere in the dark. After washing, the resin was treated with ethylenediamine (251 μ l; 375 mmol) in DMF during 1h at rt, then washed. In order to remove the allyl-protecting group, the resin was reacted with a solution of [(C₆H₅)₃P]₄Pd⁰ (87 mg; 0.075 mmol) and DMBA (137 mg; 0.875 mmol) in DCM during 2h at rt.

[0205] On-resin cyclization was accomplished by binding the deprotected Asp residue to the ethylenediamino moiety using a solution of PyBOP (195 mg; 0.375 mmol) and DIEA (131 μ l; 0.75 mmol) in DMF for 2h at rt. The resin was washed and dried in vacuum for 3h. The peptide conjugate was cleaved from the resin using a cocktail solution TFA/Thioanisole/H₂O/TIS/EDT (82.5:5:5:5:2.5) for 10 min at 0°C and then 1h at rt. Upon the addition of cold Et₂O (25 ml), a dark solid was obtained. The crude product (95 mg) was purified by RP-HPLC to give 2 mg of pure (98%) cyclic RGD conjugate 37. ESI-MS 1087 (M+H) m/z.

Example 20. Synthesis of conjugate 38

[0206] The synthesis was carried out on a 0.175 mmol scale using the same procedure as described in Example 19, but starting from the compound Bpheid 3 instead of Pd-Bpheid 7.

The crude product (160 mg) was purified by RP-HPLC to give 17 mg of pure (98%) cyclic RGD conjugate **38**. ESI-MS 982 (M+H) m/z.

Example 21. Synthesis of conjugate 39

[0207] The procedure is similar as in Example 19, but 1,4-bis(3-aminopropyl)-piperazine was used for "bridge"-formation between the Bpheid residue and the Asp-residue instead of ethylenediamine. The crude product (158 mg) was purified by RP-HPLC to give 12.5 mg of pure (99%) cyclic RGD conjugate **39**. ESI-MS 1122 (M+H) m/z.

Example 22. Synthesis of conjugate 40

[0208] Conjugate **40** was obtained by a method similar to that described for conjugate **24**, but using the linear RGD-peptidomimetic 5-(6-guanidino-hexanoylamino)-pentanoic acid (RGD-PM1). Yield: 42%. Analysis was performed on LC-MS using YMC-C18 analytical column with ammonium acetate pH 4.5/acetonitrile: ESI-MS positive mode, 1123 m/z.

Example 23. Synthesis of conjugate 41

[0209] Conjugate **41** was obtained by a method similar to that described for conjugate **24**, but using the linear RGD-peptidomimetic 1-(4-guanidino-butyryl)-piperidine-3-carbonyl]-amino]-heptanoic acid (RGD-PM2). Yield: 66%. Analysis was performed on LC-MS using YMC-C18 analytical column with ammonium acetate pH 4.5/acetonitrile: ESI-MS positive mode, 1220 m/z.

Example 24. Synthesis of conjugate 42

[0210] Conjugate **42** was obtained by a method similar to that described for conjugate **24** in Example 11, but using the peptide cycloRADfK. Yield: 30%. Analysis was performed on LC-MS using YMC-C18 analytical column with ammonium acetate pH 4.5/acetonitrile: ESI-MS positive mode, 1439 m/z.

Example 25. Synthesis of conjugate 43

[0211] The title compound was prepared starting from the synthesis of the Bacteriophage-173-(cycloRGDfK)amide conjugate 27, as described in Example 13.

[0212] Conjugate 27 (0.1 mmol) was treated on the resin with an 1,3-propylene diamine (6 mmol) in DMF at room temperature during 2 h. Then, the amine excess was washed off, and DTPA dianhydride (0.2 mmol) and triethylamine (100 ml) in anhydrous DMF (30 ml) was added. After 1-h agitation under argon atmosphere, distilled water (50 ml) was added, followed by additional agitation for 30 min. The product 43 was disconnected from the resin, deprotected with the TFA-containing cocktail, and finally purified by RP-HPLC (61 mg, 37%). Analysis was performed on LC-MS using YMC-C18 analytical column with water/acetonitrile. ESI-MS negative mode, 1643 m/z.

Example 26. Synthesis of conjugate 44

[0213] Gadolinium chloride (0.1 mmol) in a sodium acetate buffered aqueous solution (0.1 N, pH 5.5) was added into a solution of conjugate 43 (6 μ mol) in 2 mL of DMF. The mixture was allowed to stand at ambient temperature for overnight with stirring. The formation of the metal chelates was verified by LC-MS (1799 m/z). The reaction mixture was evaporated, and the product was purified on a RP-18 cartridge (Lichrolut, Merck), first using water to wash out non-reacted gadolinium salt, and then methanol for the elution of the main compound, conjugate 44, which was collected and evaporated (8 mg, 73%).

II. BIOLOGICAL SECTION

Materials and Methods

[0214]

1. (i) ***Eu-labeled RGD-4C***. RGD-4C (20 nmole in 10 μ l DDW) was added to 100 μ l of K-phosphate buffer (0.1 M, pH 8.5) containing isothiocyanatophenyl-DTPA-Eu (150 nmole, 50 μ l). The mixture was incubated overnight at room temperature with constant stirring. To terminate the reaction, 1 μ l of Tris-Cl (1 M, pH 7.5) was added, the mixture was stirred for 5 min, then loaded on Sep-Pak C-18 cartridge and washed with DDW to elute the free Eu. The column was then washed with 50% aqueous ethanol, fractions (250-500 μ l) were collected and their fluorescence measured.

In Vitro Studies

[0215]

- (ii) ***Cell culture***. Mouse embryonic heart endothelial cells (H5V) monolayers were cultured in

Dulbecco's modified Eagle's medium (DMEM)/F12 containing 25 mM HEPES, pH 7.4, 10% fetal calf serum (FCS), 2 mM glutamine, 0.06 mg/ml penicillin and 0.1 mg/ml streptomycin at 37°C, in 8% CO₂. Human umbilical vein endothelial cells (HUVEC) were maintained in M199 medium (with glutamine and EARLE's salts) containing 10 mM HEPES, pH 7.4, 20% heat inactivated FCS (56°C, 30 min), 2 mM glutamine, 50 mg/ml gentamycin, 25 µg/ml endothelial cell growth factor (ECGF), 5 IU/ml heparin at 37°C, in 5% CO₂. H5V cells were kindly provided by Dr. Annunciata Vecchi, Istituto Mario Negri, Milan, Italy. HUVEC cells were obtained from Rambam Medical Center, Haifa, Israel.

(iii) Solubilization of sensitizers, peptides and their conjugates for *in vitro* cell culture experiments. Water-soluble compound **8** and conjugate **11** were dissolved in culture medium (DMEM/F12) or 10% FCS in medium or 10 µM BSA in medium or PBS prior to use, as described for each experiment. Water insoluble compounds (RGD-4C, cycloRGDfK, compound **10** and conjugate **23**) were dissolved in 100% DMSO before use and diluted in culture medium or PBS to a final DMSO concentration of 2% v/v. Compound **24** was dissolved in 100% DMSO before use and diluted in saline to a final DMSO concentration of 5% v/v.

(iv) Light source. The light source for *in vitro* studies was home-built 100-W halogen lamp equipped with a high-pass filter ($\lambda > 650$ nm, Safelight filter 1A Eastman Kodak Co., Rochester, NY, USA) and a 4-cm water filter. The lamp was used to illuminate (20 mW/cm²/10 min (12 J/cm²)) the culture plates from the bottom at room temperature in a dark room.

(v) Phototoxicity assay of the RGD peptide-photosensitizer conjugates. To determine the pigment photodynamic efficacy *in vitro* under standard conditions, cells were cultured in 96-well plates and preincubated for 15 or 90 min at 37°C or 4°C, according to the indicated experiment protocol, with 0-25 µM conjugated or non-conjugated photosensitizer in different media conditions (culture medium DMEM/F12; 10% FCS in medium or 10 µM BSA in medium) in the absence or presence of excess free peptide (100 fold up to 1 mM). The cells were washed and illuminated (20 mW/cm² for 10 min). Plates were placed back in the culture incubator for 24 h. Cell survival was determined using Neutral Red cell viability assay. Cell survival was calculated as the percent of the dye accumulated in the untreated controls. Triplicate determinations were conducted and representative experiments are shown. Three kinds of controls were used: (i) light control: cells illuminated in the absence of pigments; (ii) dark control: cells treated with pigments but kept in the dark; and (iii) untreated cells that were kept in the dark.

(vi) Neutral Red cell viability assay. Following photosensitization and a 24-h incubation period (37°C), cell survival was determined by Neutral Red (Fluka Chemie, Buchs, Switzerland) accumulation. After subtraction of assay blanks, net optical density (570 nm) was computed as the average value of triplicates determinations. Cell survival was calculated as the percent of the dye accumulated in the untreated controls.

(vii) Cell detachment (rounding) assay: H5V cells were cultured as monolayers in 3-cm dish for 24-48 h, and further incubated for 1 h with 100 µM RGD-4C at 4°C or 37°C. The cells were washed once and re-incubated for three hours with fresh culture medium at 37°C. In the same

fashion, HUVEC were cultured as monolayers in 6-well plate pre-coated with gelatin for 48 h, and incubated for 1 h with 100 μ M RGD-4C at 37°C. The cells were washed once and re-incubated for 24 h with fresh culture medium at 37°C. The morphological changes of the cells were documented using light microscopy.

In Vivo Studies

[0216]

(viii) Animals: Male CD1 nude mice (8-week old, ~30g) were housed and handled with free access to food and water in the animal facility according to the guidelines (1996) of the Institutional Animal Care and Use Committee of the Weizmann Institute of Science, Rehovot, Israel.

(ix) Xenograft, graft and metastases tumor models. Cultured rat C6 glioma cell monolayers were scraped under saline with a rubber policeman. Single-cell suspensions of rat C6 glioma ($2-4 \times 10^6$ cells/mouse, 50 μ l) were implanted subcutaneously (s.c.) on the backs of the mice. The glial cell strain, C6, was cloned from a rat glial tumor induced by N-nitrosomethylurea after a series of alternate culture and animal passages. Tumors reached treatment size, i.e. diameter of 7-9 mm, within 2-3 weeks. Rat C6 glioma cells were kindly provided by Prof. Michal Neeman, Weizmann Institute of Science, Rehovot, Israel.

[0217] Cultured BALB/c CT26luc colon carcinoma cell monolayers transfected with luciferase were scraped under saline with a rubber policeman. Single-cell suspensions of CT26luc ($2-4 \times 10^6$ cells/mouse, 50 μ l) were implanted subcutaneously (s.c.) on the backs of the mice. CT26 is an N-nitroso-N-methylurethane-(NNMU) induced, undifferentiated colon carcinoma cell line. It was cloned to generate the cell line designated CT26WT, which was stably transduced with luciferase to obtain the lethal subclone CT261uc. Tumors reached treatment size, i.e. diameter of 7-9 mm, within 1.5-2 weeks. CT26luc cells were kindly provided by Dina Preise, Weizmann Institute, Rehovot, Israel.

[0218] Cultured BALB/cfC3H 4T1luc mammary gland tumor cell monolayers transfected with luciferase were scraped under saline with a rubber policeman. Single-cell suspensions of 4T1luc ($2-4 \times 10^6$ cells/mouse, 50 μ l) were implanted subcutaneously (s.c.) on the backs of the mice. 4T1 is a 6-thioguanine resistant cell line selected from the 410.4 tumor without mutagen treatment, which was stably transduced with luciferase to obtain the lethal subclone 4T1luc (kindly provided by Shimrit Ben-Zaken, Weizmann Institute, Rehovot, Israel). Tumors reached treatment size, i.e. diameter of 7-9 mm, within 1 week.

[0219] Cultured metastatic human breast cancer MDA-MB-231 cell (ATCC, USA) monolayers were scraped under saline with a rubber policeman. Single-cell suspensions of rat human breast cancer ($2-4 \times 10^6$ cells/mouse, 50 μ l) were implanted s.c. on the backs of the mice. Tumors reached treatment size, i.e. diameter of 7-9 mm, within 1 week.

[0220] Cultured human OVCAR-8 ovarian adenocarcinoma cell monolayers (kindly provided by Prof. Mordechai Liscovitz, Weizmann Institute, Rehovot, Israel) were scraped under saline with a rubber policeman. Single-cell suspensions of human OVCAR-8 ovarian adenocarcinoma ($2-4 \times 10^6$ cells/mouse, 50 μ l) were implanted s.c. on the backs of the mice. OVCAR-8 are derived from a chemotherapy-treated patient with a metastatic disease. Tumors reached treatment size, i.e. diameter of 7-9 mm, within 3-4 weeks.

[0221] Cultured MLS human carcinoma cell monolayers (kindly provided by Prof. Michal Neeman, Weizmann Institute, Rehovot, Israel) were scraped under saline with a rubber policeman. Single-cell suspensions of human MLS cells ($2-4 \times 10^6$ cells/mouse, 50 μ l) were implanted s.c. on the backs of the mice. Tumors reached treatment size, i.e. diameter of 7-9 mm, within one week.

[0222] *Groin metastases.* Cultured CT26luc cells (1×10^6 cells/mouse, 20 μ l) collected in saline were s.c. injected in the distal dorsal foot of the hindleg of anesthetized mice. When the needle was injected below the skin, the handle of the syringe was withdrawn to verify that it had not penetrated a blood vessel. In this way, systemic dissemination of tumor cells was avoided. Primary tumors grew to a size of 6-8 mm within 3 weeks. Metastases in the groin were inspected using Xenogen IVIS® Imaging System as described herein and by palpation.

[0223] *Lung metastases model.* Cultured CT261uc or 4T1luc cells ($0.8-1 \times 10^6$ cells/mouse, 300 μ l) collected in saline were i.v.-injected in the tail vein of anesthetized mice. Lung metastases in the lungs were inspected using Xenogen IVIS® Imaging System as described herein, 2-3 weeks after cells injection.

[0224] The mice were sacrificed (according to the guidelines of the Weizmann Institute of Science) when tumors reached the diameter of ≥ 15 mm.

(x) Anesthesia: Mice were anesthetized by an intraperitoneal (i.p.) injection of a mixture of 50 μ l ketamine (100 mg/ml; Rhone Merieux, Lyon, France) and xylazine (2%; Vitamed, Benyamina, Israel) (85:15, vol:vol).

(xi) Light source: The light source for *in vivo* studies is a 763 nm or 755 nm diode laser (1W; Ceramoptec, Bonn, Germany) according to the photosensitizer in use.

(xii) Solubilization of sensitizers and their conjugates for animal experiments. The water-soluble conjugate **11** was dissolved in PBS prior to use. The water-insoluble conjugate **24** was dissolved in 100% DMSO before use and diluted in saline or PBS to a final DMSO concentration of 5% v/v.

(xiii) Biodistribution of Pd-containing compounds. Anesthetized mice were i.v. injected (tail vein) with the different photosensitizer (pigment) conjugates (control group: untreated). The mice were sacrificed at indicated time points and samples of the indicated organs and tissues (blood, tumor, intestine, liver, spleen, kidneys, testies, heart, lung, brain, skin, muscle and fat) were placed in pre-weighted vials and immediately frozen and stored at -20° in the dark until analyzed. Two methods were used for sample preparation: (1) Each sample was thawed and homogenized in DDW (1:10 w/v). Aliquots of the homogenate (500 μ l) were lyophilized in Eppendorf test tubes. Then, 60 μ l of HNO_3 (70%, TraceSelect, Fluka) were added to each dry sample, incubated for 1 h at 90°C and diluted with DDW to 3 ml. (2) Each sample was diluted (1:2 w/v) in HNO_3 (70%, TraceSelect, Fluka). The samples were sonicated for 30 min in boiled water, and left for at least 48 h at room temperature. Then, 140 μ l from each sample was added to 3.36 ml DDW to give total volume of 3.5 ml and incubated for 1 h at 90°C . Pd concentrations were determined by ICP-MS.

(xiv) Inductively-Coupled Plasma Mass Spectrometry (ICP-MS) was performed for determination of Pd concentrations using an ELAN-6000 instrument (Perkin Elmer, CT).

(xv) In Vivo Fluorescence Optical Imaging System: The planar fluorescence optical imaging system used was Xenogen IVIS[®] Imaging System 100 Series equipt with a 1-inch CCD camera cooled to -105°C . The field-of-view was 15 cm. The Xenogen IVIS[®] Imaging System is a highly sensitive, low light-level system optimized for *in vivo* (whole, living animals) imaging. The IVIS Imaging System is a modular software and hardware system. Two images were taken; the first image is black and white, providing a photograph of the animal. The second image is a colored overlay of the emitted photon data, in the present case the NIR fluorescence of the compound (680-720 nm excitation filter and a 780-810 nm emission filter) or bioluminescence (560 nm) as described below. The CCD integration time was 10-20 sec in order to maintain a high signal-to-noise ratio. Dynamic fluorescence images were acquired immediately following the injection of a conjugate of the invention and continued for approximately 2 hours. Fluorescence images were also obtained under isoflurane anesthesia for up to 72 hr after initial injection of the conjugate. The injected dose varied from 140 to 250 nmol per animal. The CCD integration time was 20 sec in order to maintain a high signal-to-noise ratio. After completion of the image acquisition, data analysis and processing were accomplished by the Living Image[®] software that supports hardware for IVIS Imaging System 100 Series. Living Image[®] software is a custom software package developed by Xenogen that runs the IVIS System and provides tools for image display and analysis.

(xvi) Luciferin assay. Localization and viability of CT26luc and 4T1luc tumor cells transplanted in mice were accurately assessed by *in vivo* bioluminescence imaging (BLI). According to the present invention, BLI relies on the light-emitting properties of the reporter enzyme firefly luciferase, which catalyses the transformation of its substrate D-luciferin into oxyluciferin leading to the emission of photons. Luciferin is a chemical substance found in the cells of various bioluminescent organisms. When luciferin is oxidized under the catalytic effects of luciferase and ATP, a bluish-green light is produced. Firefly luciferin is a particularly good reporter for *in vivo* biophotonic imaging due to properties of its emission spectra. The emission

peak of firefly luciferase (560 nm) is contained within the spectrum of visible light and can be detected and quantified with low light imaging systems such as the IVIS system. Prior to imaging, mice were injected intraperitoneally with D-luciferin (for whole body imaging: 55 mg/kg of body weight; for lungs and lymph node metastases imaging: 77 mg/kg of body weight). *In vivo* images were acquired with the Xenogen IVIS® Imaging System 100 Series and analyzed with the Living Image® 2.5 software. Luciferin can be used in a number of ways. It can be used to monitor light production *in vivo*, and can be monitored with a Xenogen IVIS® Imaging System.

(xvii) PDT Protocol. CD-1 nude male mice bearing the different tumor xenografts were anesthetized and **24** (5-24 mg/kg body weight) or **8** (9 mg/kg body weight) were i.v. injected via the tail vein. The tumors were trans-cutaneously illuminated after 3.5, 6, 8, 12 and 24 hours for 5-30 min at light doses of 30-360 J/cm². Intensity of illumination: 100-200 mW/cm². After treatment, the mice were returned to the cage. The mice were considered cured if tumor free for 90 days after treatment. Mice were euthanatized when the tumor diameter reached 15 mm. The controls used were: (1) dark control, the mice were i.v.-injected with pigment and not illuminated; (2) light control, mice were illuminated without pigment injection; (3) untreated control; (4) compound **8** alone: the mice were i.v. injected with **8** and illuminated after indicated time point. (5) Mixture of **8** and cycloRGDfK: the mice were i.v. injected with mixture of **8** with cycloRGDfK and illuminated after indicated time point. (6) cycloRGDfK alone: the mice were i.v. injected with cycloRGDfK and illuminated after indicated time point. Images were taken at indicated time post PDT.

(xviii) MRI measurements. Conventional spin-echo images are acquired before contrast agent administration, in order to localize the tumor. IR snap images were obtained before and 2, 5, 10, 20 and 30 min after injection of **9**. The parameters used for IR snap imaging were: TR/TE = 9.2/2.7 ms, field of view (FOV) = 5 cm, number of experiments (NEX) = 1, image matrix = 128x128, slice thickness 2 mm, and a 10° flip angle. A series of seven images, using inversion times of 0.05s, 0.25s, 0.4s, 1.8s, 2.5s, 3.6s, and 5s were used for T1 evaluation.

Example 26. Evaluation of binding parameters and biological activities of the cyclic peptide RGD-4C

[0225] The binding parameters and biological activities of the cyclic nonapeptide RGD-4C were characterized in order to test its suitability for vascular photosensitizer targeting.

Characterization of RGD-4C binding activity

[0226]

- (i) Preparation of Eu-labeled RGD-4C.** The binding parameters characteristics for the $\alpha_v\beta_3$ integrin receptor expressed on endothelial cells (affinity, specificity and number of receptors/cell) were determined using time resolved emission spectroscopy with Eu-labeled RGD-4C. To this end, RGD-4C was labeled with Eu by direct conjugation of isothiocyanatophenyl-DTPA-Eu as described in Material and Methods. The separation of Eu-RGD-4C from free isothiocyanatophenyl-DTPA-Eu was carried out using Sep-Pak C-18. The column was washed with 50% aqueous ethanol, fractions were collected and their fluorescence measured as described in Materials and Methods. An additional wash with 100% ethanol did not reveal the retention of any significant amount of Eu-containing material in the column. The final product, Eu-RGD-4C, was quantitatively eluted as a single peak (**Fig. 3A**), as confirmed by mass-spectra analysis (1499 m/z) (**Fig. 3B**).
- (ii) $\alpha_v\beta_3$ integrin receptor binding assay.** The binding activity of Eu-RGD-4C to the integrin receptor was determined using mouse H5V endothelial cells in culture. For the binding assay, H5V cells were plated in 48-well plate (10^5 /well) for 48 h. The plates were incubated at 4°C (in order to inhibit receptor endocytosis), washed once with ice cold binding buffer (0.1% BSA in DMEM:F-12) and incubated for 2 h with increasing concentrations of Eu-RGD-4C in the absence (total binding) or presence of 1 μ M RGD-4C (non specific binding). The incubation was terminated by triple washing with ice cold binding buffer, and enhancement solution was added (300 μ l/well) in order to lyse the cells and release the chelated Eu. Samples (200 μ l) were taken from each well and fluorescence was determined using time-resolved fluorometry. Net specific binding was calculated by subtraction of non-specific from total values for each concentration. The percentages of non-specific binding from total added ligand were $4.9\% \pm 2.4\%$ (mean \pm SD). The ratio of total binding to non-specific binding increased from ~ 1 at low ligand concentrations to ~ 4 at the highest concentration. The binding results and the Scatchard analysis are presented in **Fig. 4** and **Fig. 5**, respectively, for a representative experiment.

The values for the binding parameters of the ligand were calculated from the Scatchard analysis: ($1/K_d=K_a$, the tested compound's affinity) and B_{max} (the maximal number of binding sites) were 37.2-41.3 nM, and 4.3-7.7 nM (1-1.8 million receptors per cell), respectively. Thus, Eu-RGD-4C binds specifically to H5V endothelial cells. These results confirm reports by others that RGD-4C is a potent ligand for $\alpha_v\beta_3$ integrin receptor (affinity constant of ~ 100 nM). Specific binding to $\alpha_v\beta_3$ integrin receptor was further demonstrated using isolated $\alpha_v\beta_3$ binding assay as follows.
- (iii) Solid-phase receptor assay.** The binding of Eu-RGD-4C to isolated $\alpha_v\beta_3$ integrin receptor was determined using time-resolved fluorometry. Each well of a microtiter plate (Nunc MaxiSorb) was coated with 50 μ l of purified receptor (1 μ g/ml in PBS) by shaking at 4°C overnight. The receptor solution was then removed, and each well was blocked with 200 μ l of milk (1% w/v milk powder in PBS, 1 hr, room temperature). The plate was then washed with 200 μ l of PBS once, and incubated for 1 h at 37°C with increasing concentrations of RGD-4C in the presence of constant amount of Eu-RGD-4C (10 million F.U./well). The ligand/competitor solution was removed and each well was washed three times with 200 μ l PBS. Enhancement solution was added (200 μ l/well) to release the

chelated Eu. Samples (100 μ l) were taken from each well and fluorescence was determined using time-resolved fluorometry (**Fig. 6**). Under these experimental conditions, 100 μ M of RGD-4C reduced by 50% Eu-RGD-4C binding to the isolated receptor. This value represents the highest attenuation of the Eu-RGD-4C binding, even at RGD-4C highest concentrations.

Characterization of RGD-4C biological activity

[0227] The biological effect of RGD-4C binding was characterized in H5V cells and Human Umbilical Vein Endothelial Cells (HUVEC) using the cell-rounding assay described in Materials and Methods. The morphological changes of the cells were documented using light microscopy. As seen in **Fig. 7B**, RGD-4C at a concentration of 100 μ M induced 99% H5V endothelial cell detachment from the dish ($n=200$), whereas only 5% rounded cells were observed in the absence of RGD-4C (see **Fig. 7A**). This effect was reversible as the cells recovered following 3 h re-incubation with fresh culture medium (8% rounded cells in dishes with previous presence of RGD-4C versus 6% in the absence of RGD-4C).

[0228] Similarly to H5V cells, 100 μ M RGD-4C induced HUVEC detachment from the dish in a reversible manner, since the cells recovered following 24 h re-incubation with fresh culture medium (**Fig. 8**: upper panels show HUVEC cell detachment in the presence of increasing concentrations of RGD-4C (0-200 μ M) while the lower panels show recovery of the cells 24 h after replacement of the medium with a fresh one).

[0229] Thus, the effect of RGD-4C is a reversible one since removal of RGD-4C by extensive washing and subsequent maintenance of the tested endothelial cells in culture for 3 h (H5V) or 24 h (HUVEC), results in complete recovery of their adhesive capacities.

Example 27. Binding, cellular uptake and localization in vitro of conjugate 24

[0230] The binding pattern of the RGD-BChI conjugates is of great importance in understanding their mode of action. Conjugate **24** presents a detectable NIR fluorescence and its cellular binding and localization was determined *in vitro* using fluorescence microscopy. Cultured H5V endothelial cells were incubated with 25 μ M **24** in DMEM/F12 medium with 10% FCS for 2 hours at 37°C. The cell culture was then washed, and PBS++ was added. Using custom made fluorescence microscope, **24** was excited at 520 nm and the emitted fluorescence was detected at 780 nm.

[0231] As shown in **Fig. 9**, conjugate **24** penetrated into endothelial cells and concentrated around the nucleus in granule-like structures.

[0232] For comparison purposes, the cellular uptake of non-conjugated compound **8** was measured. Cultured H5V cells were incubated with 25 μ M **24** or **8** in DMEM/F12 medium with 10% FCS or 75%FCS for 20 minutes or 2 hours at 37°C. The cell culture was then washed, and PBS++ was added. Excitation was carried out at 520 nm and emitted fluorescence detection at 780 nm. **Fig. 10** demonstrates that the conjugate cellular uptake was faster than that of compound **8**.

[0233] Notably, high serum concentrations (75% vs. 10% FCS) attenuate the cellular uptake of conjugate **24**. Quantitative structure function relationship studies done in our group emphasized the role of photosensitizer structure in the interactions with serum proteins. These studies suggest that there is an active involvement of serum albumin in the trafficking of compound **8** both into and out of the treated cells. Further, the cellular uptake of **8**, clearance and phototoxicity are mediated by BSA molecules that undergo continuous receptor mediated up-take and secretion. Regarding conjugate **24**, the affinity of the bacteriochlorophyll moiety to serum albumin modifies the conjugate bioavailability to the integrin receptor $\alpha_v\beta_3$. This can explain the observed decrease in cellular accumulation in the presence of high serum protein concentrations (**Fig. 10**). The higher *in vitro* accumulation of conjugate **24** compared to compound **8** at each time point that was tested could be explained by the fact that the RGD conjugate can enter the cell by integrin receptor mediated endocytosis or/and by non specific endocytosis like the non-conjugated **8**.

Example 28. *In vivo* biodistribution of conjugate **24 and compound **8****

[0234] The conjugates of the invention are potential drug carriers. Therefore, their *in vivo* biodistribution is of great importance. In order to quantify the conjugate levels in target tissues, Ion Coupled Plasma-Mass Spectroscopy (ICP-MS) was used for tracing the central M atom (e.g., Pd, Cu) in the target organ. The stable binding of the central metal atom enables monitoring and accurate determination of the time dependent concentration of the compound in the target organs. Biodistribution of conjugate **24** and of compound **8** was determined in CD1-nude male mice with tumor xenografts of rat C6 glioma as described in Materials and Methods, using method (2) for sample preparation. Biodistribution of **24** was also determined in CD1-nude male mice bearing tumor grafts of mouse CT26luc colon carcinoma and CD 1-nude male mice bearing tumor grafts of mouse of 4T1luc mammary cancer.

[0235] The results, as shown in **Figs. 11A-11D**, indicate accumulation of conjugate **24** in the different tumor tissues up to 8 hours post injection accompanied by continuous decrease of the conjugate levels in the blood. Moreover, the biodistribution pattern of **24** appears independent of the tumor's origin (rat C6 glioma (**Fig. 11A**), mouse CT26luc colon carcinoma (**Fig. 11B**), and mouse 4T1 carcinoma of the breast (**Fig. 11C**).

[0236] The biodistribution of compound **8** injected to CD1 nude mice with tumor xenografts of rat C6 glioma presented a completely different picture as shown in **Fig. 12**: compound **8** cleared rapidly from the subject and at no time showed selective accumulation or retention in

the tumor tissue. The accumulation of conjugate **24** in the tumor tissue, with maximal values at 8 h post injection, as opposed to compound **8** (Fig. 12), indicates that the potential drug carrier **24** can be used for drug targeting purposes and can be applied for imaging of tumors and angiogenesis.

[0237] Moreover, it is to be noted that the concentrations of accumulated conjugate within the tumor tissue reached the μM level, whereas labeled cycloRGDFK and cycloRGDFK conjugated to other metal chelators were reported by others to reach concentrations only in the nM range (Haubner et al., 2001; Janssen et al., 2002a; Janssen et al., 2002b; Temming, 2005). These reported results demonstrate rapid tumor up-take of the conjugated peptides with maximal peak concentration at 30 min, 1 hour or 2 hours post injection, depending on the conjugate structure. Thus, the markedly increased tumor uptake of the conjugates of the invention compared to either M-Bchl derivative alone or GRD-containing peptide conjugated to other chelators, can be attributed to the conjugation of the RGD-containing peptide to the Bchl moiety.

[0238] The relative levels of **24** in the tumor tissue and blood are illustrated in Fig. 11D, and it is shown that while 8 hours post injection the conjugate reached maximum concentration in the tumor, at 24 hours post injection its concentration in the tumor relative to the blood and surrounding normal tissue, is still sufficiently high to enable a selective vascular-targeted imaging (VTI) and possibly vascular-targeted PDT (VTP).

[0239] It is to be noted that the concentration of the conjugate in the tumor tissue relative to other organs was significantly lower in tumors where the cells are known not to express $\alpha_v\beta_3$ integrin (e.g. CT26luc). Thus, the observed accumulation in $\alpha_v\beta_3$ negative tumors is probably due to their vascular up-take.

Example 29. In vivo biodistribution of conjugate **15**

[0240] The biodistribution of Cu-conjugate **15** was determined in female CD-1 nude mice of 6-8 weeks-old, weighing 20-23 g and bearing 6-9-mm³ tumors of human adenocarcinoma cells obtained from breast tissue (MDA-MB-231 cells). The conjugate (30 mg/ml in 5%DMSO/PBS) was injected to the tail vein, and the animals were sacrificed in selected time points. Cu concentrations were determined by ICP-MS as described in Material and Methods. The ICP-MS results after the subtraction of time 0 are shown in Fig 13.

[0241] The obtained data showed an obvious accumulation of **15** in tumor with a peak at 8-12 h after injection of about 3-fold intensity in comparison with surrounding normal tissue.

Example 30. In vivo biodistribution of conjugate **42**

[0242] In order to assess the actual role of RGD/integrin recognition, the biodistribution of the conjugate **42**, in which glycine in the peptide is replaced with alanine, was measured and compared to the biodistribution of conjugate **24**. The substitution of only one amino acid was demonstrated by others to interfere with the integrin recognition (Pierschbacher and Ruoslahti, 1987). Mostly, RAD or RGE peptides were used for this purpose. The biodistribution assay was performed as described in Example 26 above using CD1 nude male mice with tumor grafts of mouse CT261uc colon cancer cells, and Pd concentrations were determined by ICP-MS. The ICP-MS results are shown in **Fig 14A**.

[0243] Comparison between the biodistribution of conjugate **24** and the conjugate **42** (**Fig. 14B**) demonstrates that RGD conjugate uptake in tumor tissue was faster than that of RAD conjugate and to a higher extent up to 24 hours. Conjugate **24** accumulated in the tumor tissue with maximal peak concentration at 8 hours post injection accompanied by a continuous decrease of the conjugate levels in the blood, while the concentrations of **42** in the tumor tissue and blood 8 hours post injection are quite the same. Importantly, both conjugates presented a prolonged basal level after administration due to non-specific binding. However, the accumulation of the RGD conjugate in the tumor site was twice as much compare to the RAD conjugate.

Example 31. In vivo fluorescence imaging of mice bearing rat C6 glioma xenografts following treatment with conjugate **24 or compound **8****

[0244] Dynamic fluorescence images were obtained from CD-1 nude male mice bearing rat C6 glioma xenografts. The fluorescence images were acquired using IVIS system as described in Materials and Methods. Clearance of the injected photosensitizers (compound **8** or conjugate **24**) was measured in mice by fluorescence imaging and is demonstrated in **Fig. 15**. Mice bearing rat C6 glioma xenografts on the back of the right posterior limb were injected with 200 nmol dose of conjugate **8** (mice in upper pictures) or 200-nmol dose of **24** (mice in lower pictures), and images were taken at 4, 24, 48 and 72 hours post-injection.

[0245] Except for a residual fluorescence from the liver and spleen, no specific signal could be seen from the animal treated with the compound **8** at times longer than 4 hours post injection in agreement with the ICP-MS data (**Figure 12**). Conjugate **24** appears to accumulate in the tumor, spleen, liver and a fat hump below the animal head. These imaging results, when combined with the ICP-MS results, suggest that the best time window for imaging and probably treatment of the tumor by VTP is at 8-24 hours after drug administration.

Example 32. Dynamic fluorescence imaging of mice bearing mouse CT26luc colon cancer grafts transfected with luciferase following treatment with conjugate **24**

[0246] Cell lines transfected with luciferase generate visible light in the presence of luciferin

when alive. The luciferin luminescence enables to monitor viable tumor cells and thus provides the means to validate the conjugate's homing at the tumor site, its imaging capability and the efficacy of VTP.

[0247] To avoid the theoretical possibility of conjugate excitation by the luciferin bioluminescence, the fluorescence images were recorded and only then the animals were i.p. injected with luciferin and the bioluminescence of the transfected tumor cells was detected.

[0248] The results show that there is a complete overlap between the region of NIR fluorescence signal coming from conjugate **24** and the region of endogenous bioluminescence signal that originates in the tumor cells themselves.

[0249] Dynamic fluorescence images were obtained from CD-1 nude male mice bearing grafts of mouse CT26luc colon cancer transfected with luciferase, following the intravenous injection of an integrin receptor targeting conjugate **24**. **Figs. 16B-16C** depict fluorescence and luminescence images of a mouse bearing a graft on the back of the right posterior limb, 24 hours after injection of 200-nmol dose of conjugate **24**. The fluorescence and luminescence images were acquired using Xenogen IVIS® Imaging System as described in Material and Methods.

[0250] The results show that there is a complete overlap between the region of NIR fluorescence signal coming from conjugate **24** and the region of endogenous bioluminescence signal that originates in the tumor cells themselves.

Example 33. Dynamic fluorescence imaging of mice bearing 4T1luc mammary cancer grafts transfected with luciferase following treatment with conjugate 24

[0251] Dynamic fluorescence images were obtained from BALB/c female mice bearing grafts of mouse 4T1luc mammary cancer transfected with luciferase, following the intravenous injection of an integrin receptor targeting conjugate **24**. **Figs. 17A-17C** show photographs fluorescence and luminescence images of two female mice bearing a subcutaneous mouse 4T1 mammary gland cancer transfected with luciferase grafts on the back of the right posterior limb, 24 hours after the injection of 200-nmol dose of conjugate **24**. The fluorescence and luminescence images were acquired using IVIS system as described in Material and Methods.

[0252] The results show that there is a complete overlap between the region of NIR fluorescence signal coming from conjugate **24** and the region of endogenous bioluminescence signal that originates in the tumor cells themselves.

Example 34. Dynamic fluorescence of mice bearing ovarian carcinoma (MLS) following treatment with conjugate 26

[0253] Conjugate **26** (8 mg/kg) was i.v. injected into animals bearing MLS ovarian carcinoma. Images on IVIS were taken after 8 and 14 hours. As shown in **Fig. 18**, the conjugate did not present accumulation after 8 hours, but at 14 hours a high level of fluorescence was observed in tumor and liver areas.

Example 35. Fluorescence imaging demonstration of *in vivo* binding specificity of conjugate **24 to $\alpha_v\beta_3$ integrin receptor**

[0254] Specific binding is defined as one inhibited by the unconjugated sensitizer. Thus, in order to demonstrate the *in vivo* binding specificity of conjugate **24**, attempts to block its accumulation were carried by competing with free cycloRGDfK for binding of the same binding sites. Fluorescence imaging was performed 24 hours after administration of 140 nmol of conjugate **24** alone (**Fig. 19**, left mouse on both panels, with tumor on the back of the right posterior limb), or administration of 140 nmol of conjugate **24** 1 hour after injection of excess "free" (8.5 μ mol) cycloRGDfK peptide to mice bearing C6 glioma xenografts (**Fig. 19**, right mouse on both panels, with tumor on the back of the left posterior limb). Fluorescence images of the blocked receptor xenografts with the same exposure time are illustrated in **Fig. 19** on the same linear color scale to allow for a qualitative comparison. The fluorescence intensity originating from the tumor was larger when conjugate **24** was administered alone as compared to when the peptide cycloRGDfK was administered one hour prior to imaging agent administration. In normal tissues, the uptake was not influenced by the pre-administration of cycloRGDfK.

[0255] The results show that the uptake of conjugate **24** in tumor regions were: (i) significantly greater than in the contralateral normal tissue regions; and (ii) blocked by pre-injection of cycloRGDfK in excess. Taken together, one can conclude that "free" cycloRGDfK inhibits the accumulation of conjugate **24**, and the reduced uptake of conjugate **24** resulting from pre-administration of cycloRGDfK in excess validates the *in vivo* molecular specificity of the conjugate to $\alpha_v\beta_3$ receptors.

Example 36. Dynamic fluorescence imaging following treatment with conjugate **42**

[0256] In order to assess the actual role of RGD/integrin recognition *in vivo*, dynamic fluorescence images were obtained from CD-1 nude male mice bearing CT26luc grafts on the back of the posterior limb, 24 hours after the administration of conjugate **24** (**Fig. 20**, left mouse in each panel) or conjugate **42**, in which glycine in the peptide is replaced with alanine (cycloRADfK); right mouse in each panel). Since the fluorescence signal of the RGD conjugate at the tumor tissue reaches a maximum at 3.5-4 hours post injection, images are presented taken 4 hours post injection. Importantly, both conjugates present a prolonged basal level of fluorescence after administration due to non-specific binding. However, the fluorescence intensity of the RGD conjugate is clearly higher than that of the RAD conjugate in the tumor

site. These results are supported quantitatively by ICP-MS measurements showing almost twice as much accumulation of the RGD conjugate in the tumor tissue (see Example 30 above and Fig. 14A).

[0257] Since the CT26luc cells lack $\alpha_v\beta_3$ (although they likely express some $\alpha_v\beta_5$) (Yao et al., 2005; Borza et al., 2006), the higher fluorescence of **24** from the tumors probably originates in their ligation (via the RGD tripeptide) to the neoendothelial $\alpha_v\beta_3$ integrins.

[0258] Fig. 21 depicts the fluorescence images of CD1 nude mice bearing tumors that originate in human ovary adenocarcinoma OVCAR-8, mouse colon cancer CT261uc, human epithelial ovarian carcinoma MLS, and mouse mammary carcinoma 4T1luc cell lines, 24 h after administration of conjugate **24**. Integrin $\alpha_v\beta_3$ is expressed on some types of solid tumor cells. Regarding the cell lines above, MLS (Schiffenbauer et al., 2002), and 4T1luc (Mi et al., 2006), overexpress integrin $\alpha_v\beta_3$ receptors on their cell surface, while mouse CT26luc lack integrin $\alpha_v\beta_3$ receptors, but express some $\alpha_v\beta_5$ (Yao et al., 2005; Borza et al., 2006), and OVCAR-8 lack α_v integrins (Ross et al., 2000). Indeed, the fluorescence signal was significantly higher for integrin $\alpha_v\beta_3$ positive cells (MLS and 4T1luc) compared to integrin $\alpha_v\beta_3$ negative cells (CT261uc and OVCAR-8), probably due to additional accumulation in the tumor cells themselves. The observed difference between the compound accumulation in the two $\alpha_v\beta_3$ negative tumors (CT261uc and OVCAR-8) probably reflects (i) a difference in their neovascularization since they both lack the $\alpha_v\beta_3$ integrins, (ii) might be due to additional accumulation in the CT26luc tumor cells themselves, since they express $\alpha_v\beta_5$ that can binds specifically the RGD-BChI conjugate.

Example 37. Dynamic fluorescence imaging of lung metastases

[0259] Detection of a 4T1luc model of breast cancer metastases in the lungs was enabled by conjugate **24**, 24 h post injection into BALB/c female mouse (15 mg/kg) (Fig. 22). These results show that the uptake of **24** in metastatic regions in the lungs can be monitored by fluorescence at relatively high accuracy.

[0260] Next, CT26luc model metastases in the lungs were detected as a function of time post **24** injection (4, 9 and 24 h, 15 mg/kg; Figs. 23A-23I). CD-1 nude male mice bearing CT26luc lung metastases that were not injected with the conjugate served as controls (Figs. 23G.23H) and a CD-1 nude male mouse without lung metastases that was i.v. injected with conjugate **24** (Fig. 23I). The fluorescence imaging results show that the uptake of **24** in metastatic regions was significantly higher than by the surrounding normal tissue regions, with best tumor to background ratio at 24 hours after administration.

Example 38. Dynamic fluorescence imaging of lymph node metastases

[0261] CD-1 nude male mouse bearing CT26luc primary tumor on the back of its left leg and metastases in the near lymph node, was imaged and photographed 24 hours after the i.v. injection of conjugate **24** (15 mg/kg). Detection of the CT26luc metastases in the lymph node was aided by localization of conjugate **24**. The black & white photograph, bioluminescence signal originated from the reaction of luciferin with the luciferase transfected tumor cells, and the fluorescence image of the mouse are shown in **Fig. 24**.

[0262] These results indicate that tumors in both primary and metastatic regions (lungs, lymph nodes) can be monitored by fluorescence at relatively high accuracy.

Example 39. *In vivo* magnetic resonance imaging (MRI) of mice bearing rat C6 glioma xenografts using compound **9 as a contrast agent**

[0263] Measurements were performed on CD1 nude male mice (average weight ~30 g) bearing the C6-glioma xenografts (10-15 mm diameter; left flank, subcutaneous). Seven mice were used for MRI enhanced with Mn-13²-OH-Bpheid (compound **9**) (15 µmol/kg).

[0264] Calculated graphs of signal intensity ratio and relaxivity ratio revealed that compound **9** at a dose of 15 µmol/kg increased the tumor/normal relaxivity ratio from 0.8-1.0 up to -1.4, in about 10 min after injection of the substance. The contrast effect obtained with **9** was higher than that known for Gd-containing contrast agents.

[0265] Taking the higher contrast obtained by compound **9** in comparison with Gd agents and the expected prolonged residence of the corresponding Mn-containing cycloRGDfK conjugate **12** in the tumor, that enables long integration of the MR signal, we anticipate superior imaging with this conjugate over other contrast agents such as Gd-DTPA.

Example 40. *In vitro* targeted phototoxicity

[0266] In order to evaluate the photodynamic potency of the RGD peptide-photosensitizer conjugate versus that of the non-conjugated photosensitizer, the phototoxicity of conjugate **23** and the unconjugated photosensitizer **10** were determined by monitoring the survival of cultured H5V endothelial cells following PDT.

[0267] H5V cells were incubated for 90 min at 37°C with 0-25 µM of conjugate **23** or compound **10** in different media conditions, illuminated and their survival was determined using Neutral Red viability assay as described in Materials and Methods. The dose-response survival curves of the H5V cells treated with the photosensitizers under different conditions are shown in **Figs. 25A-25C**: 10% FCS in medium (**Fig. 25A**), culture medium DMEM/F12 (**25B**) and 10 µM BSA in medium (**25C**).

[0268] The phototoxic effects of conjugate **23** and compound **10** in different media were found to be light- and drug concentration-dependent. Based on the LD₅₀ values we can conclude that the photodynamic potency of the conjugate **23** is higher than that of the non-conjugated photosensitizer **10**.

[0269] Targeted phototoxicity is defined as one inhibited by the free ligand. Thus, further experiments attempted to block phototoxicity by administration of the free cycloRGDfK, which competes for the cellular binding of conjugate **23**. H5V cells were incubated for 90 min at 37 °C with 0-25 µM of compound **10** or conjugate **23** in different media (10% FCS in medium or 10 µM BSA in medium) in the absence or presence of free excess cycloRGDfK (100-fold up to 1 mM). The cells were illuminated and cell survival was determined using Neutral Red viability assay, as described above.

[0270] As shown in Figs 26A-26D, presenting the dose-response survival curves of treated cells, and as indicated by the LD₅₀ values presented in Table 2, the phototoxic effects of **23** and **10** were not influenced by the presence of excess cycloRGDfK.

Table 2. LD₅₀ values of conjugate **23 and compound **10** in absence and presence of free peptide in excess in different reaction conditions**

Compound Reaction Conditions	Conj. 23	Conj. 23 with free peptide in excess	Comp. 10	Comp. 10 with free peptide in excess
10µM BSA in medium (90 min, 37°C)	0.5-1µM (Figs. 16C, 17D)	1µM (Fig. 17D)	3.5-5µM (Figs. 16C, 17B)	5µM (Fig. 17B)
culture medium (90 min, 37°C)	1µM (Fig. 16B)	Not done	7µM (Fig. 16B)	Not done
10% FCS (90 min, 37°C)	1-4µM (Figs. 16A, 17C)	4µM (Fig. 17C)	5-7µM (Figs. 16A, 17A)	5µM (Fig. 17A)
10% FCS (15 min, 37°C)	3.5µM (Fig. 18A)	2.4µM (Fig. 18A)	Not done	Not done
10% FCS (15 min, 4°C)	20µM (Fig. 18B)	8µM (Fig. 18B)	Not done	Not done

[0271] These results suggest that the conjugate is entering the cell via integrin-independent fluid-phase endocytosis, thus the free cycloRGDfK cannot compete for the cellular binding with the conjugate. The integrin-independent cell entry can be attributed to either parts of the conjugate, the photosensitizer moiety or the cycloRGDfK peptide. There is one report in the literature indicating that cycloRGDfK internalizes by an integrin-independent fluid-phase endocytosis that does not alter the number of functional integrin receptors on the cell surface (Hart et al., 1994; Castel et al., 2001).

[0272] In order to test the endocytosis theory and since the endocytic process is time- and temperature-dependent, H5V cells were incubated at 37°C and 4°C for 15 min with 0-20 µM of

conjugate **23** in medium containing 10% FCS, in the presence or absence of excess cycloRGDfK (100-fold up to 1 mM). Cells were illuminated and their survival was determined as described above. The dose-response survival curves of the treated H5V cells are shown in **Figs. 27A-27B**.

[0273] The LD₅₀ values measured for 15-min incubation at 37°C or 4°C increased relatively to the values obtained upon incubation of the cells at 37°C for 90 min (**Table 2**). The LD₅₀ values of conjugate **23** changed to 3.5 μM and to 20 μM following 15-min incubation at 37°C and 4°C, respectively, compared to 1 μM obtained for incubation at 37°C for 90 min. The increase in LD₅₀ values upon lowering the temperature supports the hypothesis of a possible role for endocytosis in the conjugate uptake.

[0274] Unexpectedly, not only the photocytotoxic effect of conjugate **23** was unblocked by the presence of excess cycloRGDfK, but in fact, the photodynamic activity of **23** under 15-min incubation at 37°C or 4°C was higher in the presence of free cycloRGDfK. There is a possibility that the excess of free peptide causes the cells to be more sensitive to the PDT effect of the conjugate due to enhanced detachment of the cells from the dish and/or induced apoptotic signal transduction.

[0275] The phototoxicity of conjugate **24** was determined by monitoring the survival of cultured H5V endothelial cells following PDT. H5V cells were incubated for 2 hours at 37°C with 0-25 μM conjugate **24** in culture medium DMEM/F12 with 10% FCS. The cells were illuminated and their survival was determined as described above.

[0276] As shown in the dose-response survival curve (**Fig. 28**), the phototoxic effects of conjugate **24** on H5V cells after 2 hr incubation at 37°C were found to be light- and drug concentration-dependent.

[0277] The phototoxicity of a third conjugate, **11**, and of compound **8** was also determined using H5V endothelial cells. Cells were incubated for 90 min at 37°C in the presence of 0-20 μM conjugate **11** or compound **8** in 10 μM BSA in medium, illuminated and their survival was determined as described above.

[0278] As shown in the dose-response survival curve (**Fig. 29**), the phototoxic effects of conjugate **11** and compound **8** were found to be light- and drug concentration-dependent. The LD₅₀ values are represented in **Table 3**.

Table 3. LD₅₀ values of conjugate **11 and compound **8** in absence and presence of free peptide excess**

Compound Reaction Conditions	Conj. 11	Conj. 11 with free peptide excess	Comp. 8	Comp. 8 with free peptide excess
10μM BSA in	7-10μM	5μM	1.8-2μM	2μM

medium (90 min, 37 °C)	(Figs. 19, 20)	(Fig. 20)	(Figs. 19, 20)	(Fig. 20)
---------------------------	-------------------	-----------	----------------	-----------

[0279] As for the cycloRGDfK peptide, blockage of the phototoxicity of conjugate **11** by adding free cyclic RGD-4C to the cell culture failed (Figs. 30A-30B, Table 3). H5V cells were incubated for 90 min at 37°C with 0-10 µM conjugate **11** or compound **8** in 10 µM BSA in medium in the absence or presence of RGD-4C in excess (1 mM). The cells were illuminated and their survival was determined as described above.

[0280] Again, this result suggests that the photosensitizer's moiety (compound **8**) determines the cellular uptake of the conjugate **11** via free endocytosis.

Example 41. In vivo PDT in rat C6 glioma tumor using conjugate **24**

[0281] Based on the results above we developed a new treatment protocols for PDT of solid tumors using conjugate **24**. The protocol parameters should include: *Time of treatment (drug-light interval)*- Illumination 3 to 24 hours post-drug administration; *Dose (mg/kg)* - 5-24 mg/kg; *Duration of illumination (min)*- 5-30 min; *Intensity of illumination (mW/cm²)* - 100-200 mW/cm²; *Delivered energy (J/cm²)*- 30-360 J/cm².

[0282] The initial tumor models used comprised rat C6 glioma tumor xenografts, since these tumor cells express $\alpha_v\beta_3$ (Zhang et al., 2006) and $\alpha_v\beta_5$ integrins (Milner et al., 1999) in addition to integrin $\alpha_v\beta_3$ expressed on the tumor neovasculature.

[0283] CD-1 nude male mice bearing C6 glioma grafts were i.v. injected with 15 or 24 mg/kg body doses of conjugate **24** or 9 mg/kg body dose of compound **8**.

[0284] For each protocol we used at least 3 animals, but due to high mortality rate we were left with limited number of animals. The results are presented in Table 4.

Table 4. Therapeutic results of different VTP protocols applying conjugate **24 to mice bearing rat C6 glioma.**

Time to treatment (hours)	Dose (mg/kg)	Duration of illumination (min)	Intensity of illumination (mW)	Delivered energy (J/cm ²)	comments	No. of animals
3.5	15	5	100	30	Extensive necrosis	2
6	15	10	100	60	Extensive necrosis	2
8	15	5	100	30	Limited necrosis	2

Time to treatment (hours)	Dose (mg/kg)	Duration of illumination (min)	Intensity of illumination (mW)	Delivered energy (J/cm ²)	comments	No. of animals
8	15	10	100	60	Limited necrosis	1
8	24	10	100	60	Limited necrosis	1
8	24	10	100	60	Extensive necrosis	1
8	15	15	100	90	Extensive necrosis	1

[0285] The protocols that appeared optimal and provided the best therapeutic results appear in bold in **Table 4**: 15 mg/kg, 15-min illumination (90 J/cm²) 8 hours post injection, and 24 mg/kg, 10-min illumination (60 J/cm²) 8 hours post injection.

[0286] **Figs. 31A and 31B** show the therapeutic results of those protocols, respectively. In dark control (**Fig. 31C**), the mice were i.v. injected with conjugate **24** and not illuminated; In light control (**Fig. 31D**), mice were illuminated without conjugate **24** injection; and in unconjugated photosensitizer control (**Fig. 31E**), the mice were i.v. injected with compound **8** and illuminated after 8 hours.

[0287] The different controls showed no PDT effect. In contrast, the animals treated with conjugate **24** and light presented extensive edema few hours post PDT treatment that developed to inflammation and necrosis below the skin at 3 days post PDT. Tumor flattening and long period of tumor regression as well as wound healing was observed.

Example 42. In vivo PDT in mouse CT26 colon tumor using conjugate **24**

[0288] Using the rat C6 glioma model we could not get immediate assessment of VTP outcome, a major disadvantage in course of a screening process. To overcome this problem we used the mouse CT26luc colon carcinoma model consisting of luciferase transfected cells, which enable fast evaluation of the therapeutic effect.

[0289] CD-1 nude male mice bearing CT26luc tumors were subjected to different protocols of PDT with conjugate as shown in **Table 5**.

Table 5. Therapeutic results of different VTP protocols applying conjugate **24 to mice bearing mice CT26luc colon cancer.**

Time to treatment (hrs)	Dose (mg/kg)	Duration of illumination (min)	Intensity of illumination (mW)	Delivered energy (J/cm ²)	Comments	No. of animals
8	9	15	100	90	Reduction in luminescence signal, no necrosis	3
8	9	10	100	60	Reduction in luminescence signal, no necrosis*	5
8	11	10	100	60	Reduction in luminescence signal, extensive necrosis	4
8	12	10	100	60	Reduction in luminescence signal, extensive necrosis	3
8	15	10	100	60	Reduction in luminescence signal, extensive necrosis	4
12	15	15	100	90	Reduction in luminescence signal, limited necrosis*	5
24	15	30	200	360	Reduction in luminescence signal, no necrosis*	3
24	15	30	100	180	Reduction in luminescence signal, no necrosis	2
24	24	30	100	180	Reduction in luminescence signal, no necrosis	2
24	24	30	150	270	Reduction in luminescence signal, no necrosis	2
24	24	30	200	360	Reduction in luminescence signal, limited	2

Time to treatment (hrs)	Dose (mg/kg)	Duration of illumination (min)	Intensity of illumination (mW)	Delivered energy (J/cm ²)	Comments	No. of animals
					necrosis	

[0290] Figs. **32A-E** show the therapeutic results of applying 15 mg/kg, 10 min illumination (60 J/cm²), 8 hours post injection of conjugate **24** to mice bearing CT26Luc tumors (bolded protocol in **Table 5**). **32A** - conjugate **24** was i.v. injected 15 mg/kg, 10 min illumination (60 J/cm²) 8 hours post injection; **32B** - overlaid images taken after i.p. injection of luciferin to the mouse described in **32A**, using the IVIS system. The first image is black and white, which gives the photograph of the animal. The second image is color overlay of the emitted photon data. All images are normalized to the same scale. **32C** - Bioluminescence signal quantification (photon/sec/cm²) of the data shown in B. **32D** - control with compound **8** alone: the mice were i.v. injected with compound **8** and illuminated after 8 hours. **32E** - control with mixture of compound **8** and cycloRGDfK: the mice were i.v. injected with mixture of compound **8** with cycloRGDfK and illuminated after 8 hours. **32F** - control with cycloRGDfK alone: the mice were i.v. injected with cycloRGDfK and illuminated after 8 hours. Images were taken at indicated time post PDT.

[0291] Fig. **32B** are overlaid images taken with the IVIS system after i.p. injection of luciferin to the mouse depicted in Fig. **32A**. Fig. **32C** provides quantitative description of the bioluminescence shown in Fig. **32 B**. The controls used were (1) compound **8** alone (Fig. **32D**); (2) mixture of unconjugated compound **8** and cycloRGDfK (Fig. **32E**); and (3) cycloRGDfK alone (Fig. **32F**). The different controls showed no PDT effect. In contrast, the animals treated with the targeted conjugate developed necrosis within 4 days post PDT (Fig. **32A**). Significant bioluminescence signal from residual tumor cells appear 8 days post PDT (Fig. **32B**), although no tumor was palpated or visually detected. Wound healing and tumor flattening were observed in all responding animals.

[0292] Fig. **33** shows the Kaplan-Mayer curve for the protocols indicated in the Table 5 with asterisk.

Example 43. Tumor diagnosis and PDT treatment of breast tumors with conjugate 13

[0293] Human breast cancer MDA-MB-231 cells (ATCC) were transfected with red fluorescent protein (RFP) as follows.

[0294] *Plasmids* - the plasmid that was used for the transfection of the cells was pDsRed-Monomer-Hyg-C1 (Clontech, Palo Alto, CA) that carries the RFP gene and resistance gene for hygromycin in which the DsRed-Monomer gene was replaced with pDsRed2 (from the pDsRed2-N1 plasmid).

[0295] Transfection process - For the transfection process, Lipofectamine™ 2000 (Invitrogen) was used according to the manufacturer protocol: 4 µg DNA were incubated for 5 min with 250 µl Opti-MEM medium (supplied by the manufacturer Invitrogen). In a separate test tube, 10 µl of Lipofectamine were incubated for 5 min with 250 µl Opti-MEM medium. After incubation, the DNA and Lipofectamine solutions were mixed and incubated for 20 min at room temperature and the content was evenly scattered on one out of a 6-well plate that was 50-60% confluent with the MDA-MB-231 cells.

[0296] Selection of stable clone - 24hr after the transfection of the MDA-MB-231 cells, the plate was checked under a fluorescence microscope (Nikon). A transient transfection was detectable at this stage. The medium was replaced with fresh medium containing antibiotics (hygromycin) at a concentration of 250 µg/ml. When the plates reached confluency, the cells were detached from the culture plate following a 30-60 sec treatment with trypsin, and plated in a 96-well plate at a concentration of 0.5 cells/well. Wells that contained one clone only and the clone was fluorescent, were collected and plated in a 6-well plate. After reaching confluency they were further plated in a 10 cm plate. **Figs. 34A-34B** show the fluorescent MDA-MB-231 RFP clone 3 (resistant to hygromycin) after 1 sec and 3 sec exposure, respectively.

[0297] For the PDT experiments, MDA-MB-231 RFP cells (4×10^6) were implanted subcutaneously on the backs of the mice and tumors developed to the treatment size (6-8 mm) within 2-3 weeks.

[0298] PDT Protocol: Anaesthetized mice were i.v. injected with conjugate **13** (7.5 mg drug/kg body weight). The tumors were illuminated for 10 min. The drug light interval used was 8hr post drug injection. Transdermal illumination through the mouse skin with 755 nm diode laser at 100 mW/cm² (CeramOptec, Germany) was used. After the treatment, the mice were returned to the cage. In the dark control group, the mice were i.v. injected with the sensitizer conjugate **13** and placed in dark cage for 24hr. In the light control group, the mice were illuminated for 10 min with 100mW/cm². During the first 2 days post PDT, as needed, the mice received analgesia (2.5 mg/kg Flunixin daily) and 3 days Oxycodone in the drinking water. The end point of animal survival is when the size of the tumor reaches 10% of animal weight. Mice are sacrificed at this time (up to 90 days) by cervical dislocation.

[0299] Figs. 35A-35B show two representative examples to local response of human MDA-MB-231-RFP to PDT. Mice with MDA-MB-231-RFP xenografts (~0.5 cm³) on their backs were i.v. injected with 7.5 mg/kg of conjugate **13** and illuminated 8 h later through the mouse skin with 755nm diode laser at 100mW/cm². **35A** - Photographs taken from day 0 (before treatment) and after treatment at 1, 4, 7, 12 and 90 days. By day 4 partial necrosis was seen, by day 7 tumor flattening was observed, after 90 days the wound healed and the animal was cured. **35B** - In vivo whole-body red fluorescence imaging of CD-1 nude male mice bearing MDA-MB-231-RFP orthotopic tumor. No signal was detected 90 days after treatment.

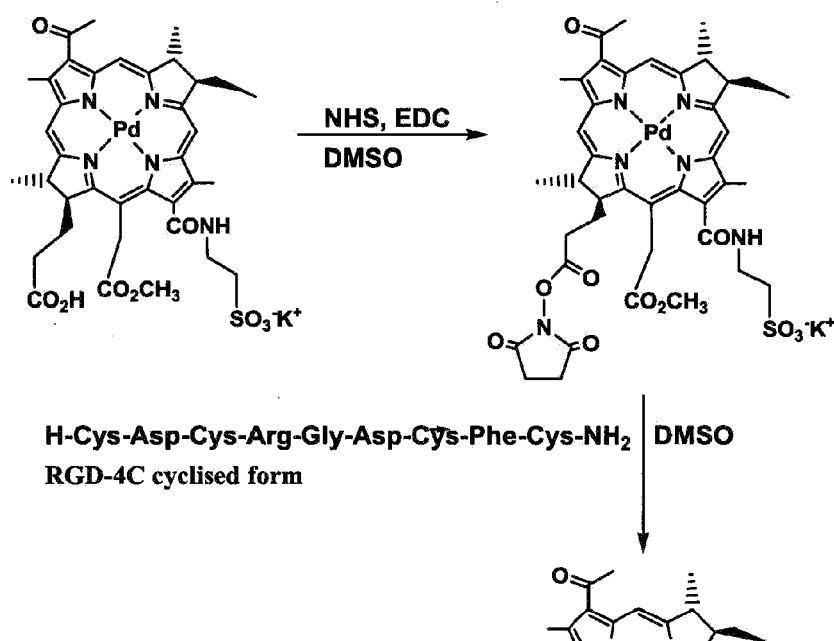
[0300] In order to study the accumulation of the photosensitizer in primary mammary tumors, the MDA-MB-231-RFP cells (4×10^6) were implanted orthotopically in the mammary pad of the mice. Tumors developed to the wanted size, bigger than 1 cm^3 , within 3-4 weeks.

[0301] For the accumulation assessment, mice were anesthetized by i.p. injection of 30 μl mixture of 85:15 ketamine: xylazine, and received an i.v. injection to the tail vein of 15 mg drug/kg body weight conjugate **13**. Fluorescence of both tumor cells and conjugate **13** are monitored by IVIS®100 Imaging system (Xenogen). Tumor imaging main filter set comprised: excitation filter 500-550 nm, emission filter 575-650 nm; Background filter set for subtraction the tissue auto fluorescence: excitation filter 460-490 nm, emission filter 575-650 nm. Photosensitizer imaging main filter set: excitation filter 665-695 nm, emission filter 810-875 nm.

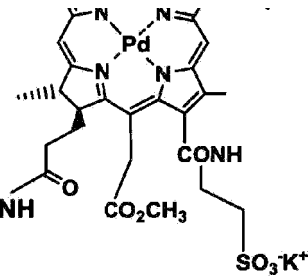
[0302] Images were taken at these time points post drug injection: 15 min, 1, 2, 3, 4.5, 6, 7.5, 9, 24 hr, 2, 3, 4, 5, 6, 7 days. The results are shown in Figs. 36 and 37.

[0303] Fig. 36 shows accumulation of conjugate **13** in orthotopic human breast MDA-MB-231-RFP primary tumor (tumor size $\sim 1 \text{ cm}^3$). Images were taken from 15 min to 24 hr post drug injection. Top panel - In vivo whole-body red fluorescence imaging of CD-1 nude female mice bearing MDA-MB-231-RFP orthotopic tumor. Bottom panel - In vivo whole-body NIR fluorescence imaging of conjugate **13** accumulation. The drug shows no specific accumulation in the tumor during the first 24 h.

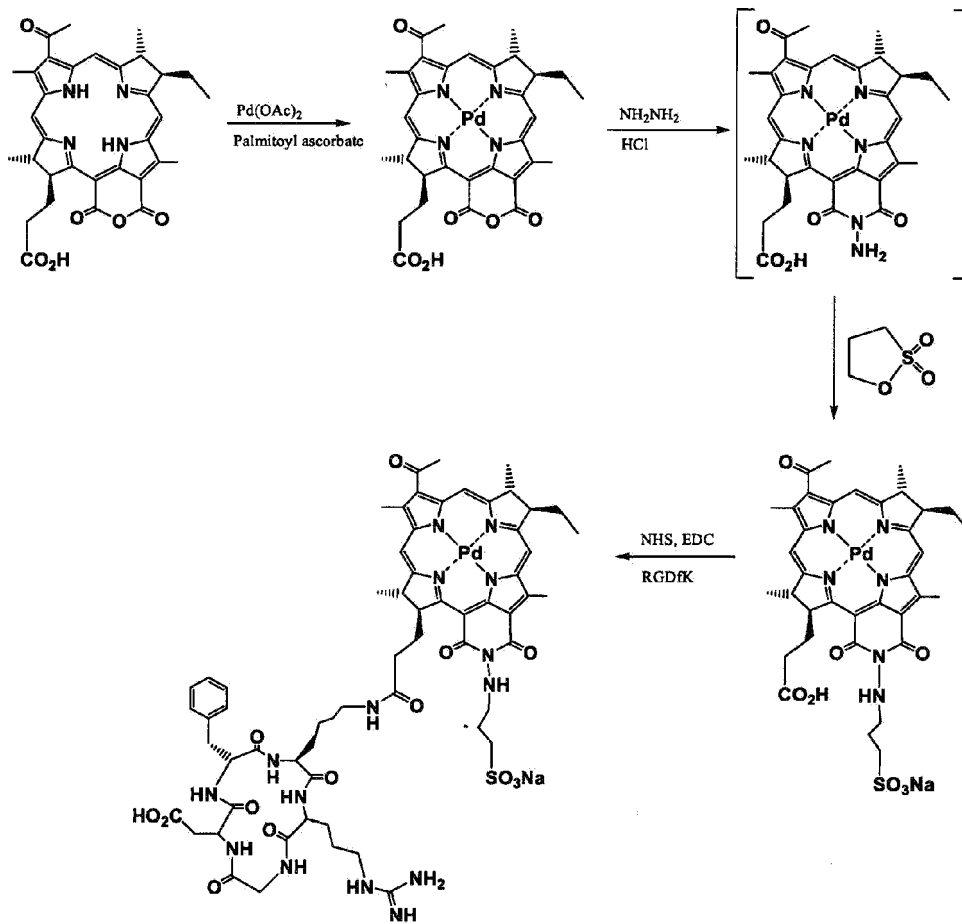
[0304] Fig. 37 shows accumulation of conjugate **13** in orthotopic human breast MDA-MB-231-RFP primary tumor (tumor size $\sim 1 \text{ cm}^3$). Images were taken from day 1 to 6 post drug injection. Top panel - In vivo whole-body red fluorescence imaging of CD-1 nude female mice bearing MDA-MB-231-RFP orthotopic tumor. Bottom panel - In vivo whole-body NIR fluorescence imaging of conjugate **13** accumulation. The drug shows accumulation in the tumor, reaching peak concentration specifically in the tumor from day 2 post injection.



H-Cys-Asp-Cys-Arg-Gly-Asp-Cys-Phe-Cys-NH
 RGD-4C cyclised form

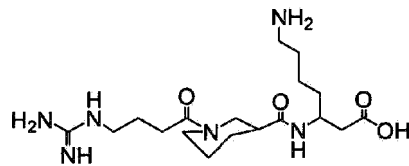
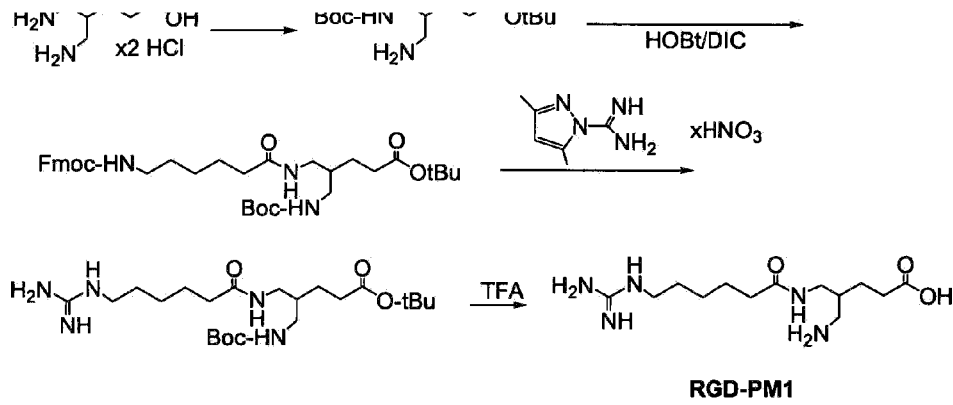


Scheme 1



Scheme 2





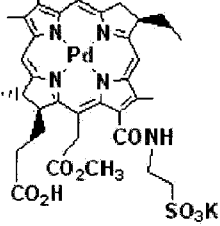
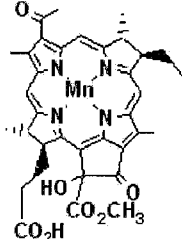
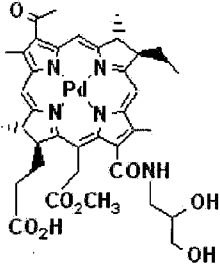
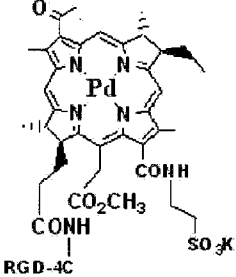
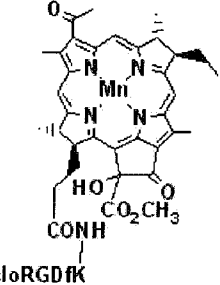
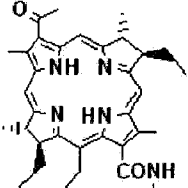
Scheme 3

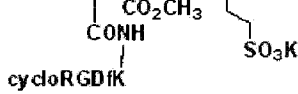
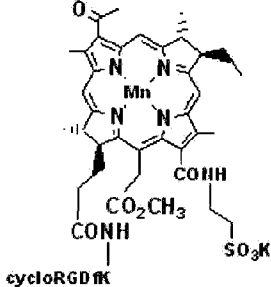
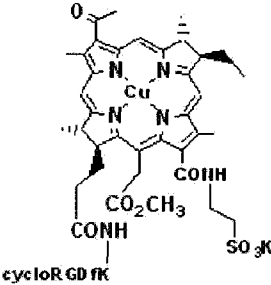
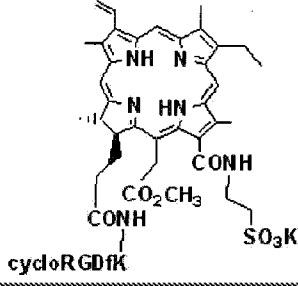
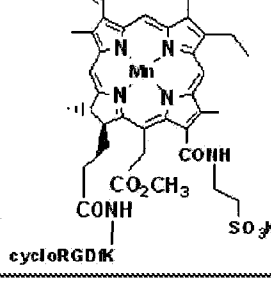
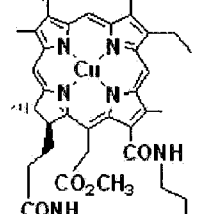
Appendix

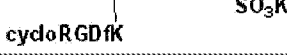
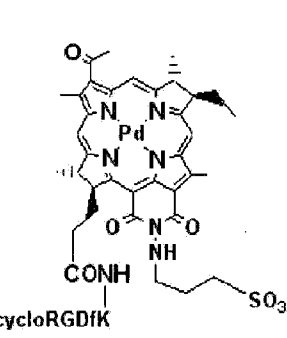
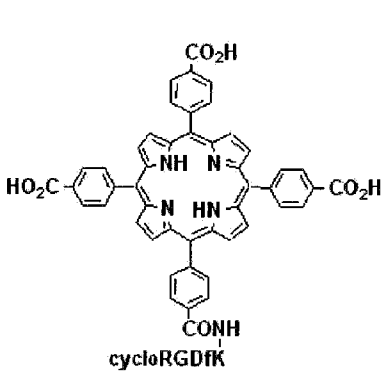
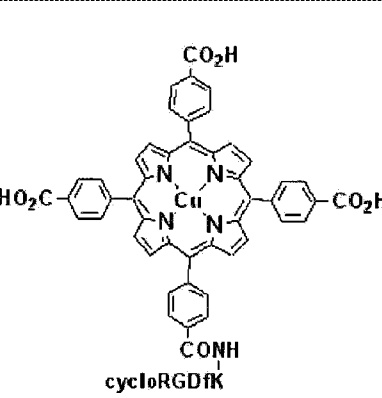
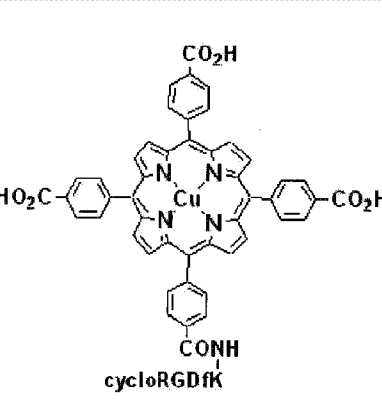
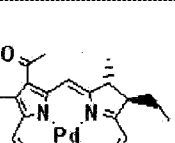
Compound Number	Chemical Name	Structure
<u>1</u>	Bacteriochlorophyll a	<p style="text-align: center;">CO_2CH_3 $\text{CO}_2\text{C}_{20}\text{H}_{39}$</p>
<u>2</u>	13 ² -OH-Bacteriochlorophyll a	<p style="text-align: center;">HO CO_2CH_3 $\text{CO}_2\text{C}_{20}\text{H}_{39}$</p>

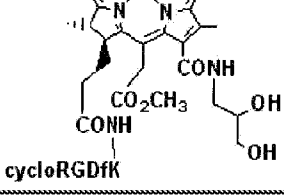
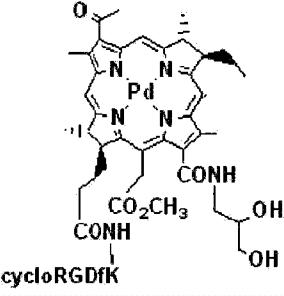
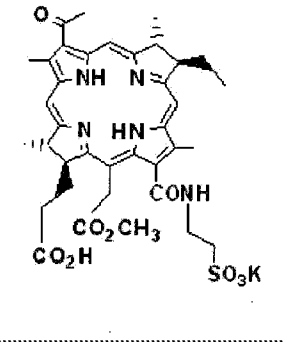
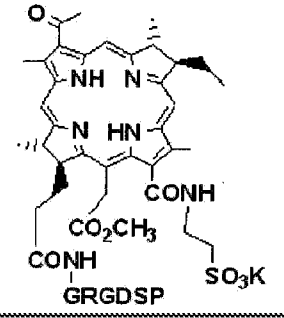
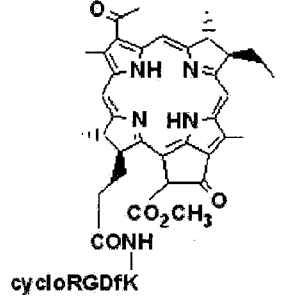
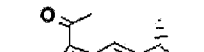
Compound Number	Chemical Name	Structure
<u>3</u>	Bacteriopheophorbide a	
<u>4</u>	13 ² -OH-Bacteriopheophorbide a	
<u>4a</u>	Bacteriopurpurin 18	
<u>5</u>	Chlorophyll a	
<u>6</u>	Pheophorbide a	
<u>7</u>	Palladium Bacteriopheophorbide a	

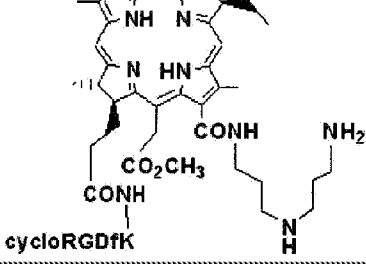
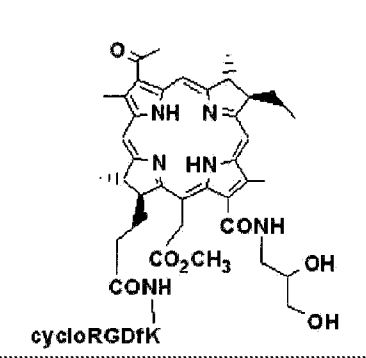
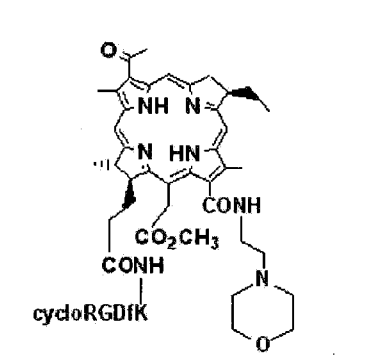
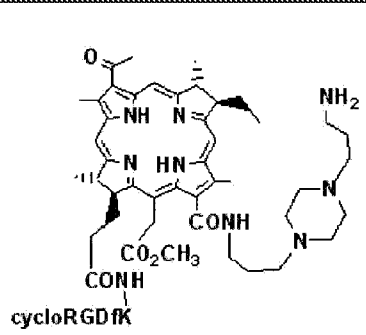
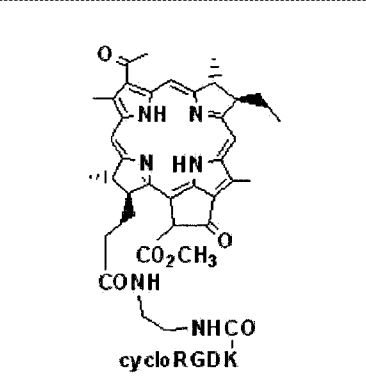


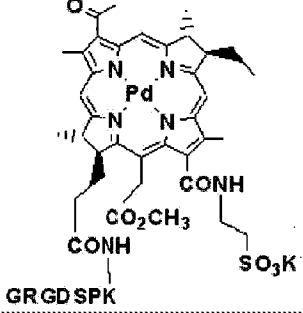
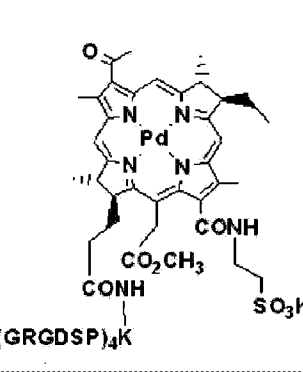
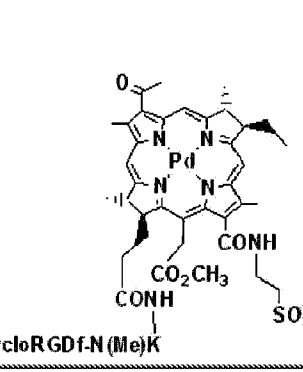
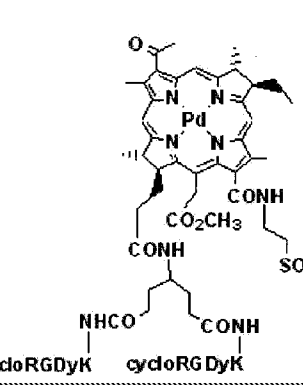
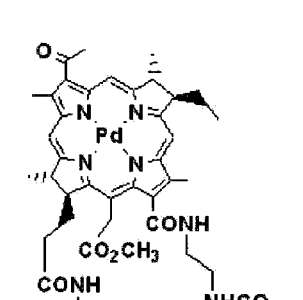
Compound Number	Chemical Name	Structure
<u>8</u>	Palladium 3 ¹ -oxo-15-methoxycarbonylmethyl-Rhodobacteriochlorin 13 ¹ -(2-sulfoethyl)amide potassium salt	
<u>9</u>	Manganese(III) 13 ² -OH-Bacteriopheophorbide a	
<u>10</u>	Palladium 3 ¹ -oxo-15-methoxycarbonylmethyl-Rhodobacteriochlorin-13 ¹ -(2,3-dihydroxypropyl)amide potassium salt	
<u>11</u>	Palladium 3 ¹ -oxo-15-methoxycarbonylmethyl-Rhodobacteriochlorin 13 ¹ -(2-sulfoethyl)amide-17 ³ -(RGD-4C)amide potassium salt	
<u>12</u>	Manganese(III) 13 ² -OH-Bacteriopheophorbide-17 ³ -(cycloRGDfK)amide	
<u>13</u>	3 ¹ -oxo-15-methoxycarbonylmethyl-Rhodobacteriochlorin 13 ¹ -(2-sulfoethyl)amide-17 ³ -	

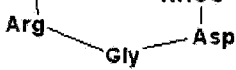
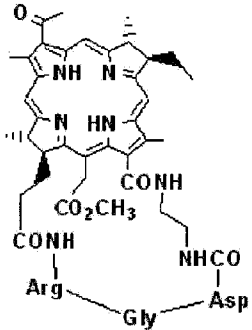
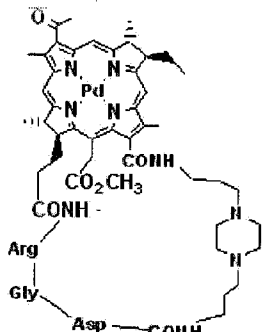
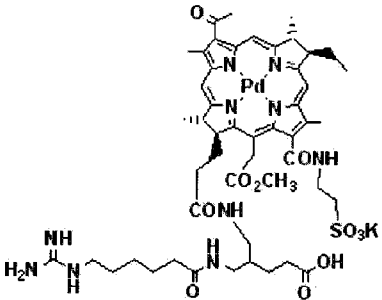
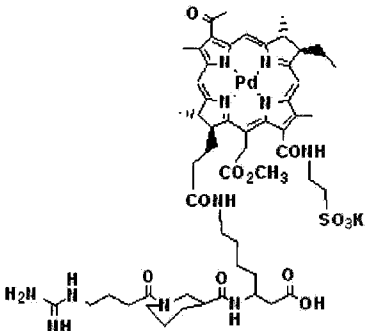
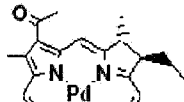
Compound Number	Chemical Name	Structure
	(cycloRGDfK)amide potassium salt	
<u>14</u>	Manganese(III) 3 ¹ -oxo-15-methoxycarbonylmethyl-Rhodobacteriochlorin 13 ¹ -(2-sulfoethyl)amide-17 ³ -(cycloRGDfK)amide potassium salt	
<u>15</u>	Copper(II) 3 ¹ -oxo-15-methoxycarbonylmethyl-Rhodobacteriochlorin 13 ¹ -(2-sulfoethyl)amide-17 ³ -(cycloRGDfK)amide potassium salt	
<u>16</u>	3 ¹ ,3 ² -Didehydrorhodochlorin 13 ¹ -(2-sulfoethyl)amide-17 ³ -(cycloRGDfK)amide potassium salt	
<u>17</u>	Manganese(III) 3 ¹ ,3 ² -Didehydrorhodochlorin 13 ¹ -(2-sulfoethyl)amide-17 ³ -(cycloRGDfK)amide potassium salt	
<u>18</u>	Copper(II) 3 ¹ ,3 ² -Didehydrorhodochlorin 13 ¹ -(2-sulfoethyl)amide-17 ³ -(cycloRGDfK)amide potassium salt	

Compound Number	Chemical Name	Structure
		
<u>19</u>	Palladium Bacteriopurpurin N-(3-sulfopropylamino)imide-17 ³ -(cycloRGDfK)amide potassium salt	
<u>20</u>	Meso-5-(4-cycloRGDfK-benzamido)-10,15,20-tris(4-carboxyphenyl)porphine	
<u>21</u>	Copper(II) meso-5-(4-cycloRGDfK-benzamido)-10,15,20-tris(4-carboxyphenyl) porphine	
<u>22</u>	Gadolinium(III) meso-5-(4-cycloRGDfK-benzamido)-10,15,20-tris(4-carboxy phenyl)porphine	
	Palladium 3 ¹ -oxo-15-methoxycarbonylmethyl-	

Compound Number	Chemical Name	Structure
<u>23</u>	Rhodobacteriochlorin-13 ¹ -(2,3-dihydroxypropyl)amide-17 ³ -(cycloRGDfK)amide	
<u>24</u>	Palladium 3 ¹ -oxo-15-methoxycarbonylmethyl-Rhodobacteriochlorin 13 ¹ -(2-sulfoethyl)amide-17 ³ -(cycloRGDfK)amide potassium salt	
<u>25</u>	3 ¹ -oxo-15-methoxycarbonylmethyl-Rhodobacteriochlorin 13 ¹ -(2-sulfoethyl)amide potassium salt	
<u>26</u>	3 ¹ -oxo-15-methoxycarbonylmethyl-Rhodobacteriochlorin 13 ¹ -(2-sulfoethyl)amide-17 ³ -(GRGDSP)amide potassium salt	
<u>27</u>	Bacteriopheophorbide-17 ³ -(cycloRGDfK)amide	
		

Compound Number	Chemical Name	Structure
<u>28</u>	3 ¹ -oxo-15-methoxycarbonylmethyl-Rhodobacteriochlorin 13 ¹ -(3-[(3-aminopropyl)amino]propyl)amide-17 ³ -(cycloRGDfK)amide	
<u>29</u>	3 ¹ -oxo-15-methoxycarbonylmethyl-Rhodobacteriochlorin 13 ¹ -(2,3-dihydroxypropyl)amide-17 ³ -(cycloRGDfK)amide	
<u>30</u>	3 ¹ -oxo-15-methoxycarbonylmethyl-Rhodobacteriochlorin 13 ¹ -(2-morpholino-N-ethyl)amide-17 ³ -(cycloRGDfK)amide	
<u>31</u>	3 ¹ -oxo-15-methoxycarbonylmethyl-Rhodobacteriochlorin 13 ¹ -(3-[4-(3-aminopropyl)-piperazin-1-yl]-propyl)amide-17 ³ -(cycloRGDfK)amide	
<u>32</u>	Bacteriopheophorbide-17 ³ -(2-cycloRGDK-amido-N-ethyl)amide	

Compound Number	Chemical Name	Structure
<u>33</u>	Palladium 3 ¹ -oxo-15-methoxycarbonylmethyl-Rhodobacteriochlorin 13 ¹ -(2-sulfoethyl)amide-17 ³ -(GRGDSPK)amide potassium salt	 <p>GRGDSPK</p>
<u>34</u>	Palladium 3 ¹ -oxo-15-methoxycarbonylmethyl-Rhodobacteriochlorin 13 ¹ -(2-sulfoethyl)amide-17 ³ -[(GRGDSP) ₄ K]amide potassium salt	 <p>(GRGDSP)₄K</p>
<u>35</u>	Palladium 3 ¹ -oxo-15-methoxycarbonylmethyl-Rhodobacteriochlorin 13 ¹ -(2-sulfoethyl)amide-17 ³ -(cycloRGDf-N(Me)K)amide potassium salt	 <p>cycloRGDf-N(Me)K</p>
<u>36</u>	Palladium 3 ¹ -oxo-15-methoxycarbonylmethyl-Rhodobacteriochlorin 13 ¹ -(2-sulfoethyl)-17 ³ -N-[4-heptanedioic acid bis-(cycloRGDyK-amido)]amide potassium salt	 <p>cycloRGDyK cycloRGDyK</p>
<u>37</u>	Palladium 3 ¹ -oxo-15-methoxycarbonylmethyl-Rhodobacteriochlorin 13 ¹ ,17 ³ -cyclo(2-RGD-amido-N-ethyl)diamide	 <p>NHCO</p>

Compound Number	Chemical Name	Structure
		
38	3 ¹ -oxo-15-methoxycarbonylmethyl-Rhodobacteriochlorin 13 ¹ ,17 ³ -cyclo(2-RGD-amido-N-ethyl)diamide	
39	Palladium 3 ¹ -oxo-15-methoxycarbonylmethyl-Rhodobacteriochlorin 13 ¹ ,17 ³ -cyclo{3-[4-(3-aminopropyl-RGD-amido)-piperazin-1-yl]-propyl} diamide	
40	Palladium 3 ¹ -oxo-15-methoxycarbonylmethyl-Rhodobacteriochlorin 13 ¹ -(2-sulfoethyl)amide-17 ³ -[4-(methyl-5-(6-guanidino-hexanoylamino)-pentanoic acid)]amide potassium salt	
41	Palladium 3 ¹ -oxo-15-methoxycarbonylmethyl-Rhodobacteriochlorin 13 ¹ -(2-sulfoethyl)amide-17 ³ -[7-amido-3-[[1-(4-guanidino-butyl)-piperidine-3-carbonyl]-amino]-heptanoic acid] potassium salt	
	Palladium 3 ¹ -oxo-15-methoxycarbonylmethyl-	

Assa-Munt N., Jia X., Laakkonen P. and Ruoslahti E. (2001) "Solution structures and integrin binding activities of an RGD peptide with two isomers", *Biochemistry*, 40:2373-2378.

Bauminger S. and Wilchek M. (1980) "The use of carbodiimides in the preparation of immunizing conjugates. *Methods Enzymol*", 70(A): 151-159.

Bogdanowich-Knipp S.J., Jois D.S. and Siahaan T.J. (1999) "The effect of conformation on the solution stability of linear vs. cyclic RGD peptides", *J. Pept. Res.*, 53(5):523-9.

Bonnett R. (1999) "Photodynamic therapy in historical perspective", *Rev. Contemp. Pharmacother.*, 10:1-17.

Borza CM, Pozzi A, Borza DB, Pedchenko V, Hellmark T, Hudson BG, Zent R. (2006) "Integrin alpha3beta1, a novel receptor for alpha3(IV) noncollagenous domain and a trans-dominant Inhibitor for integrin alphavbeta3", *J Biol Chem*. 281(30):20932-20939.

Brandis A., Mazor O., Gross S., Koudinova N., Hami R., Kalin-Kammhuber N., Rosenbach-Belkin V., Greenwald M., Bondon A., Simonneaux G., Scheer H., Salomon Y. and Scherz A. (2003) "Novel palladium-bacteriochlorophyll derivatives for antivasular Photodynamic therapy: synthesis, phototoxicity, pharmacokinetics and efficacy", *J. Med. Chem.* submitted.

Brandis A., Mazor O., Neumark E., Rosenbach-Belkin V., Salomon Y. and Scherz A. (2005) "Novel water-soluble bacteriochlorophyll derivatives for vascular-targeted photodynamic therapy: synthesis, solubility, phototoxicity, and the effect of serum proteins", *Photochem Photobiol.*, 81, 983-993.

Brooks P.C., Clark R.A. and Cheresh D.A. (1994a) "Requirement of vascular integrin alpha v beta 3 for angiogenesis", *Science*, 264(5158):569-571.

Brooks P.C., Montgomery A.M., Rosenfeld M., Reisfeld R.A., Hu T., Klier G. and Cheresh D.A. (1994b) "Integrin alpha v beta 3 antagonists promote tumor regression by inducing apoptosis of angiogenic blood vessels", *Cell*, 79(7):1157-1164.

Brooks P.C., Stromblad S., Klemke R., Visscher D., Sarkar F.H. and Cheresh D.A. (1995) "Antiintegrin alpha v beta 3 blocks human breast cancer growth and angiogenesis in human skin", *J. Clin. Invest.*, 96(4):1815-1822.

Burrows F.J. and Thorpe P.E. (1994) "Vascular targeting-a new approach to the therapy of solid tumors", *Pharmacol. Ther.*, 64(1):155-74.

Castel S., Pagan R., Mitjans F., Piulats J., Goodman S., Jonczyk A., Huber F., Vilaro S. and Reina M. (2001) "RGD peptides and monoclonal antibodies, antagonists of α v-integrin, enter the cells by independent endocytic pathways", *Lab. Invest.*, 81(12):1615-1626.

Chaleix V., Sol V., Huang Y.M., Guilloton M., Granet R., Blais J.C., and Krausz P. (2003) "RGD-porphyrin conjugates: synthesis and potential application in photodynamic therapy", *Eur. J. Org. Chem.*, 1486-1493.

Chang Y.S., di Tomaso E., McDonald D.M., Jones R. and Jain R.K. (2000) "Mosaic blood vessels in tumors: frequency of cancer cells in contact with flowing blood", *Proc. Acad. Sci. U.S.A.*, 97(26):14608-14613.

Dougherty D.J., Gomer C.J., Henderson B.W., Jori G., Kessel D., Korbek M., Moan J. and Qian P. (1998) "Photodynamic therapy", *JNCI*, 90(12):889-905.

D'Souza S.E., Ginsberg M.H. and Plow E.F. (1991) "Arginyl-glycyl-aspartic acid (RGD): a cell adhesion motif", *Trends Biochem. Sci.*, 16(7):246-250.

Elceiri B.P. and Cheresh D.A. (1999) "The role of alphav integrins during angiogenesis: insights into potential mechanisms of action and clinical development", *J. Clin. Invest.*, 103(9):1227-1230.

Ellerby H.M., Arap W., Ellerby L.M., Kain R., Andrusiak R., Del Rio G., Krajewski S., Rao R., Ruoslahti E., Bredesen D.E. and Pasqualini R. (1999) "Anticancer activity of targeted pro-apoptotic peptides", *Nat. Med.*, 5(9):1032-1038.

Fiedor L., Rosenbach-Belkin V. and Scherz A. (1992) "The stereospecific interaction between chlorophylls and chlorophyllase. Possible implication for chlorophyll biosynthesis and degradation", *J. Biol. Chem.* 267:22043-22047.

Freidinger R.M., Hinkle J.S., Perlow D.S., and Arison B.H. (1983) "Synthesis of 9-Fluorenylmethyloxycarbonyl-Protected N-Alkyl Amino Acids by Reduction of Oxazolidinones", *J. Org. Chem.* 48: 77-81.

Goligorsky M.S., Kessler H. and Romanov V.I. (1998) "Molecular mimicry of integrin ligation: therapeutic potential of arginine-glycine aspartic acid (RGD) peptides", *Nephrol. Dial. Transplant.*, 13:254-263.

Gross S., Brandis A., Chen L., Rosenbach-Belkin V., Roehrs S., Scherz A., and Salomon Y. (1997) "Protein-A-mediated targeting of bacteriochlorophyll-IgG to *Staphylococcus aureus*: a model for enhanced site-specific photocytotoxicity", *Photochem Photobiol.*, 66(6):872-8.

Gross S., Gilead A. Scherz A. Neeman M. and Salomon Y. (2003b) "Monitoring Photodynamic Therapy of Solid Tumors Online by BOLD Contrast MRI", *Nature Medicine in Press*.

Gross S., Gilead A., Brandis A., Schreiber S., Machluf Y., Neeman M., Scherz A. and Salomon Y. (2003a) "Selective vascular and tumor responses of photodynamic therapy (PDT) with Pd bacteriopheophorbide (TOOKAD®): online and offline analyses", *Proceedings of the 94th annual meeting of the American association for cancer research (AACR)*, Toronto, April 5-9, 44: 27.

Hahn S.M. and Glatstein E. (1999) "The emergence of photodynamic therapy as a major modality in cancer treatment", *Rev. Contemp. Pharmacother.*, 10:69-74.

Hardan I., Weiss L., Hershkovitz R., Greenspoon N., Alon R., Cahalon L., Reich S., Slavin S. and Lider O. (1993) "Inhibition of metastatic cells colonization in murine lungs and tumor-

induced morbidity by non-peptidic Arg-Gly-Asp mimetics", *Int. J. Cancer*, 55:1023-1028.

Hart S.L., Knight A.M., Harbottle R.P., Mistry A., Hunger H.D., Cutler D.F., Williamson R. and Coutelle C. (1994) "Cell binding and internalization by filamentous phage displaying a cyclic Arg-Gly-Asp-containing peptide", *J. Biol. Chem.*, 269(17):12468-12474.

Haubner R. et al. (1999) "Radiolabeled $\alpha\beta 3$ integrin antagonists: a new class of tracers for tumor targeting", *J Nucl Med.* 40:1061-1071

Haubner R., Wester H.J., Weber W.A., Mang C., Ziegler S.L., Goodman S.L., Senekowitsch-Schmidtke R., Kessler H. and Schwaiger M. (2001) "Noninvasive imaging of $\alpha\beta 3$ integrin expression using ^{18}F -labeled RGD-containing glycopeptide and positron emission tomography", *Cancer res.*, 61:1781-1785.

Horrocks W.D. Jr. and Hove E.G., 1978, "Water-Soluble Lanthanide Porphyrins: Shift Reagents for Aqueous Solution", *Journal of the American Chemical Society*, 100: 4386-4392.

Huang X., Molema G., King S., Watkins L., Edgington T.S. and Thorpe P.E. (1997) "Tumor infarction in mice by antibody-directed targeting of tissue factor to tumor vasculature", *Science*, 275:547-550.

Janssen M.L., Oyen W.J., Dijkgraaf I., Massuger L.F., Frielink C., Edwards D.S., Rajopadhye M., Boonstra H., Corstens F.H., Boerman O.C. (2002a) Tumor Targeting with Radiolabeled $\alpha\beta 3$ Integrin Binding Peptides in a Nude Mouse Model. *Cancer research* 62: 6146-6151.

Janssen M, Oyen WJ, Massuger LF, Frielink C, Dijkgraaf I, Edwards DS, Radjopadhye M, Corstens FH, Boerman OC. (2002b) Comparison of a monomeric and dimeric radiolabeled RGD-peptide for tumor targeting. *Cancer Biother Radiopharm.* 17(6):641-646.

Joshi P., Chung C.Y., Aukhil I. and Erickson H.P. (1993) "Endothelial cells adhere to the RGD domain and the fibrinogen-like terminal knob of tenascin. J", *Cell Sci.*, 106 (Pt 1):389-400.

Kawaguchi M., Hosotani R., Ohishi S., Fujii N., Tulachan S.S., Koizumi M., Toyoda E., Masui T., Nakajima S., Tsuji S., Ida J., Fujimoto K., Wada M., Doi R., and Imamura M. (2001) "A novel synthetic Arg-Gly-Asp-containing peptide cyclo(-RGDf-V-) is the potent inhibitor of angiogenesis", *Biochem. Biophys. res. com.*, 288:711-717.

Kessel D. and Dougherty T.J. (1999) "Agents used in Photodynamic therapy", *Rev. Contemp. Pharmacother*, 10:19-24.

Koivunen E., Wang B. and Ruoslahti E. (1995) "Phage libraries displaying cyclic peptides with different ring sizes: ligand specificities of the RGD-directed integrins", *Biotechnology (N Y)*, 13(3):265-70.

Koivunen E., Wang B., Dickinson C.D. and Ruoslahti E. (1994) "Peptides in cell adhesion research", *Methods Enzymol.*, 245:346-369.

Koudinova N.V., Pinthus J.H., Brandis A., Brenner O., Bendel P., Ramon J., Eshhar Z., Scherz

- A. and Salomon Y. (2003) "Photodynamic therapy with Pd-Bacteriopheophorbide (TOOKAD): successful in vivo treatment of human prostatic small cell carcinoma xenografts", *Int J Cancer.*, 104(6):782-789.
- Mazon M.D. (1999) "Cellular aspects of photodynamic therapy for cancer", *Rev. Contemp. Pharmacother.*, 10:25-37.
- Mi Z, Guo H, Wai PY, Gao C, Kuo PC. (2006) "Integrin-linked kinase regulates osteopontin-dependent MMP-2 and uPA expression to convey metastatic function in murine mammary epithelial cancer cells", *Carcinogenesis.* 27(6):1134-1145.
- Mironov A.F. et al. (2003) "New bacteriochlorin derivatives with a fused N-aminoimide ring", *J. Porphyrins Phthalocyanins*, 7: 725-730.
- Mironov A.F., Kozyrev A.N. and Brandis A.S. (1992) "Sensitizers of second generation for photodynamic therapy of cancer based on chlorophyll and bacteriochlorophyll derivatives", *Proc. SPIE*, 1922:204-208.
- Omata T. and Murata N. (1983) "Preparation of Chlorophyll a, Chlorophyll b and Bacteriochlorophyll a by column chromatography with DEAE-Sepharose C1-6B and Sepharose C1-6B", *Plant Cell Physiol.*, 24:1093-1100
- Pasqualini R. and Ruoslahti E. (1996) "Organ targeting in vivo using phage display peptide libraries", *Nature*, 380(6572):364-366.
- Pasqualini R., Koivunen E. and Ruoslahti E. (1997) "Alpha v integrins as receptors for tumor targeting by circulating ligands", *Nat. Biotechnol.*, 15(6):542-546.
- Pasqualini R., Koivunen E., Kain R., Lahdenranta J., Sakamoto M., Stryhn A., Ashmun R.H., Shapiro L.H., Arap W. and Ruoslahti E. (2000) "Aminopeptidase N is a receptor for tumor-homing peptides and a target for inhibiting angiogenesis", *Cancer res.*, 60:722-727.
- Pierschbacher M. and Ruoslahti E. (1984) "Cell attachment activity of fibronectin can be duplicated by small synthetic fragments of the molecule", *Nature*, 309:30-33.
- Pierschbacher M.D. and Ruoslahti E. (1987) "Influence of stereochemistry of the sequence Arg-Gly-Asp-Xaa on binding specificity in cell adhesion", *J. Biol. Chem.*, 262(36):17294-17298.
- Preise D., Mazor O., Koudinova N., Liscovitch M., Scherz A. and Salomon Y. (2003) "Bypass Of Tumor Drug Resistance By Antivascular Therapy", *Neoplasia*, in Press.
- Rajotte D., ArapW., Hagedorn M., Koivunen E., Pasqualini R. and Ruoslahti E. (1998) "Molecular Heterogeneity of the vascular endothelium revealed by in vivo phage display", *J. Clin. Invest.*, 102:430-437.
- Romanov V.I. and Goligorsky M.S. (1999) "RGD-recognizing integrins mediate interactions of human prostate carcinoma cells with endothelial cells in vitro", *The prostate*, 39:108-118.
- Rosenbach-Belkin V., Chen L., Fiedor L., Tregub I., Paviotsky F., Brumfeld V., Salomon Y. and

- Scherz A. (1996) "Serine conjugates of chlorophyll and bacteriochlorophyll: photocytotoxicity in vitro and tissue distribution in mice bearing melanoma tumors", *Photochem Photobiol.*, 64(1):174-181.
- Ross D.T. et al., (2000) "Systematic variation in gene expression patterns in human cancer cell lines", *Nat Genet.* 24(3):227-235.
- Ruoslahti E. (1996) "RGD and other recognition sequences for integrins", *Annu. Rev. Cell Dev. Biol.*, 12:697-715.
- Ruoslahti E. (2000) "Targeting tumor vasculature with homing peptides from phage display", *Seminars in cancer biology*, 10:435-442.
- Ruoslahti E. (2002) "Drug targeting to specific vascular sites", *DDT*, 7(22):1138-1143.
- Ruoslahti E. and Pierschbacher M.D. (1987) "New perspectives in cell adhesion: RGD and integrins", *Science*, 238(4826):491-497.
- Ruoslahti E. and Rajotte D. (2000) "An address system in the vasculature of normal tissues and tumors", *Annu. Rev. Immunol.*, 18:813-827.
- Saiki I., Murata J., Iida J., Sakurai T., Nishi N., Matsuno K. and Azuma I. (1989) "Antimetastatic effects of synthetic polypeptides containing repeated structures of the cell adhesive Arg-Gly-Asp (RGD) and Tyr-Ile-Gly-Ser-Arg (YIGSR) sequence", *Br. J. Cancer*, 60:722-728.
- Scherz A. and Parson W.W. (1984) "Oligomers of bacteriochlorophyll and bacteriopheophytin with spectroscopic properties resembling those found in photosynthetic bacteria", *Biochim. Biophys. Acta*, 766:653-665.
- Schiffenbauer YS, Meir G, Maoz M, Even-Ram SC, Bar-Shavit R, Neeman M. (2002) "Gonadotropin stimulation of MLS human epithelial ovarian carcinoma cells augments cell adhesion mediated by CD44 and by alpha(v)-integrin", *Gynecol. Oncol.* 84(2):296-302.
- Schreiber S., Gross S., Brandis A., Harmelin A., Rosenbach-Belkin V., Scherz A. and Salomon Y. (2002) "Local photodynamic therapy (PDT) of rat C6 glioma xenografts with Pd-bacteriopheophorbide leads to decreased metastases and increase of animal cure compared with surgery", *Int. J. Cancer*, 99: 279-285.
- Struck A., Cmiel E., Katheder I., Schafer W. and Scheer H. (1992) "Bacteriochlorophylls modified at position C-3: long-range intramolecular interaction with position C-13[2]", *Biochimica et Biophysica Acta*, 1101 (3): 321-328.
- Su Z.F., Liu G., Gupta S., Zhu Z., Rusckowski M. and Hnatowich D.J. (2002) "In vitro and in vivo evaluation of a Technetium-99m-labeled cyclic RGD peptide as a specific marker of alpha(V)beta(3) integrin for tumor imaging", *Bioconjug. Chem.*, 13(3):561-570.
- Temming K. et al. (2005) RGD-based strategies for selective delivery of therapeutics and imaging agents to the tumour vasculature. *Drug resistance updates.* 8(6):381-402.

Vaillancourt V.A. et al. (2001) "Synthesis and Biological Activity of Aminoguanidine and Diaminoguanidine Analogues of the Antidiabetic/Antiobesity Agent 3-Guanidinopropionic Acid", *J. Med. Chem.*, 44:1231-1248.

van Hagen P.M., Breeman W.A., Bernard H.F., Schaar M., Mooij C.M., Srinivasan A., Schmidt M.A., Krenning E.P. and de Jong M. (2000) "Evaluation of a radiolabelled cyclic DTPA-RGD analogue for tumour imaging and radionuclide therapy", *Int. J. Cancer*, 90:186-198.

Wanunu M., Vaskevich A., Cohen S.R., Cohen H., Arad-Yellin R., Shanzer A., Rubinstein I. (2005) "Branched Coordination Multilayers on Gold", *JACS*, 127: 17877-17887.

Wasielewski M.R. and Svec W.A. (1980) "Synthesis of Covalently Linked Dimeric Derivatives of Chlorophyll a, Pyrochlorophyll a, Chlorophyll b, and Bacteriochlorophyll a", *J. Org. Chem.*, 45(10):1969-1974.

Yao B. et al. (2005) "Enhanced antitumor effect of the combination of tumstatin gene therapy and gemcitabine in murine models", *Hum Gene Ther.* 16(9):1075-1086.

Zhang S.Z., Lipsky M.M., Trump B.F. and Hsu I.C. (1990) "Neutral Red (NR) assay for cell viability and xenobiotic-induced cytotoxicity in primary cultures of human and rat hepatocytes", *Cell. Biol. Toxicol.*, 6:219-234.

Zilberstein J., Bromberg A., Frantz A., Rosenbach-Belkin V., Kritzman A., Pfefermann R., Salomon Y. and Scherz A. (1997) "Light-dependent oxygen consumption in bacteriochlorophyll-serine-treated melanoma tumors: on-line determination using a tissue-inserted oxygen microsensor", *Photochem Photobiol.*, 65(6):1012-1019.

Zilberstein J., Schreiber S., Bloemers M. C. W. M., Bendel P., Neeman M., Schechtman E., Kohen F., Scherz A. and Salomon Y. (2001) "Antivascular treatment of solid melanoma tumors with bacteriochlorophyll-serine-based photodynamic therapy", *Photochem. Photobiol.*, 73: 257-266.

Zitzmann S., Ehemann V. and Schwab M. (2002) "Arginine-Glycine-Aspartic acid (RGD)-peptide bind to both tumor and tumor-endothelial cells in vivo", *Cancer res.*, 62:5139-5143.

SEQUENCE LISTING

[0306]

<110> Yeda Research and Development Co.Ltd Scherz, AVIGDOR Salomon, YORAM Rubinstein, Efrat Brandis, Alexander Eren, Doron Neimann, Karin

<120> CONJUGATES OF RGD PEPTIDES AND PORPHYRIN OR (BACTERIO)CHLOROPHYLL PHOTOSYNTHESIZERS AND THEIR USES

<130> STEBA-007 PCT

<150> 60/839,409

<151> 2006-08-23

<160> 8

<170> PatentIn version 3.3

<210> 1

<211> 5

<212> PRT

<213> Artificial

<220>

<223> INTEGRIN BINDING MOTIF

<220>

<221> CYCLO

<222> (1)..(5)

<220>

<221> D-AMINO ACID

<222> (4)..(4)

<400> 1

Arg Gly Asp Phe Lys
1 5

<210> 2

<211> 9

<212> PRT

<213> Artificial

<220>

<223> INTEGRIN BINDING MOTIF

<220>

<221> CYCLIC

<222> (1)..(9)

<223> spontaneous oxidative formation of disulfide bonds

<400> 2

Cys Asp Cys Arg Gly Asp Cys Phe Cys
1 5

<210> 3

<211> 6

<212> PRT

<213> Artificial

<220>

<223> INTEGRIN BINDING MOTIF

<220>

<221> LINEAR

<222> (1)..(6)

<400> 3

Gly Arg Gly Asp Ser Pro
1 5

<210> 4

<211> 4

<212> PRT

<213> Artificial

<220>

<223> INTEGRIN BINDING MOTIF

<220>

<221> CYCLO

<222> (1)..(4)

<400> 4

Arg Gly Asp Lys
1

<210> 5

<211> 7

<212> PRT

<213> Artificial

<220>

<223> INTEGRIN BINDING MOTIF

<400> 5

Gly Arg Gly Asp Ser Pro Lys
1 5

<210> 6

<211> 25

<212> PRT

<213> Artificial

<220>

<223> INTEGRIN BINDING MOTIF

<400> 6

Gly Arg Gly Asp Ser Pro Gly Arg Gly Asp Ser Pro Gly Arg Gly Asp
1 5 10 15

Ser Pro Gly Arg Gly Asp Ser Pro Lys
 20 25

<210> 7

<211> 5

<212> PRT

<213> Artificial

<220>

<223> INTEGRIN BINDING MOTIF

<220>

<221> CYCLIC

<222> (1)..(5)

<220>

<221> N-METHYL

<222> (4)..(5)

<220>

<221> D-AMINO ACID

<222> (4)..(4)

<400> 7

Arg Gly Asp Phe Lys
 1 5

<210> 8

<211> 5

<212> PRT

<213> Artificial

<220>

<223> INTEGRIN BINDING MOTIF

<220>

<221> CYCLIC

<222> (1)..(5)

<220>

<221> D-AMINO ACID

<222> (4)..(4)

<400> 8

Arg Gly Asp Tyr Lys
 1 5

REFERENCES CITED IN THE DESCRIPTION

This list of references cited by the applicant is for the reader's convenience only. It does not form part of the European patent document. Even though great care has been taken in compiling the references, errors or omissions cannot be excluded and the EPO disclaims all liability in this regard.

Patent documents cited in the description

- [US6576239B](#) [0017] [0044]
- [EP0927045B1](#) [0017]
- [WO98010795A](#) [0017]
- [US5726169A](#) [0018] [0024]
- [US5650292A](#) [0018] [0024]
- [US5955585A](#) [0018] [0024]
- [US6147195A](#) [0018] [0024]
- [US6740637B](#) [0018] [0024]
- [US6333319B](#) [0018] [0024]
- [US6569846B](#) [0018] [0024]
- [US7045117B](#) [0018] [0024]
- [DE4121876](#) [0018] [0024]
- [EP1246826A](#) [0018] [0024]
- [WO2004045492A](#) [0018] [0024] [0067] [0161] [0161]
- [WO2005120573A](#) [0018] [0024] [0082]
- [EP0927045A](#) [0044]
- [WO9309795A](#) [0053] [0162]
- [WO2000033833A](#) [0161]
- [WO60839409A](#) [0306]

Non-patent literature cited in the description

- CHALEIX et al. Eur. J. Org Chem., 2003, vol. 8, 1486-1493 [0023]
- CHALEIX et al. Tetrahedron Letters, 2004, vol. 45, 5295-5299 [0023]
- STERNBERG et al. Tetrahedron, 1998, vol. 54, 174151-4202 [0023]
- PDT. FROCHOT et al. Bioorganic Chemistry, 2007, vol. 35, 3205-220 [0023]
- ARAP W.HAEDICKE W.BERNASCONI M.KAIN R.RAJOTTE D.KRAJEWSKI

- S.ELLERBY H.M.BREDESEN D.E.PASQUALINI R.RUOSLAHTI E.Targeting the prostate for destruction through a vascular addressProc. Natl. Acad. Sci. U.S.A., 2002, vol. 99, 31527-1531 [0305]
- **ARAP W.PASQUALINI R.RUOSLAHTI E.**Cancer treatment by targeted drug delivery to tumor vasculature in a mouse modelScience, 1998, vol. 279, 377-380 [0305]
 - **ASSA-MUNT N.JIA X.LAAKKONEN P.RUOSLAHTI E.**Solution structures and integrin binding activities of an RGD peptide with two isomersBiochemistry, 2001, vol. 40, 2373-2378 [0305]
 - **BAUMINGER S.WILCHEK M**The use of carbodiimides in the preparation of immunizing conjugatesMethods Enzymol, 1980, vol. 70, A151-159 [0305]
 - **BOGDANOWICH-KNIPP S.J.JOIS D.S.SIAHAAN T.J.**The effect of conformation on the solution stability of linear vs. cyclic RGD peptidesJ. Pept. Res., 1999, vol. 53, 5523-9 [0305]
 - **BONNETT R.**Photodynamic therapy in historical perspectiveRev. Contemp. Pharmacother., 1999, vol. 10, 1-17 [0305]
 - **BORZA CMPOZZI ABORZA DBPEDCHENKO VHELLMARK THUDSON BGZENT R.**Integrin alpha3beta1, a novel receptor for alpha3(IV) noncollagenous domain and a trans-dominant Inhibitor for integrin alphavbeta3J Biol Chem., 2006, vol. 281, 3020932-20939 [0305]
 - **BRANDIS A.MAZOR O.GROSS S.KOUDINOVA N.HAMI R.KALIN-KAMMHUBER N.ROSENBAACH-BELKIN V.GREENWALD M.BONDON A.SIMONNEAUX G.**Novel palladium-bacteriochlorophyll derivatives for antivasular Photodynamic therapy: synthesis, phototoxicity, pharmacokinetics and efficacyJ. Med. Chem. submitted, 2003, [0305]
 - **BRANDIS A.MAZOR O.NEUMARK E.ROSENBAACH-BELKIN V.SALOMON Y.SCHERZ A**Novel water-soluble bacteriochlorophyll derivatives for vascular-targeted photodynamic therapy: synthesis, solubility, phototoxicity, and the effect of serum proteinsPhotochem Photobiol., 2005, vol. 81, 983-993 [0305]
 - **BROOKS P.C.CLARK R.A.CHERESH D.A.**Requirement of vascular integrin alpha v beta 3 for angiogenesisScience, 1994, vol. 264, 5158569-571 [0305]
 - **BROOKS P.C.MONTGOMERY A.M.ROSENFELD M.REISFELD R.A.HU T.KLIER G.CHERESH D.A.**Integrin alpha v beta 3 antagonists promote tumor regression by inducing apoptosis of angiogenic blood vesselsCell, 1994, vol. 79, 71157-1164 [0305]
 - **BROOKS P.C.STROMBLAD S.KLEMKE R.VISSCHER D.SARKAR F.H.CHERESH D.A.**Antiintegrin alpha v beta 3 blocks human breast cancer growth and angiogenesis in human skinJ. Clin. Invest., 1995, vol. 96, 41815-1822 [0305]
 - **BURROWS F.J.THORPE P.E.**Vascular targeting-a new approach to the therapy of solid tumorsPharmacol. Ther., 1994, vol. 64, 1155-74 [0305]
 - **CASTEL S.PAGAN R.MITJANS F.PIULATS J.GOODMAN S.JONCZYC A.HUBER F.VILARO S.REINA M.**RGD peptides and monoclonal antibodies, antagonists of α v-integrin, enter the cells by independent endocytic pathwaysLab. Invest., 2001, vol. 81, 121615-1626 [0305]
 - **CHALEIX V.SOL V.HUANG Y.M.GUILLOTON M.GRANET R.BLAIS J.C.KRAUSZ P.**RGD-porphyrin conjugates: synthesis and potential application in photodynamic

- therapy *Eur. J. Org. Chem.*, 2003, 1486-1493 [0305]
- **CHANG Y.S. DI TOMASO E. MCDONALD D.M. JONES R. JAIN R.K.** Mosaic blood vessels in tumors: frequency of cancer cells in contact with flowing blood *Proc. Acad. Sci. U.S.A.*, 2000, vol. 97, 2614608-14613 [0305]
 - **DOUGHERTY D.J. GOMER C.J. HENDERSON B.W. JORI G. KESSEL D. KORBELIK M. MOAN J. QIAN P.** Photodynamic therapy *JNCI*, 1998, vol. 90, 12889-905 [0305]
 - **D'SOUZA S.E. GINSBERG M.H. PLOW E.F.** Arginyl-glycyl-aspartic acid (RGD): a cell adhesion motif *Trends Biochem. Sci.*, 1991, vol. 16, 7246-250 [0305]
 - **ELCEIRI B.P. CHERESH D.A.** The role of alpha v integrins during angiogenesis: insights into potential mechanisms of action and clinical development *J. Clin. Invest.*, 1999, vol. 103, 91227-1230 [0305]
 - **ELLERBY H.M. ARAP W. ELLERBY L.M. KAIN R. ANDRUSIAK R. DEL RIO G. KRAJEWSKI S. RAO R. RUOSLAHTI E. BREDESEN D.E.** Anticancer activity of targeted pro-apoptotic peptides *Nat. Med.*, 1999, vol. 5, 91032-1038 [0305]
 - **FIEDOR L. ROSENBAACH-BELKIN V. SCHERZ A.** The stereospecific interaction between chlorophylls and chlorophyllase. Possible implication for chlorophyll biosynthesis and degradation *J. Biol. Chem.*, 1992, vol. 267, 22043-22047 [0305]
 - **FREIDINGER R.M. HINKLE J.S. PERLOW D.S. ARISON B.H.** Synthesis of 9-Fluorenylmethyloxycarbonyl-Protected N-Alkyl Amino Acids by Reduction of Oxazolidinone *J. Org. Chem.*, 1983, vol. 48, 77-81 [0305]
 - **GOLIGORSKY M.S. KESSLER H. ROMANOV V.I.** Molecular mimicry of integrin ligation: therapeutic potential of arginine-glycine aspartic acid (RGD) peptides *Nephrol. Dial. Transplant.*, 1998, vol. 13, 254-263 [0305]
 - **GROSS S. BRANDIS A. CHEN L. ROSENBAACH-BELKIN V. ROEHRS S. SCHERZ A. SALOMON Y.** Protein-A-mediated targeting of bacteriochlorophyll-IgG to *Staphylococcus aureus*: a model for enhanced site-specific photocytotoxicity *Photochem Photobiol.*, 1997, vol. 66, 6872-8 [0305]
 - **GROSS S. GILEAD A. SCHERZ A. NEEMAN M. SALOMON Y.** Monitoring Photodynamic Therapy of Solid Tumors Online by BOLD Contrast MRI *Nature Medicine in Press*, 2003, [0305]
 - **GROSS S. GILEAD A. BRANDIS A. SCHREIBER S. MACHLUF Y. NEEMAN M. SCHERZ A. SALOMON Y.** Selective vascular and tumor responses of photodynamic therapy (PDT) with Pd bacteriopheophorbide (TOOKAD®): online and offline analyses *Proceedings of the 94th annual meeting of the American association for cancer research (AACR)*, 2003, vol. 44, 27- [0305]
 - **HAHN S.M. GLATSTEIN E.** The emergence of photodynamic therapy as a major modality in cancer treatment *Rev. Contemp. Pharmacother.*, 1999, vol. 10, 69-74 [0305]
 - **HARDAN I. WEISS L. HERSHKOVITZ R. GREENSPOON N. ALON R. CAHALON L. REICH S. SLAVIN S. LIDER O.** Inhibition of metastatic cells colonization in murine lungs and tumor-induced morbidity by non-peptidic Arg-Gly-Asp mimetics *Int. J. Cancer*, 1993, vol. 55, 1023-1028 [0305]
 - **HART S.L. KNIGHT A.M. HARBOTTLE R.P. MISTRY A. HUNGER H.D. CUTLER D.F. WILLIAMSON R. COUTELLE C.** Cell binding and internalization by filamentous phage displaying a cyclic Arg-Gly-Asp-containing peptide *J. Biol. Chem.*, 1994, vol. 269,

1712468-12474 [0305]

- **HAUBNER R. et al.** Radiolabeled $\alpha\beta 3$ integrin antagonists: a new class of tracers for tumor targeting *J Nucl Med.*, 1999, vol. 40, 1061-1071 [0305]
- **HAUBNER R. WESTER H.J. WEBER W.A. MANG C. ZIEGLER S.L. GOODMAN S.L. SENEKOWITSCH-SCHMIDTKE R. KESSLER H. SCHWAIGER M.** Noninvasive imaging of $\alpha\beta 3$ integrin expression using 18F-labeled RGD-containing glycopeptide and positron emission tomography *Cancer res.*, 2001, vol. 61, 1781-1785 [0305]
- **HORROCKS W.D. JR. HOVE E.G.** Water-Soluble Lanthanide Porphyrins: Shift Reagents for Aqueous Solution *Journal of the American Chemical Society*, 1978, vol. 100, 4386-4392 [0305]
- **HUANG X. MOLEMA G. KING S. WATKINS L. EDGINGTON T.S. THORPE P.E.** Tumor infarction in mice by antibody-directed targeting of tissue factor to tumor vasculature *Science*, 1997, vol. 275, 547-550 [0305]
- **JANSSEN M.L. OYEN W.J. DIJKGRAAF I. MASSUGER L.F. FRIELINK C. EDWARDS D.S. RAJOPADHYE M. BOONSTRA H. CORSTENS F.H. BOERMAN O.C.** Tumor Targeting with Radiolabeled $\alpha\beta 3$ Integrin Binding Peptides in a Nude Mouse Model *Cancer research*, 2002, vol. 62, 6146-6151 [0305]
- **JANSSEN MOYEN W. MASSUGER L. FRIELINK C. DIJKGRAAF I. EDWARDS D. SRADJOPADHYE M. CORSTENS F. H. BOERMAN O. C.** Comparison of a monomeric and dimeric radiolabeled RGD-peptide for tumor targeting *Cancer Biother Radiopharm.*, 2002, vol. 17, 6641-646 [0305]
- **JOSHI P. CHUNG C.Y. AUKHIL I. ERICKSON H.P.** Endothelial cells adhere to the RGD domain and the fibrinogen-like terminal knob of tenascinJ", *Cell Sci.*, 1993, vol. 106, 389-400 [0305]
- **KAWAGUCHI M. HOSOTANI R. OHISHI S. FUJII N. TULACHAN S.S. KOIZUMI M. TOYODA E. MASUI T. NAKAJIMA S. TSUJI S.A.** A novel synthetic Arg-Gly-Asp-containing peptide cyclo(-RGDf=V-) is the potent inhibitor of angiogenesis *Biochem. Biophys. res. com.*, 2001, vol. 288, 711-717 [0305]
- **KESSEL D. DOUGHERTY T.J.** Agents used in Photodynamic therapy *Rev. Contemp. Pharmacother*, 1999, vol. 10, 19-24 [0305]
- **KOIVUNEN E. WANG B. RUOSLAHTI E.** Phage libraries displaying cyclic peptides with different ring sizes: ligand specificities of the RGD-directed integrins *Biotechnology*, 1995, vol. 13, 3265-70 [0305]
- **KOIVUNEN E. WANG B. DICKINSON C.D. RUOSLAHTI E.** Peptides in cell adhesion research *Methods Enzymol.*, 1994, vol. 245, 346-369 [0305]
- **KOUDINOVA N.V. PINTHUS J.H. BRANDIS A. BRENNER O. BENDEL P. RAMON J. ESHHAR Z. SCHERZ A. SALOMON Y.** Photodynamic therapy with Pd-Bacteriopheophorbide (TOOKAD): successful in vivo treatment of human prostatic small cell carcinoma xenografts *Int J Cancer.*, 2003, vol. 104, 6782-789 [0305]
- **MAZON M.D.** Cellular aspects of photodynamic therapy for cancer *Rev. Contemp. Pharmacother.*, 1999, vol. 10, 25-37 [0305]
- **MI ZGUO HWAI PYGAO CKUO PC** Integrin-linked kinase regulates osteopontin-dependent MMP-2 and uPA expression to convey metastatic function in murine mammary epithelial cancer cells *Carcinogenesis*, 2006, vol. 27, 61134-1145 [0305]

- **MIRONOV A.F. et al.** New bacteriochlorin derivatives with a fused N-aminoimide ring. *J. Porphyrins Phthalocyanins*, 2003, vol. 7, 725-730 [0305]
- **MIRONOV A.F.KOZYREV A.N.BRANDIS A.S.** Sensitizers of second generation for photodynamic therapy of cancer based on chlorophyll and bacteriochlorophyll derivatives *Proc. SPIE*, 1922, 204-208 [0305]
- **OMATA T.MURATA N** Preparation of Chlorophyll a, Chlorophyll b and Bacteriochlorophyll a by column chromatography with DEAE-Sepharose C1-6B and Sepharose C1-6B *Plant Cell Physiol.*, 1983, vol. 24, 1093-1100 [0305]
- **PASQUALINI R.RUOSLAHTI E.** Organ targeting in vivo using phage display peptide libraries *Nature*, 1996, vol. 380, 6572364-366 [0305]
- **PASQUALINI R.KOIVUNEN E.RUOSLAHTI E.** Alpha v integrins as receptors for tumor targeting by circulating ligands *Nat. Biotechnol.*, 1997, vol. 15, 6542-546 [0305]
- **PASQUALINI R.KOIVUNEN E.KAIN R.LAHDENRANTA J.SAKAMOTO M.STRYHN A.ASHMUN R.H.SHAPIRO L.H.ARAP W.ROUSLAHTI E.** Aminopeptidase N is a receptor for tumor-homing peptides and a target for inhibiting angiogenesis *Cancer res.*, 2000, vol. 60, 722-727 [0305]
- **PIERSCHBACHER M.RUOSLAHTI** Cell attachment activity of fibronectin can be duplicated by small synthetic fragments of the molecule *Nature*, 1984, vol. 309, 30-33 [0305]
- **PIERSCHBACHER M.D.ROUSLAHTI** Influence of stereochemistry of the sequence Arg-Gly-Asp-Xaa on binding specificity in cell adhesion *J. Biol. Chem.*, 1987, vol. 262, 3617294-17298 [0305]
- **PREISE D.MAZOR O.KOUDINOVA N.LISCOVITCH M.SCHERZ A.SALOMON Y.** Bypass Of Tumor Drug Resistance By Antivascular Therapy *Neoplasia*, 2003, [0305]
- **RAJOTTE D.ARAPW.HAGEDORN M.KOIVUNEN E.PASQUALINI R.RUOSLAHTI E.** Molecular Heterogeneity of the vascular endothelium revealed by in vivo phage display *J. Clin. Invest.*, 1998, vol. 102, 430-437 [0305]
- **ROMANOV V.I.GOLIGORSKY M.** SRGD-recognizing integrins mediate interactions of human prostate carcinoma cells with endothelial cells in vitro *The prostate*, 1999, vol. 39, 108-118 [0305]
- **ROSENBAACH-BELKIN V.CHEN L.FIEDOR L.TREGUB I.PAVIOTSKY F.BRUMFELD V.SALOMON Y.SCHERZ A.** Serine conjugates of chlorophyll and bacteriochlorophyll: photocytotoxicity in vitro and tissue distribution in mice bearing melanoma tumors *Photochem Photobiol.*, 1996, vol. 64, 1174-181 [0305]
- **ROSS D.T. et al.** Systematic variation in gene expression patterns in human cancer cell lines *Nat Genet.*, 2000, vol. 24, 3227-235 [0305]
- **RUOSLAHTI E.** RGD and other recognition sequences for integrins *Annu. Rev. Cell Dev. Biol.*, 1996, vol. 12, 697-715 [0305]
- **RUOSLAHTI E.** Targeting tumor vasculature with homing peptides from phage display *Seminars in cancer biology*, 2000, vol. 10, 435-442 [0305]
- **RUOSLAHTI E.** Drug targeting to specific vascular sites *DDT*, 2002, vol. 7, 221138-1143 [0305]
- **RUOSLAHTI E.PIERSCHBACHER M.D.** New perspectives in cell adhesion: RGD and integrins *Science*, 1987, vol. 238, 4826491-497 [0305]

- **RUOSLAHTI E. RAJOTTE D.** An address system in the vasculature of normal tissues and tumors *Annu. Rev. Immunol.*, 2000, vol. 18, 813-827 [0305]
- **SAIKI I. MURATA J. IIDA J. SAKURAI T. NISHI N. MATSUNO K. AZUMA I.** Antimetastatic effects of synthetic polypeptides containing repeated structures of the cell adhesive Arg-Gly-Asp (RGD) and Tyr-Ile-Gly-Ser-Arg (YIGSR) sequence *Br. J. Cancer*, 1989, vol. 60, 722-728 [0305]
- **SCHERZ A. PARSON W. W.** Oligomers of bacteriochlorophyll and bacteriopheophytin with spectroscopic properties resembling those found in photosynthetic bacteria *Biochim. Biophys. Acta*, 1984, vol. 766, 653-665 [0305]
- **SCHIFFENBAUER YSMEIR GMAOZ MEVEN-RAM SCBAR-SHAVIT RNEEMAN M.** Gonadotropin stimulation of MLS human epithelial ovarian carcinoma cells augments cell adhesion mediated by CD44 and by alpha(v)-integrin *Gynecol. Oncol.*, 2002, vol. 84, 2296-302 [0305]
- **SCHREIBER S. GROSS S. BRANDIS A. HARMELIN A. ROSENBAACH-BELKIN V. SCHERZ A. SALOMON Y.** Local photodynamic therapy (PDT) of rat C6 glioma xenografts with Pd-bacteriopheophorbide leads to decreased metastases and increase of animal cure compared with surgery *Int. J. Cancer*, 2002, vol. 99, 279-285 [0305]
- **STRUCK A. CMIEL E. KATHEDER I. SCHAFFER W. SCHEER H.** Bacteriochlorophylls modified at position C-3: long-range intramolecular interaction with position C-13 [2] *Biochimica et Biophysica Acta*, 1992, vol. 1101, 3321-328 [0305]
- **SU Z. F. LIU G. GUPTA S. ZHU Z. RUSCKOWSKI M. HNATOWICH D. J.** In vitro and in vivo evaluation of a Technetium-99m-labeled cyclic RGD peptide as a specific marker of alpha(V)beta(3) integrin for tumor imaging *Bioconjug. Chem.*, 2002, vol. 13, 3561-570 [0305]
- **TEMMING K. et al.** RGD-based strategies for selective delivery of therapeutics and imaging agents to the tumour vasculature *Drug resistance updates*, 2005, vol. 8, 6381-402 [0305]
- **VAILLANCOURT V. A. et al.** Synthesis and Biological Activity of Aminoguanidine and Diaminoguanidine Analogues of the Antidiabetic/Antiobesity Agent 3-Guanidinopropionic Acid *J. Med. Chem.*, 2001, vol. 44, 1231-1248 [0305]
- **VAN HAGEN P. M. BREEMAN W. A. BERNARD H. F. SCHAAR M. MOOIJ C. M. SRINIVASAN A. SCHMIDT M. A. KRENNING E. P. DE JONG M.** Evaluation of a radiolabelled cyclic DTPA-RGD analogue for tumour imaging and radionuclide therapy *Int. J. Cancer*, 2000, vol. 90, 186-198 [0305]
- **WANUNU M. VASKEVICH A. COHEN S. R. COHEN H. ARAD-YELLIN R. SHANZER A. RUBINSTEIN I.** Branched Coordination Multilayers on Gold *JACS*, 2005, vol. 127, 17877-17887 [0305]
- **WASIELEWSKI M. R. SVEC W. A.** Synthesis of Covalently Linked Dimeric Derivatives of Chlorophyll a, Pyrochlorophyll a, Chlorophyll b, and Bacteriochlorophyll a *J. Org. Chem.*, 1980, vol. 45, 101969-1974 [0305]
- **YAO B. et al.** Enhanced antitumor effect of the combination of tumstatin gene therapy and gemcitabine in murine models *Hum Gene Ther.*, 2005, vol. 16, 91075-1086 [0305]
- **ZHANG S. Z. LIPSKY M. M. TRUMP B. F. HSU I. C.** Neutral Red (NR) assay for cell viability and xenobiotic-induced cytotoxicity in primary cultures of human and rat

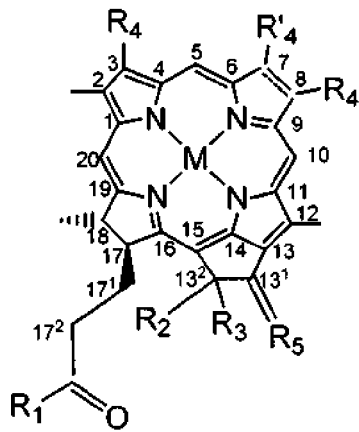
hepatocytes *Cell. Biol. Toxicol.*, 1990, vol. 6, 219-234 [0305]

- ZILBERSTEIN J. BROMBERG A. FRANTZ A. ROSENBACH-BELKIN V. KRITZMANN A. PFEFERMANN R. SALOMON Y. SCHERZ A. Light-dependent oxygen consumption in bacteriochlorophyll-serine-treated melanoma tumors: on-line determination using a tissue-inserted oxygen microsensor *Photochem Photobiol.*, 1997, vol. 65, 61012-1019 [0305]
- ZILBERSTEIN J. SCHREIBER S. BLOEMERS M. C. W. M. BENDEL P. NEEMAN M. SCHECHTMAN E. KOHEN F. SCHERZ A. SALOMON Y. Antivascular treatment of solid melanoma tumors with bacteriochlorophyll-serine-based photodynamic therapy *Photochem. Photobiol.*, 2001, vol. 73, 257-266 [0305]
- ZITZMANN S. EHEMANN V. SCHWAB M. Arginine-Glycine-Aspartic acid (RGD)-peptide bind to both tumor and tumor-endothelial cells in vivo *Cancer res.*, 2002, vol. 62, 5139-5143 [0305]

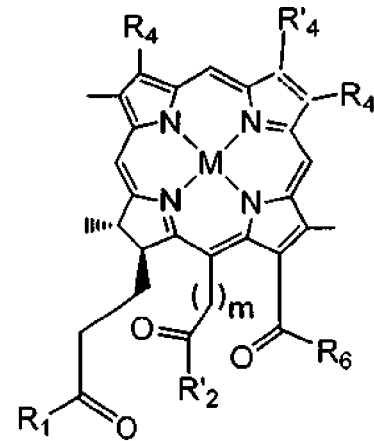
KONJUGATER AF RGD-PEPTIDER OG (BAKTERIE)CHLOROPHYL- FOTOSENSIBILISATORER SAMT ANVENDELSER DERAFT

PATENTKRAV

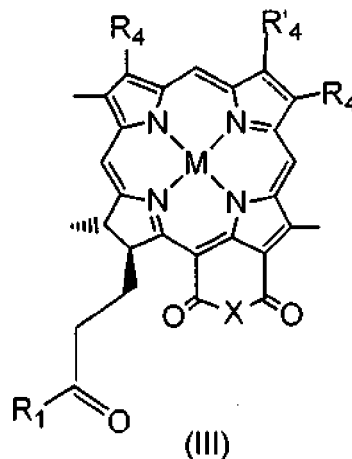
1. Konjugat af et RGD-holdigt peptid eller en ikke-peptidforbindelse, der efterligner peptider med RGD-motivet (i nærværende ansøgning RGD-peptidmimetikum), og en fotosensibilisator, som er valgt blandt et chlorophyll eller et bakteriechlorophyll med formlen I, II eller III:



(I)



(II)



(III)

hvor

M angiver 2H eller et atom, som er valgt blandt Mg, Pd, Pt, Co, Ni, Sn, Cu, Zn, Mn, In, Eu, Fe, Au, Al, Gd, Er, Yb, Lu, Ga, Y, Rh, Ru, Si, Ge, Cr, Mo, P, Re, Tc eller Tl og isotoper deraf, fortrinsvis 2H, Cu, Mn eller Pd;

X er O eller N-R₇;

R₁, R'₂ og R₆ hver især uafhængigt af hinanden er Y-R₈, -NR₉R'₉ eller -N⁺R₉R'₉R''₉A⁻; eller R₁ og R₆ tilsammen danner en ring, der omfatter en RGD-peptid- eller RGD-peptidmimetikumrest;

Y er O eller S;

R₂ er H, OH eller COOR₉;

R₃ er H, OH, C₁-C₁₂-alkyl eller C₁-C₁₂-alkoxy;

R₄ er -CH=CR₉R'₉, -CH=CR₉Hal, -CH=CH-CH₂-NR₉R'₉, -CH=CH-CH₂-N⁺R₉R'₉R''₉A⁻, CHO, -CH=NR₉, -CH=N⁺R₉R'₉A⁻, -CH₂-OR₉, -CH₂-SR₉, -CH₂-Hal, -CH₂-R₉, -CH₂-NR₉R'₉, -CH₂-N⁺R₉R'₉R''₉A⁻, -CH₂-CH₂R₉, -CH₂-CH₂Hal, -CH₂-CH₂OR₉, -CH₂-CH₂SR₉, -CH₂-CH₂-NR₉R'₉, -CH₂-CH₂-N⁺R₉R'₉R''₉A⁻, -COCH₃, C(CH₃)=CR₉R'₉, -C(CH₃)=CR₉Hal, -C(CH₃)=NR₉, -CH(CH₃)=N+R₉R'₉A⁻, -CH(CH₃)-Hal, -CH(CH₃)-OR₉, -CH(CH₃)-SR₉, -CH(CH₃)-NR₉R'₉, -CH(CH₃)-N+R₉R'₉R''₉A⁻ eller -C≡CR₉;

R'₄ er methyl eller formyl;

R₅ er =O, =S, =N-R₉, =N⁺R₉R'₉A⁻, =CR₉R'₉ eller =CR₉-Hal;

R₇, R₈, R₉, R'₉ og R''₉ hver især uafhængigt af hinanden er:

(a) H;

(b) C₁-C₂₅-hydrocarbyl;

(c) C₁-C₂₅-hydrocarbyl, der er substitueret med én eller flere funktionelle grupper, som er valgt blandt halogen, nitro, oxo, OR, SR, epoxy, epithio, -NRR', -CONRR', -CONR-NRR', -NHCONRR', -NHCONRNR', -COR, COOR'', -OSO₃R, -SO₃R'', -SO₂R, -NHSO₂R, -SO₂NRR', =N-OR, -(CH₂)_n-CO-NRR', -O-(CH₂)_n-OR, -O-(CH₂)_n-O-(CH₂)_n-R, -OPO₃RR', -PO₂HR og -PO₃R''R'', hvor n er et heltal fra 1 til 6, R og R' hver især uafhængigt af hinanden er H, hydrocarbyl eller heterocyclyl, R' kan yderligere være en rest af et RGD-peptid eller RGD-peptidmimetikum, eller R og R' sammen med det N-atom, hvortil de er bundet, danner en 5-7-leddet mættet ring, der valgfrit indeholder et yderligere heteroatom, som er valgt blandt O, S og N, hvor det yderligere N-atom kan være substitueret, og R'' er H, en kation, hydrocarbyl eller heterocyclyl;

(d) C₁-C₂₅-hydrocarbyl, der er substitueret med én eller flere funktionelle grupper, som er valgt blandt positivt ladede grupper, negativt ladede grupper, basiske grupper, der under fysiologiske betingelser er omdannet til positivt ladede grupper, og sure grupper, der under fysiologiske betingelser er omdannet til negativt ladede grupper;

(e) C₁-C₂₅-hydrocarbyl, der indeholder ét eller flere heteroatomer og/eller én eller

flere carbocykliske eller heterocykliske grupper;

(f) C₁-C₂₅-hydrocarbyl, der indeholder ét eller flere heteroatomer og/eller én eller flere carbocykliske eller heterocykliske grupper og er substitueret med én eller flere funktionelle grupper som defineret i (c) og (d) ovenfor;

(g) C₁-C₂₅-hydrocarbyl, der er substitueret med en rest af en aminosyre, et peptid, et protein, et monosaccharid, et oligosaccharid, et polysaccharid eller en polydentatligand og de chelaterende komplekser med metaller; eller

(h) en rest af en aminosyre, et peptid, et protein, et monosaccharid, et oligosaccharid, et polysaccharid; eller en polydentatligand og de chelaterende komplekser med metaller;

R₇ endvidere kan være -NRR', hvor R og R' hver især er H eller C₁-C₂₅-hydrocarbyl, der valgfrit er substitueret med en negativt ladet gruppe, fortrinsvis SO₃;

R₈ endvidere kan være H⁺ eller en kation R⁺₁₀, når R₁, R'₂ og R₆ hver især uafhængigt af hinanden er Y-R₈;

R⁺₁₀ er et metal, en ammoniumgruppe eller en organisk kation;

A⁻ er en fysiologisk acceptabel anion;

m er 0 eller 1;

den punkterede linje i positionerne 7-8 angiver en valgfri dobbeltbinding; og

farmaceutisk acceptable salte og optiske isomerer deraf;

hvor chlorophyl- eller bakteriechlorophylderivatet med formlen I, II eller III indeholder mindst ét RGD-holdigt peptid eller én RGD-peptidmimetikumrest, hvor det RGD-holdige peptid er et ligekædet eller cyklisk udelukkende L-, udelukkende D- eller et L,D-peptid sammensat af 4-100, fortrinsvis 5-50, 5-30, 5-20, mere fortrinsvis 4, 5, 6, 7, 9 eller 25 aminosyrerester, der kan være valgfrit modificerede naturlige eller ikke-naturlige aminosyrer, og RGD-peptidmimetikummet er en ikke-peptidforbindelse, der omfatter et guanidin og en carboxylterminal gruppe med en kæde på 11 atomer placeret derimellem, idet mindst 5 af atomerne er carbonatomer, hvilken kæde omfatter ét eller flere O-, S- eller N-atomer og valgfrit kan være substitueret med oxo, thioxo, halogen, amino, C₁-C₆-alkyl, hydroxyl eller carboxy, eller ét eller flere atomer i kæden kan danne en 3-6-leddet carbocyklisk eller heterocyklisk ring.

2. Konjugat ifølge krav 1, hvor det RGD-holdige peptid er et cyklisk peptid, som er valgt blandt:

(i) pentapeptidet cycloRGDfK (SEQ ID NO:1), hvor f angiver D-Phe,

- (ii) nonapeptidet, der i nærværende ansøgning er betegnet RGD-4C (SEQ ID NO:2),
 - (iii) tetrapeptidet cycloRGDK (SEQ ID NO:4),
 - (iv) pentapeptidet cycloRGDf-n(Me)K (SEQ ID NO:7), hvor f angiver D-Phe; eller
 - (v) pentapeptidet cycloRGDyK (SEQ ID NO:8), hvor y angiver D-Tyr;
- eller et ligekædet peptid, som er valgt blandt:
- (i) hexapeptidet GRGDSP (SEQ ID NO:3),
 - (ii) heptapeptidet GRGDSPK (SEQ ID NO:5) eller
 - (iii) peptidet ifølge sekvens (GRGDSP)₄K (SEQ ID NO:7);

og RGD-peptidmimetikummet har formlen:

- (i) $\text{H}_2\text{N}-\text{C}(=\text{NH})\text{NH}-(\text{CH}_2)_5-\text{CO}-\text{NH}-\text{CH}(\text{CH}_2)-(\text{CH}_2)_2-\text{COOH}$.

3. Konjugat ifølge krav 1, hvor den punkterede linje i positionerne 7-8 enten angiver en dobbeltbinding, og fotosensibilisatoren er et chlorophyl med formlen I, II eller III, eller den punkterede linje i positionerne 7-8 er fraværende, og fotosensibilisatoren er et bakteriechlorophyl med formlen I, II eller III; hvor hvert R₄, uafhængigt af hinanden, er acetyl, vinyl, ethyl eller 1-hydroxyethylradikal eller en ether eller ester af 1-hydroxyethylradikalet, og et hvilket som helst af C₁-C₂₅-hydrocarbyl er et C₁-C₂₅-alkyl, fortrinsvis C₁-C₁₀-alkyl, mere fortrinsvis C₂-C₃-alkyl.

4. Konjugat ifølge krav 1, hvor fotosensibilisatoren enten er et bakteriechlorophyl med formlen I eller II, hvor R₄ i position 3 er acetyl, R₄ i position 8 er ethyl, R'₄ er methyl, og positionerne 7-8 er hydrogeneret, eller et chlorophyl med formlen I eller II, hvor R₄ i position 3 er vinyl, R₄ i position 8 er ethyl, R'₄ er methyl, og der er en dobbeltbinding i positionerne 7-8.

5. Konjugat ifølge krav 1, hvor fotosensibilisatoren er et bakteriechlorophyl med formlen I, II eller III, og M er Pd, eller fotosensibilisatoren er et chlorophyl med formlen II, og M er 2H, Cu eller Mn.

6. Konjugat ifølge krav 1, hvor chlorophylet eller bakteriechlorophylet med formlen I, II eller III indeholder mindst én negativt ladet gruppe, som er valgt blandt COO⁻, COS⁻, SO₃⁻ eller PO₃²⁻, eller mindst én sur gruppe, som ved den fysiologiske pH-værdi er omdannet til en negativt ladet gruppe, og som er valgt blandt COOH, COSH, SO₃H eller PO₃H₂ eller et

salt deraf.

7. Konjugat ifølge krav 1, hvor chlorophylet eller bakteriechlorophylet med formlen I, II eller III indeholder mindst én positivt ladet gruppe, som er valgt blandt:

- (i) en kation, der er afledt af en N-holdig gruppe, som er valgt blandt $-N^+(RR'R'')$, $-(R)N-N^+(RR'R'')$, $O\leftarrow N^+(RR')$, $>C=N^+(RR')$, $-C(=NR)-N^+RR'R''$ og $-(R)N-C(=NR)-N^+RR'R''$ -gruppe, hvor R, R' og R'' hver især uafhængigt af hinanden er H, hydrocarbyl eller heterocyclyl, eller to af R, R' og R'' sammen med det N-atom, hvortil de er bundet, danner en 3-7-leddet mættet ring, der valgfrit indeholder ét eller flere heteroatomer, som er valgt blandt O, S eller N, og valgfrit yderligere er substitueret i det yderligere N-atom;
- (ii) en kation, der er afledt af en heteroaromatisk forbindelse, der indeholder ét eller flere N-atomer og valgfrit O- eller S-atomer, som er valgt blandt pyrazolium, imidazolium, oxazolium, thiazolium, pyridinium, quinolinium, isoquinolinium, pyrimidinium, 1,2,4-triazinium, 1,3,5-triazinium og purinium; eller
- (iii) en oniumgruppe, som er valgt blandt $-O^+(RR')$, $-S^+(RR')$, $-Se^+(RR')$, $-Te^+(RR')$, $-P^+(RR'R'')$, $-As^+(RR'R'')$, $-Sb^+(RR'R'')$ og $-Bi^+(RR'R'')$, hvor R, R' og R'' hver især uafhængigt af hinanden er H, hydrocarbyl eller heterocyclyl.

8. Konjugat ifølge krav 1, der indeholder mindst én basisk gruppe, som under fysiologiske betingelser er omdannet til en positivt ladet gruppe, hvor den mindst ene basiske gruppe er $-NRR'$, $-C(=NR)-NR'R''$, $-NR-NR'R''$, $-(R)N-C(=NR)-NR'R''$, $O\leftarrow NR-$ eller $>C=NR$, hvor hvert af R, R' og R'' uafhængigt af hinanden er H, valgfrit substitueret hydrocarbyl eller heterocyclyl, eller to af R, R' og R'' sammen med N-atomet danner en 3-7-leddet mættet ring, der valgfrit indeholder et O-, S- eller N-atom og valgfrit yderligere er substitueret i det yderligere N-atom, hvilken ring er valgt blandt aziridin, pyrrolidin, piperidin, morpholin, thiomorpholin, azepin eller piperazin, som i det yderligere N-atom valgfrit er substitueret med C₁-C₆-alkyl, der valgfrit er substitueret med halogen, hydroxyl eller amino, eller den basiske gruppe er et N-holdigt heteroaromatisk radikal, som er valgt blandt pyrazolyl, imidazolyl, oxazolyl, thiazolyl, pyridyl, quinoliny, isoquinoliny, pyrimidyl, 1,2,4-triaziny, 1,3,5-triaziny eller puriny, hvor den basiske gruppe er en endegruppe eller en gruppe, der er lokaliseret i en alkylkæde.

9. Konjugat ifølge et hvilket som helst af kravene 1 og 3 til 8, hvor fotosensibilisatoren er valgt blandt:

(i) et chlorophyll eller bakteriechlorophyll med formlen II, og R_6 er en basisk gruppe $-NR_9R'_9$, hvor R_9 er H, og R'_9 er C_1 - C_6 -alkyl, der er substitueret med en basisk gruppe $-NH-(CH_2)_{2-6}-NRR'$, hvor hvert af R og R' uafhængigt af hinanden er H, C_1 - C_6 -alkyl, der valgfrit er substitueret med NH_2 , eller R og R' sammen med N-atomet danner en 5-6-leddet mættet ring, der valgfrit indeholder et O- eller N-atom og i det yderligere N-atom valgfrit yderligere er substitueret med $-(CH_2)_{2-6}-NH_2$, hvor R_6 fortrinsvis er $-NH-(CH_2)_3-NH-(CH_2)_3-NH_2$, $-NH-(CH_2)_2$ -1-morpholino eller $-NH-(CH_2)_3$ -piperazino- $(CH_2)_3-NH_2$;

(ii) et chlorophyll eller bakteriechlorophyll med formlen II, og R_1 og R_6 tilsammen danner en cyklisk ring, der omfatter et RGD-peptid eller RGD-peptidmimetikum;

(iii) et chlorophyll eller bakteriechlorophyll med formlen III, hvor X er $-N-R_7$, R_7 er $-NRR'$, R er H, og R' er C_2 - C_6 -alkyl, der er substitueret med SO_3^- eller et alkalinsalt deraf, hvor R_7 fortrinsvis er $-NH-(CH_2)_3-SO_3K$;

(iv) et chlorophyll eller bakteriechlorophyll med formlen II, og R_6 er $-NR_9R'_9$, R_9 er H, og R'_9 er $HOCH_2-CH(OH)-CH_2^-$;

(v) et chlorophyll eller bakteriechlorophyll med formlen II, og R_6 er $-NR_9R'_9$, R_9 er H, og R'_9 er C_1 - C_6 -alkyl, der er substitueret med en polydentatligand eller de chelaterende komplekser med metaller, fortrinsvis et bakteriechlorophyll med formlen II, og polydentatliganden er EDTA, DTPA eller DOTA; R_6 er $-NR_9R'_9$, fortrinsvis $-NH-(CH_2)_3-NH-DTPA$, R_9 er H, og R'_9 er C_1 - C_6 -alkyl, der er substitueret med en polydentatligand eller de chelaterende komplekser med metaller såsom Gd; eller

(vi) et chlorophyll eller bakteriechlorophyll med formlen II, og R_6 er $-NR_9R'_9$, hvor R_9 er H, og R'_9 er C_1 - C_{10} -alkyl, der er substitueret med SO_3H eller et alkalinsalt deraf, fortrinsvis er R_6 $-NH-(CH_2)_2-SO_3K$.

10. Konjugat ifølge krav 1, som er valgt blandt:

(i) et konjugat, hvor fotosensibilisatoren er et bakteriechlorophyll med formlen II, hvor M er Pd; m er 1; R_1 er NH-P, hvor P er resten af RGD-peptidmimetikummet; R'_2 er methoxy; R_4 er i position 3 acetyl og er i position 8 ethyl; R'_4 er methyl; og R_6 er $-NH-(CH_2)_2-SO_3K$ (konjugat **40**) eller $-NH-(CH_2)_2-SO_3K$ (konjugat **41**);

(ii) et konjugat, hvor fotosensibilisatoren er et bakteriechlorophyll med formlen II,

hvor m er 1; R'_2 er methoxy; R_4 er i position 3 acetyl og er i position 8 ethyl; R'_4 er methyl; og enten R_1 og R^6 tilsammen danner en cyklisk ring, der omfatter $-\text{NH-RGD-CO-NH}-(\text{CH}_2)_2-\text{NH}-$, og M er Pd (konjugat **37**), eller M er 2H (konjugat **38**), eller R_1 og R_6 tilsammen danner en cyklisk ring, der omfatter $-\text{NH-RGD-CO-NH}-(\text{CH}_2)_3\text{-piperazino}-(\text{CH}_2)_3-\text{NH}-$, og M er Pd (konjugat **39**);

(iii) et konjugat, hvor fotosensibilisatoren er et chlorophyl med formlen II, hvor m er 1; R'_2 er methoxy; R_1 er NH-P, hvor P er resten af det RGD-holdige peptid ifølge SEQ ID NO:1; R_4 er i position 3 vinyl og er i position 8 ethyl; R'_4 er methyl; R_6 er $-\text{NH}-(\text{CH}_2)_2-\text{SO}_3\text{K}$, og M er 2H (konjugat **16**), M er Mn (konjugat **17**) eller M er Cu (konjugat **18**);

(iv) et konjugat, hvor fotosensibilisatoren er et bakteriechlorophyl med formlen I, hvor R_1 er NH-P, hvor P er resten af det RGD-holdige peptid ifølge SEQ ID NO:1; R_2 er OH; R_3 er COOCH_3 ; R_4 er i position 3 acetyl og er i position 8 ethyl; R'_4 er methyl; R_5 er O; og M er Mn (konjugat **12**) eller R_2 er H, og M er 2H (konjugat **27**);

(v) et konjugat, hvor fotosensibilisatoren er et bakteriechlorophyl med formlen I, hvor M er 2H; R_1 er $\text{NH}-(\text{CH}_2)_2-\text{NH-CO-P}$, hvor P er resten af det RGD-holdige peptid ifølge SEQ ID NO:4; R_2 er H; R_3 er COOCH_3 ; R_4 er i position 3 acetyl og er i position 8 ethyl; R'_4 er methyl; og R_5 er O (konjugat **32**);

(vi) et konjugat, hvor fotosensibilisatoren er et bakteriechlorophyl med formlen II, hvor M er Pd; m er 1; R_1 er NH-P, hvor P er resten af det RGD-holdige peptid ifølge SEQ ID NO:2; R'_2 er methoxy; R_4 er i position 3 acetyl og er i position 8 er ethyl; R'_4 er methyl; og R_6 er $-\text{NH}-(\text{CH}_2)_2-\text{SO}_3\text{K}$ (konjugat **11**);

(vii) konjugat, hvor fotosensibilisatoren er et bakteriechlorophyl med formlen II, hvor m er 1; R_1 er NH-P, hvor P er resten af det RGD-holdige peptid ifølge SEQ ID NO:1; R'_2 er methoxy; R_4 er i position 3 acetyl og er i position 8 ethyl; R'_4 er methyl; og R_6 er $-\text{NH}-(\text{CH}_2)_2-\text{SO}_3\text{K}$; og M er 2H (konjugat **13**), M er Mn (konjugat **14**), M er Cu (konjugat **15**), eller M er Pd (konjugat **24**);

(viii) et konjugat, hvor fotosensibilisatoren er et bakteriechlorophyl med formlen III, hvor M er Pd; R_1 er NH-P, hvor P er resten af det RGD-holdige peptid ifølge SEQ ID NO:1; R_4 er i position 3 acetyl og er i position 8 ethyl; R'_4 er methyl; X er N- R_7 , og R_7 er $-\text{NH}-(\text{CH}_2)_3-\text{SO}_3\text{K}$ (konjugat **19**);

(ix) et konjugat, hvor fotosensibilisatoren er et bakteriechlorophyl med formlen II, hvor M er 2H; m er 1; R_1 er NH-P, hvor P er resten af det RGD-holdige peptid ifølge

SEQ ID NO: 3; R'₂ er methoxy; R₄ er i position 3 acetyl og er i position 8 ethyl; R'₄ er methyl; og R₆ er -NH-(CH₂)₂-SO₃K (konjugat **26**);

(x) et konjugat, hvor fotosensibilisatoren er et bakteriechlorophyl med formlen II, hvor M er Pd; m er 1; R'₂ er methoxy; R₄ er i position 3 acetyl og er i position 8 ethyl; R'₄ er methyl; R₆ er -NH-(CH₂)₂-SO₃K, og R₁ er NH-P, hvor P er resten af det RGD-holdige peptid ifølge SEQ ID NO:5 (konjugat **33**), SEQ ID NO:6 (konjugat **34**) eller SEQ ID NO:7 (konjugat **35**);

(xi) et konjugat, hvor fotosensibilisatoren er et bakteriechlorophyl med formlen II, hvor M er Pd; m er 1; R₁ er NH-CH(-(CH₂)₂-CO-NH-P)₂, hvor P er resten af det RGD-holdige peptid ifølge SEQ ID NO:8; R'₂ er methoxy; R₄ er i position 3 acetyl og er i position 8 ethyl; R'₄ er methyl; og R₆ er -NH-(CH₂)₂-SO₃K (konjugat **36**);

(xii) et konjugat, hvor fotosensibilisatoren er et bakteriechlorophyl med formlen II, hvor M er Pd; m er 1; R₁ er NH-P, hvor P er resten af det RGD-holdige peptid ifølge SEQ ID NO:1; R'₂ er methoxy; R₄ er i position 3 acetyl og er i position 8 ethyl; R'₄ er methyl; og R₆ er -NH-CH₂-CH(OH)-CH₂OH (konjugat **23**); eller

(xiii) et konjugat, hvor fotosensibilisatoren er et bakteriechlorophyl med formlen II, hvor M er 2H; m er 1; R₁ er NH-P, hvor P er resten af det RGD-holdige peptid ifølge SEQ ID NO:1; R'₂ er methoxy; R₄ er i position 3 acetyl og er i position 8 ethyl; R'₄ er methyl; og R₆ er -NH-(CH₂)₃-NH-CO-DTPA (konjugat **43**) eller chelatkomplekset med Gd (konjugat **44**).

11. Bakteriechlorophyl med formlen II i krav 1, hvor M er Pd; R₁ er COOH; m er 1; R'₂ er methoxy; R₄ er i position 3 acetyl og er i position 8 ethyl; R'₄ er methyl; og R₆ er -NH-CH₂-CH(OH)-CH₂-OH (forbindelse **10**).

12. Farmaceutisk sammensætning, der omfatter et konjugat af et RGD-holdigt peptid eller et RGD-peptidmimetikum og en fotosensibilisator, som er valgt blandt et chlorophyl eller et bakteriechlorophyl som defineret i et hvilket som helst af kravene 1 til 11, og en farmaceutisk acceptabel bærer.

13. Farmaceutisk sammensætning ifølge krav 12, hvor konjugatet er valgt blandt:

(i) palladium 3¹-oxo-15-methoxycarbonylmethyl-rhodobacteriochlorin 13¹-(2-sulfoethyl)amid-17³-(RGD-4C)amid-kaliumsalt (konjugat **11**);

- (ii) mangan(III) 13²-OH-bacteriopheophorbid-17³-(cycloRGDfK)amid (konjugat **12**);
- (iii) 3¹-oxo-15-methoxycarbonylmethyl-rhodobacteriochlorin 13¹-(2-sulfoethyl)amid-17³-(cycloRGDfK)amid-kaliumsalt (konjugat **13**);
- (iv) kobber(II) 3¹-oxo-15-methoxycarbonylmethyl-rhodobacteriochlorin 13¹-(2-sulfoethyl)amid-17³-(cycloRGDfK)amid-kaliumsalt (konjugat **15**);
- (v) 3¹,3²-didehydrorhodochlorin 13¹-(2-sulfoethyl)amid-17³-(cycloRGDfK)amid-kaliumsalt (konjugat **16**);
- (vi) mangan(III) 3¹,3²-didehydrorhodochlorin 13¹-(2-sulfoethyl)amid-17³-(cycloRGDfK)amid-kaliumsalt (konjugat **17**);
- (vii) kobber(II) 3¹,3²-didehydrorhodochlorin 13¹-(2-sulfoethyl)amid-17³-(cycloRGDfK)amid-kaliumsalt (konjugat **18**);
- (viii) palladium-bacteriopurpurin N-(3-sulfopropylamino)imid-17³-(cycloRGDfK)amid-kaliumsalt (konjugat **19**);
- (ix) palladium 3¹-oxo-15-methoxycarbonylmethyl-rhodobacteriochlorin-13¹-(2,3-dihydroxypropyl)amid-17³-(cycloRGDfK)amid (konjugat **23**);
- (x) palladium 3¹-oxo-15-methoxycarbonylmethyl-rhodobacteriochlorin 13¹-(2-sulfoethyl)amid-17³-(cycloRGDfK)amid-kaliumsalt (konjugat **24**);
- (xi) 3¹-oxo-15-methoxycarbonylmethyl-rhodobacteriochlorin 13¹-(2-sulfoethyl)amid-17³-(GRGDSP)amid-kaliumsalt (konjugat **26**);
- (xii) bacteriopheophorbid-17³-(cycloRGDfK)amid (konjugat **27**);
- (xiii) 3¹-oxo-15-methoxycarbonylmethyl-rhodobacteriochlorin 13¹-(3-[(3-aminopropyl)amino]propyl)amid-17³-(cycloRGDfK)amid (konjugat **28**);
- (xiv) 3¹-oxo-15-methoxycarbonylmethyl-rhodobacteriochlorin 13¹-(2,3-dihydroxypropyl)amid-17³-(cycloRGDfK)amid (konjugat **29**);
- (xv) 3¹-oxo-15-methoxycarbonylmethyl-rhodobacteriochlorin 13¹-(2-morpholino-N-ethyl)amid-17³-(cycloRGDfK)amid (konjugat **30**);
- (xvi) 3¹-oxo-15-methoxycarbonylmethyl-rhodobacteriochlorin 13¹-{3-[4-(3-aminopropyl)-piperazin-1-yl]-propyl}amid-17³-(cycloRGDfK)amid (konjugat **31**);
- (xvii) bacteriopheophorbid-17³-(2-cycloRGDK-amido-N-ethyl)amid (konjugat **32**);
- (xviii) palladium 3¹-oxo-15-methoxycarbonylmethyl-rhodobacteriochlorin 13¹-(2-sulfoethyl)amid-17³-(GRGDSPK)amid-kaliumsalt (konjugat **33**);

- (xix) palladium 3¹-oxo-15-methoxycarbonylmethyl-rhodobacteriochlorin 13¹-(2-sulfoethyl)amid-17³-[(GRGDSP)₄K]amid-kaliumsalt (konjugat **34**);
- (xx) palladium 3¹-oxo-15-methoxycarbonylmethyl-rhodobacteriochlorin 13¹-(2-sulfoethyl)amid-17³-(cycloRGDf-N(Me)K)amid-kaliumsalt (konjugat **35**);
- (xxi) palladium 3¹-oxo-15-methoxycarbonylmethyl-rhodobacteriochlorin 13¹-(2-sulfoethyl)-17³-N-[4-heptandisyre bis-(cycloRGDyK-amido)]amid-kaliumsalt (konjugat **36**);
- (xxii) palladium 3¹-oxo-15-methoxycarbonylmethyl-rhodobacteriochlorin 13¹-(2-sulfoethyl)amid-17³-[4-(methyl-5-(6-guanidino-hexanoylamino)-pentansyre)]amid-kaliumsalt (konjugat **40**);
- (xxiii) palladium 3¹-oxo-15-methoxycarbonylmethyl-rhodobacteriochlorin 13¹-(2-sulfoethyl)amid-17³-[7-amido-3-[[1-(4-guanidino-butyryl)-piperidin-3-carbonyl]-amino]-heptansyre]-kaliumsalt (konjugat **41**);
- (xxiv) 3¹-oxo-15-methoxycarbonylmethyl-rhodobacteriochlorin 13¹-(3-DTPA-amido-N-propyl)amid-17³-(cycloRGDfK)amid (konjugat **43**); og
- (xxv) 3¹-oxo-15-methoxycarbonylmethyl-rhodobacteriochlorin 13¹-(3-Gd-DTPA-amido-N-propyl)amid-17³-(cycloRGDfK)amid (konjugat **44**),
- fortrinsvis palladium 3¹-oxo-15-methoxycarbonylmethyl-rhodobacteriochlorin 13¹-(2-sulfoethyl)amid-17³-(cycloRGDfK)amid-kaliumsalt (konjugat **24**).

14. Farmaceutisk sammensætning ifølge krav 12 eller 13 til anvendelse ved fotodynamisk terapi (PDT) eller vaskulær PDT (VTP).

15. Farmaceutisk sammensætning ifølge krav 14 til anvendelse ved behandling af: (i) tumorer, herunder primære tumorer eller metastatiske tumorer såsom melanom, kolon-, bryst-, lunge-, prostata-, hjerne- eller hoved- og halscancer; (ii) ikke-neoplastisk væv; (iii) aldersrelateret makuladegeneration; og (iv) adipositas.

16. Farmaceutisk sammensætning ifølge krav 12 eller 13 til anvendelse til diagnostiske formål, herunder: visualisering af organer og væv samt diagnose af tumorer, herunder:

(i) tumordiagnose ved dynamisk fluorescensbilleddannelse, hvor M i fotosensibilisatoren er 2H eller et metal, som er valgt blandt Cu, Pd Gd, Pt, Zn, Al, Eu, Er, Yb eller isotoper deraf;

(ii) tumordiagnose ved radiodiagnostisk teknik, hvor M i fotosensibilisatoren er en

radioisotop, som er valgt blandt ^{64}Cu , ^{67}Cu , $^{99\text{m}}\text{Tc}$, ^{67}Ga , ^{201}Tl , ^{195}Pt , ^{60}Co , ^{111}In og ^{51}Cr , fortrinsvis hvor den radiodiagnostiske teknik er positronemissionstomografi (PET), og M er ^{64}Cu eller ^{67}Cu , eller hvor den radiodiagnostiske teknik er enkeltfotonemissionstomografi (SPET), og M er en radioisotop, som er valgt blandt $^{99\text{m}}\text{Tc}$, ^{67}Ga , ^{195}Pt , ^{111}In , ^{51}Cr og ^{60}Co ; og

(iii) tumordiagnose ved hjælp af molekylær magnetisk resonansbilleddannelse (MRI), hvor M er et paramagnetisk metal, som er valgt blandt Mn^{3+} , Cu^{2+} , Fe^{3+} , Eu^{3+} , Gd^{3+} og Dy^{3+} , eller fotosensibilisatoren er substitueret med et metal-chelat-kompleks af en polydentatligand, og metallet er som defineret ovenfor.

17. Farmaceutisk sammensætning ifølge krav 12 til anvendelse ved tumorradioterapi, hvor M er en radioisotop, som er valgt blandt ^{103}Pd , ^{195}Pt , ^{105}Rh , ^{106}Rh , ^{188}Re , ^{177}Lu , ^{164}Er , $^{117\text{m}}\text{Sn}$, ^{153}Sm , ^{90}Y , ^{67}Cu og ^{32}P .

DRAWINGS

Fig. 1A

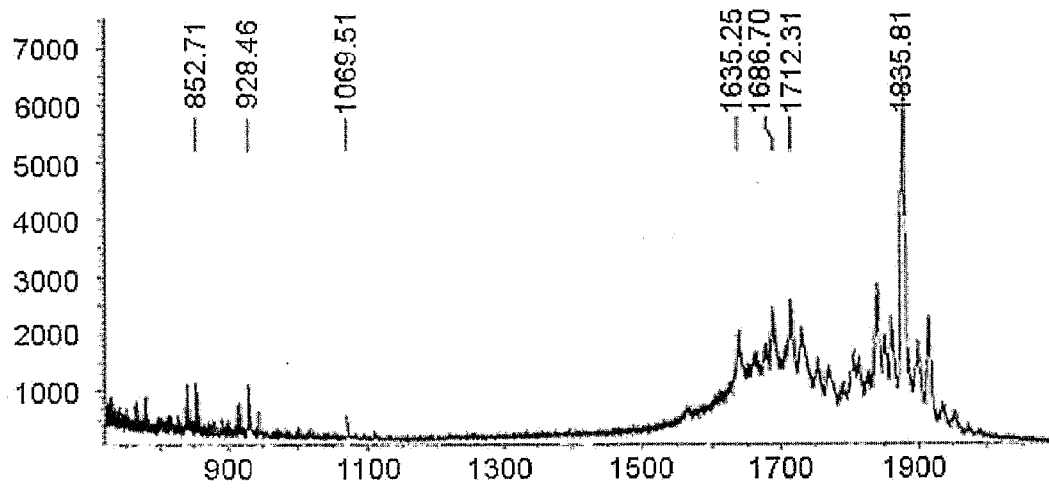


Fig. 1B

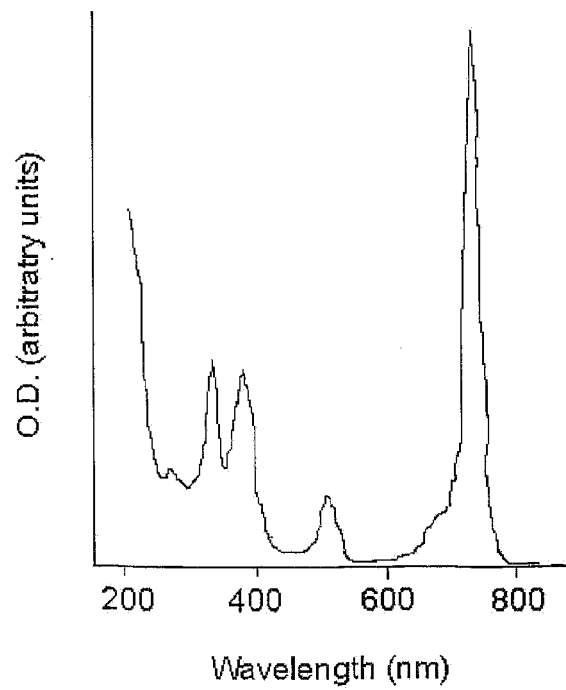


Fig. 1C

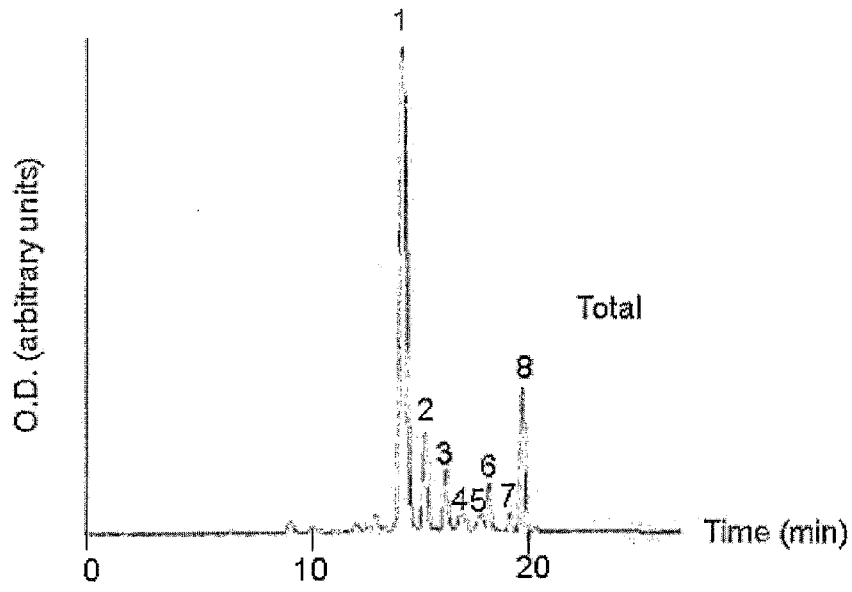


Fig. 2A

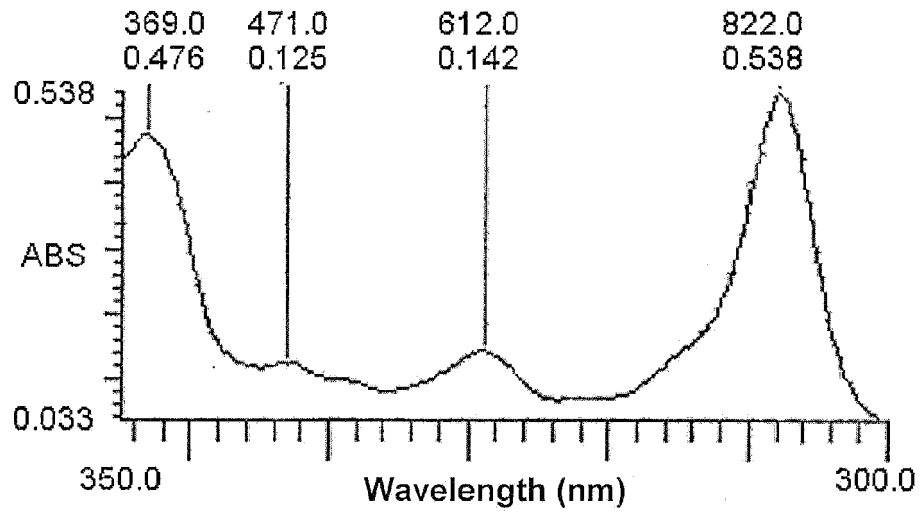


Fig. 2B

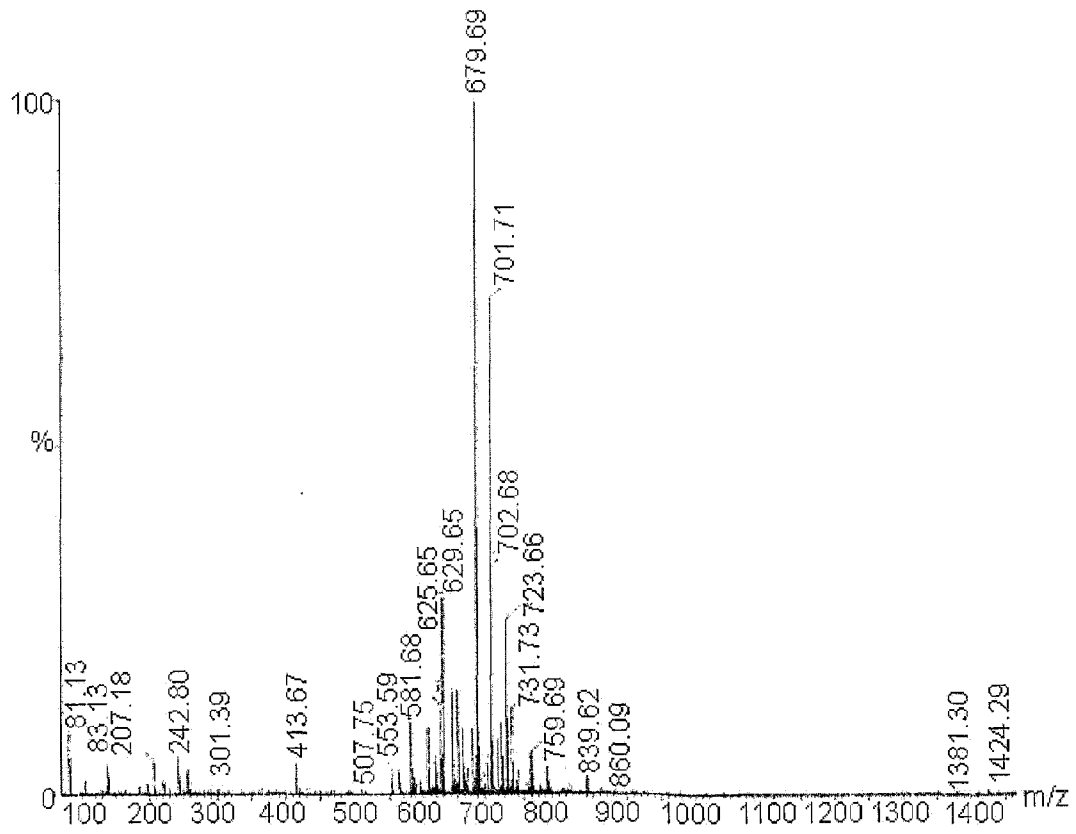


Fig. 3A

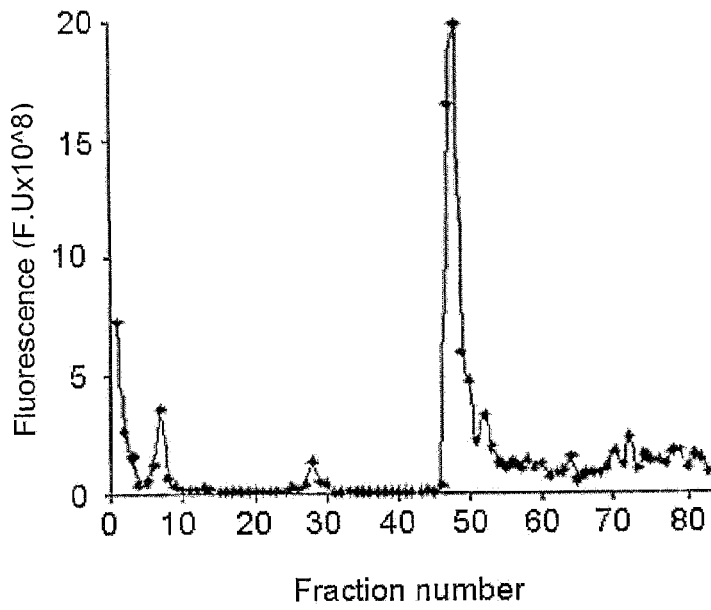


Fig. 3B

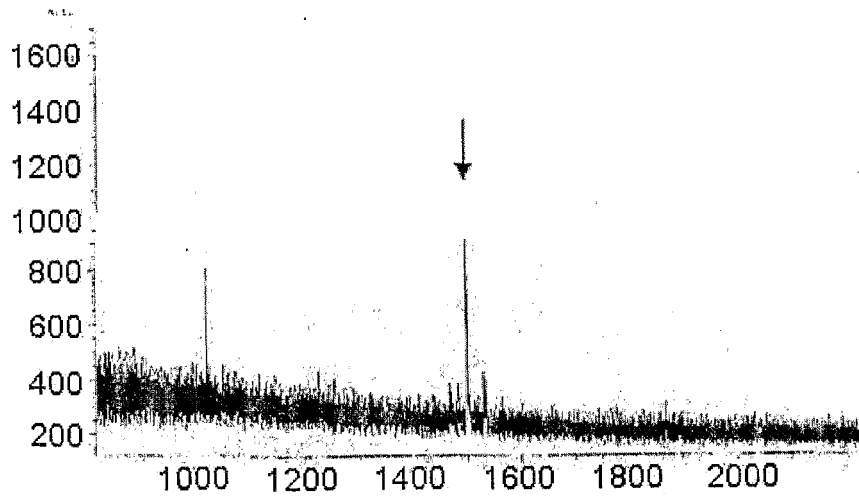


Fig. 4

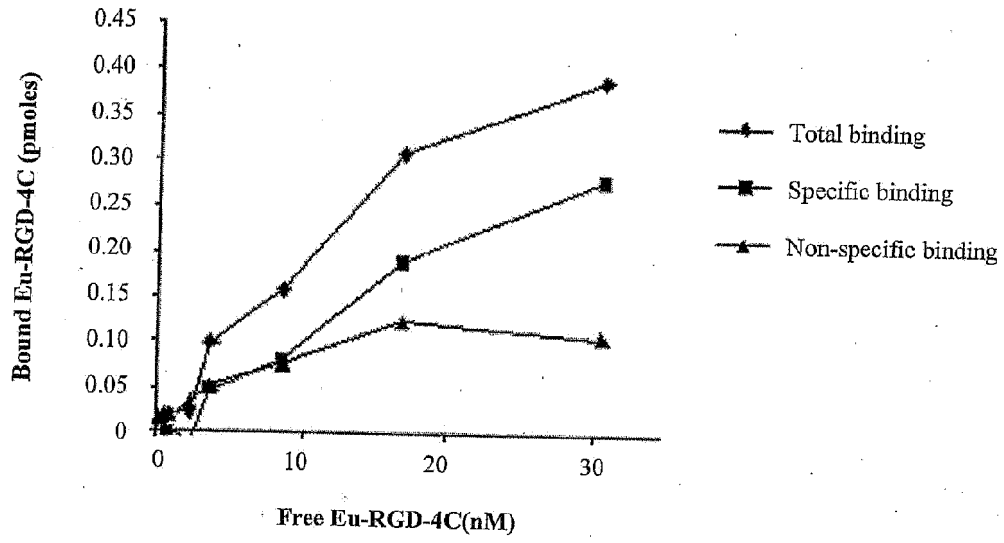


Fig. 5

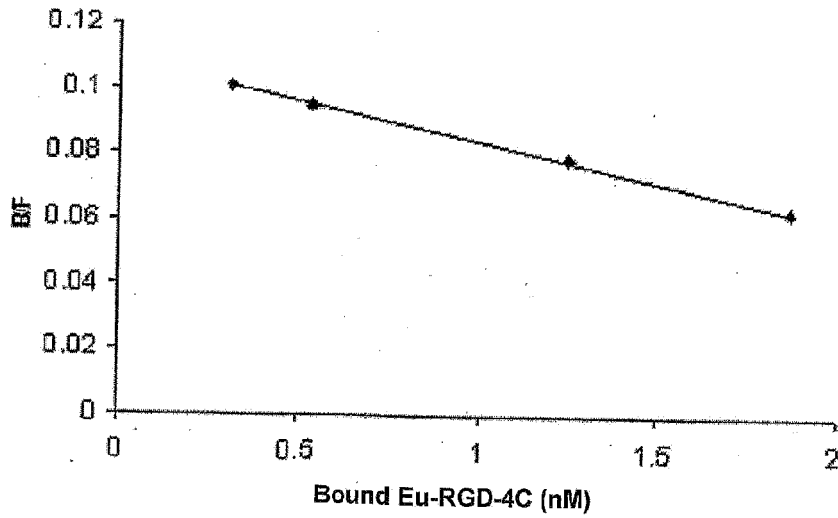


Fig. 6

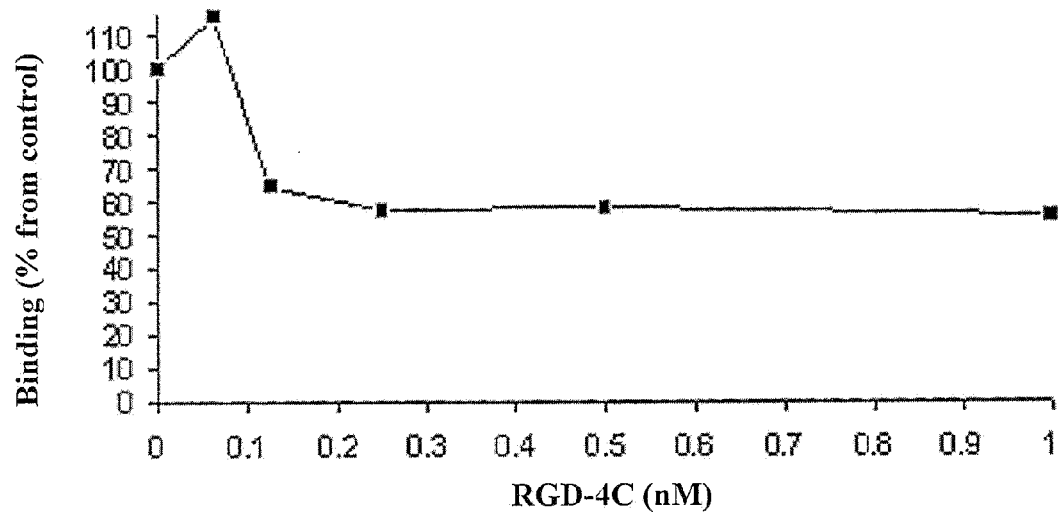


Fig. 7A

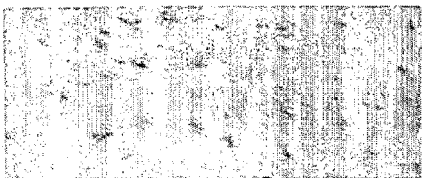


Fig. 7B

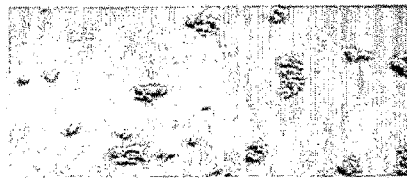


Fig. 8

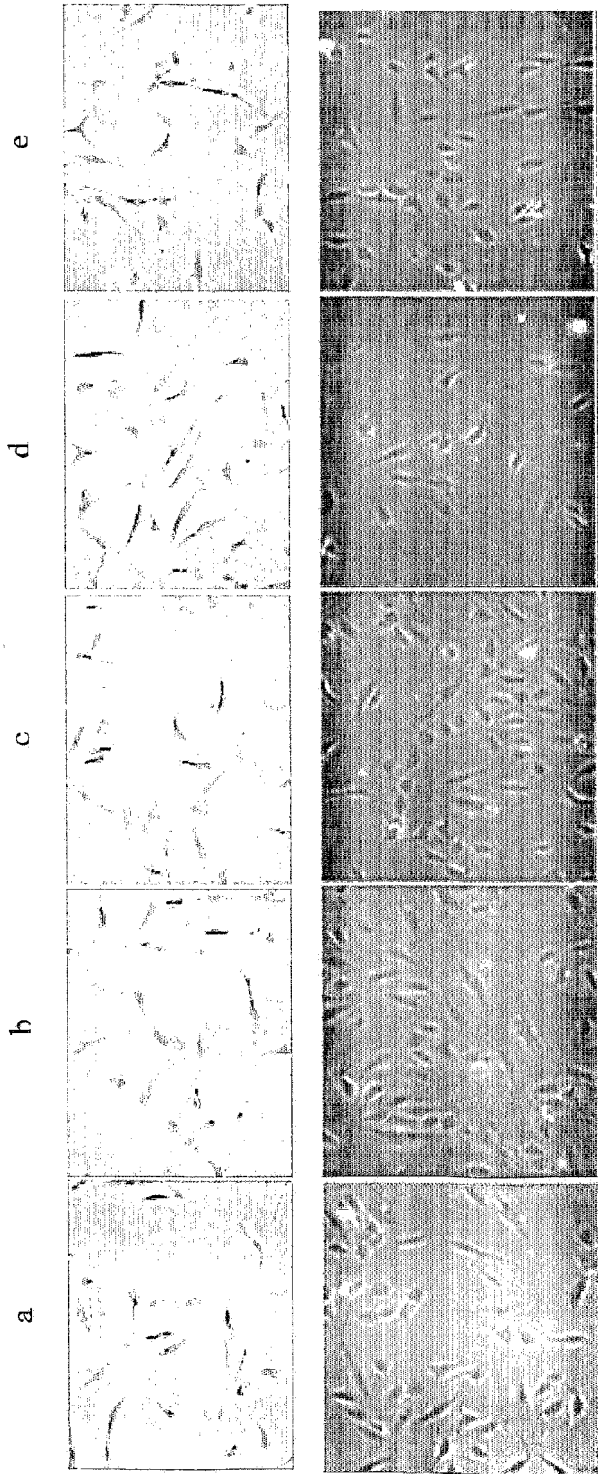


Fig. 9

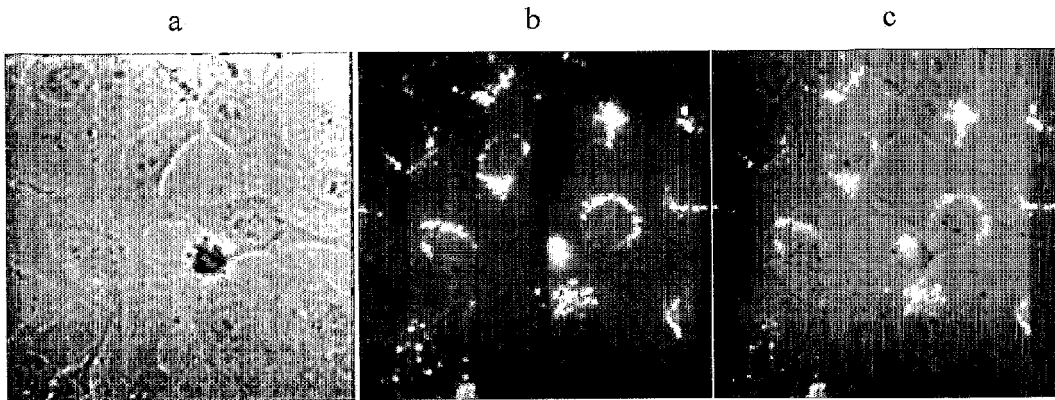


Fig. 10

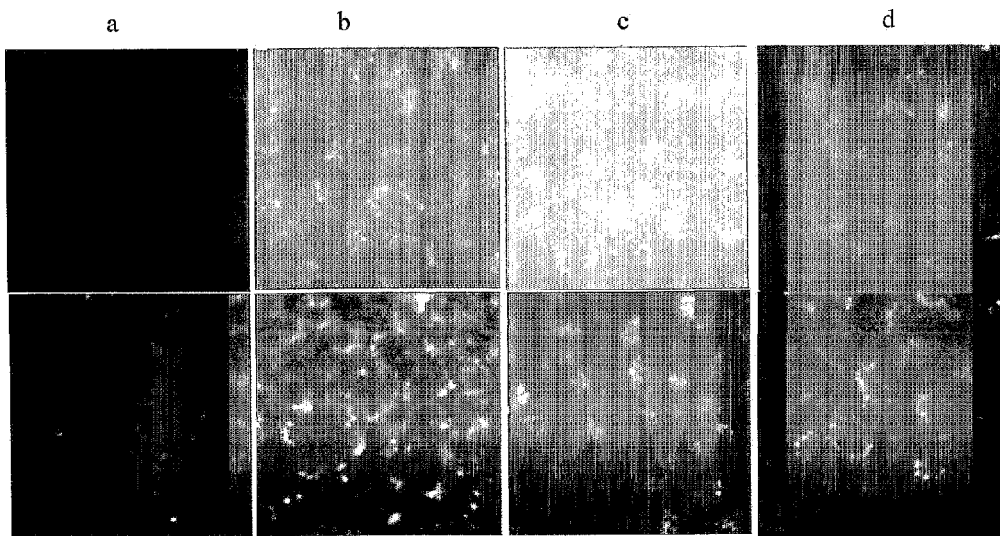


Fig. 11A

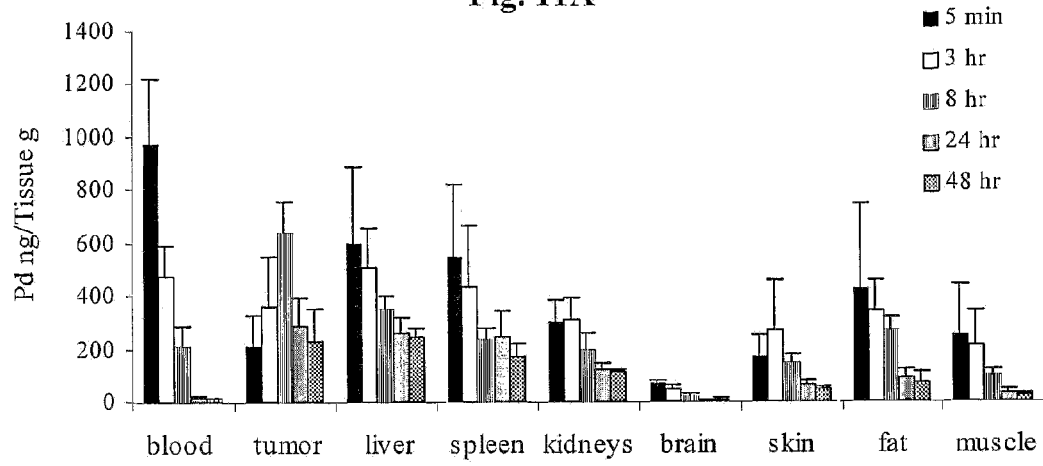


Fig. 11B

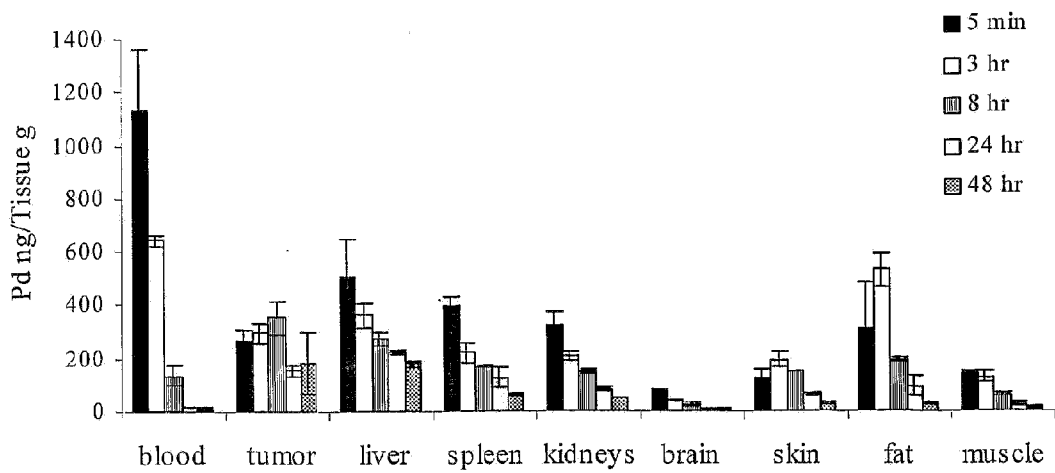


Fig. 11C

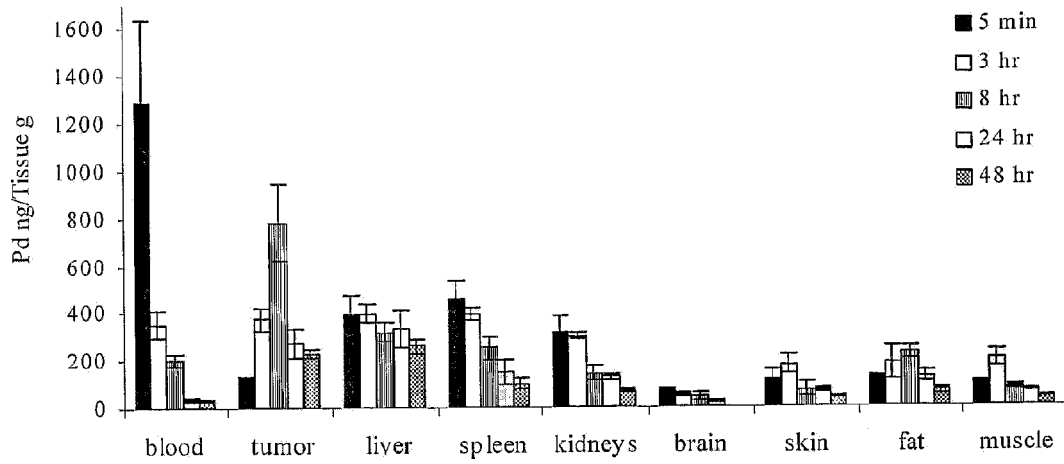


Fig. 12

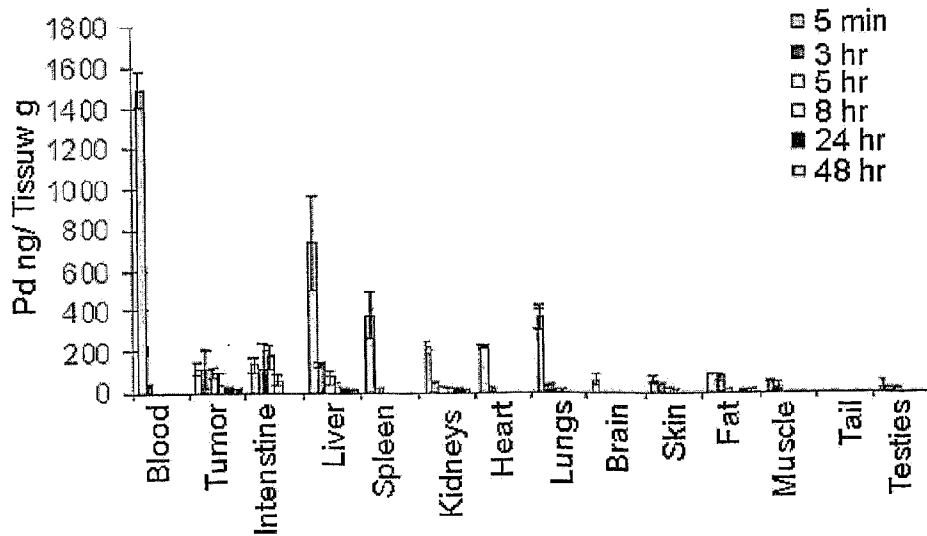


Fig. 13

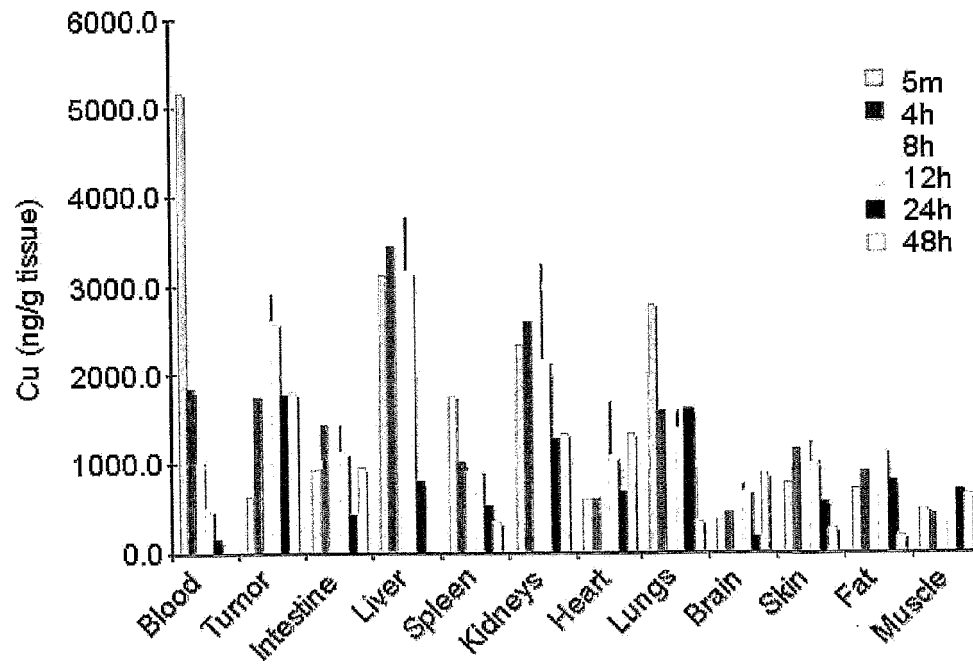


Fig. 14A

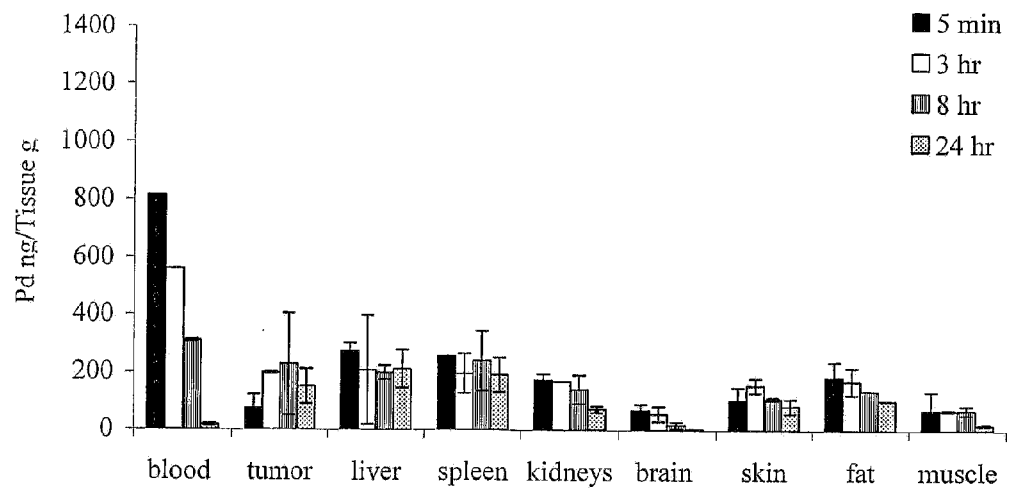


Fig. 14B

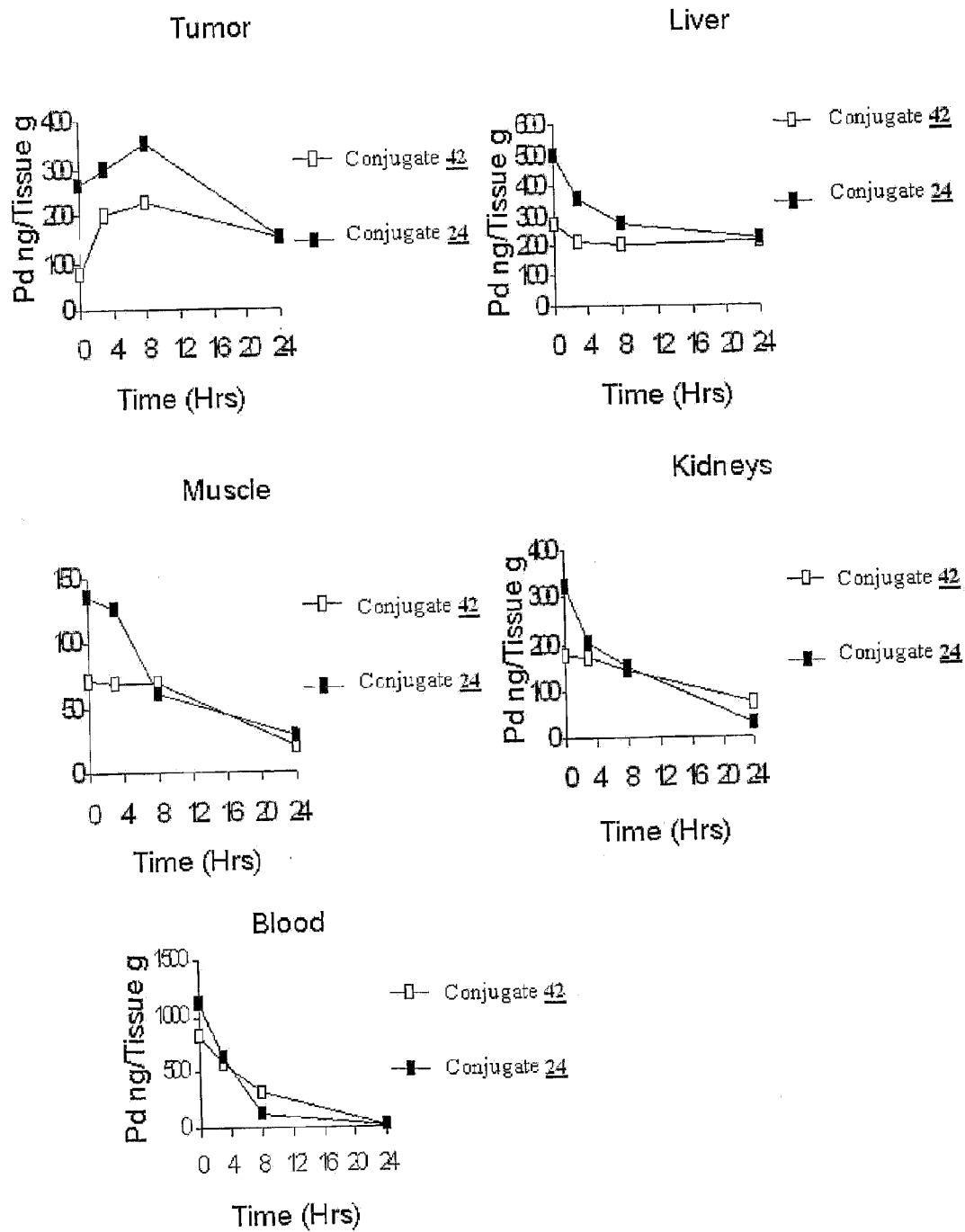


Fig. 15

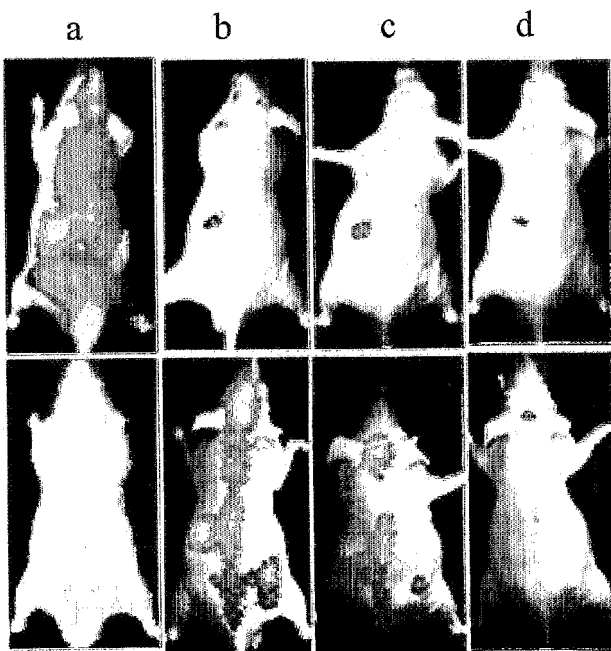


Fig. 16A



Fig. 16B

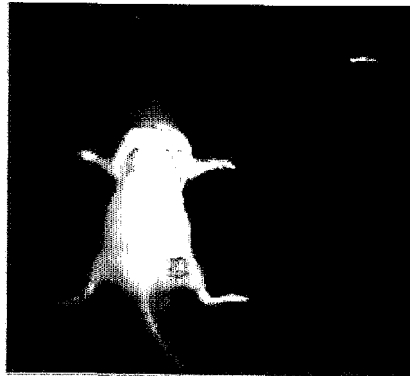


Fig. 16C



Fig. 17A

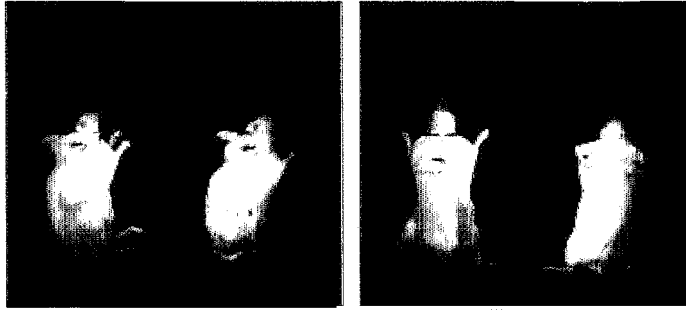


Fig. 17B

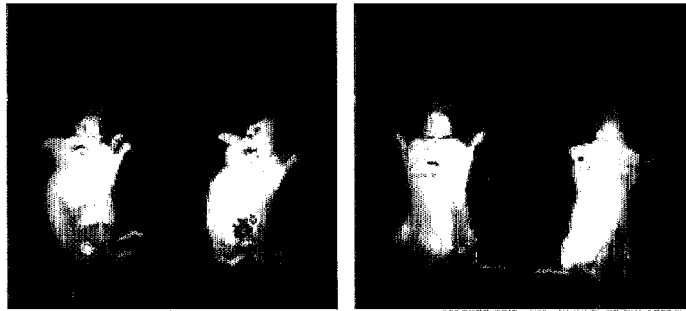


Fig. 17C

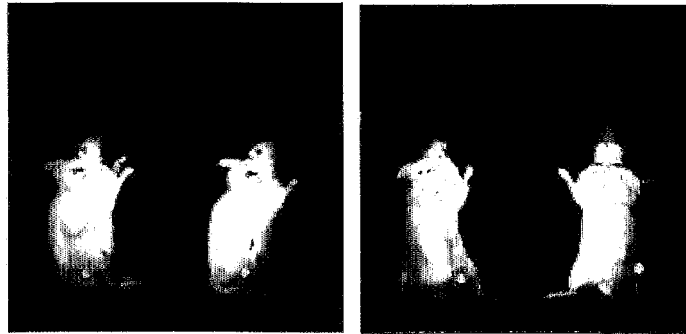


Fig. 18

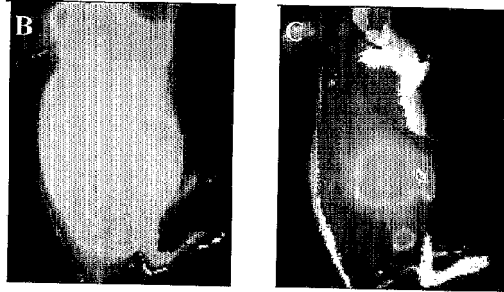


Fig. 19

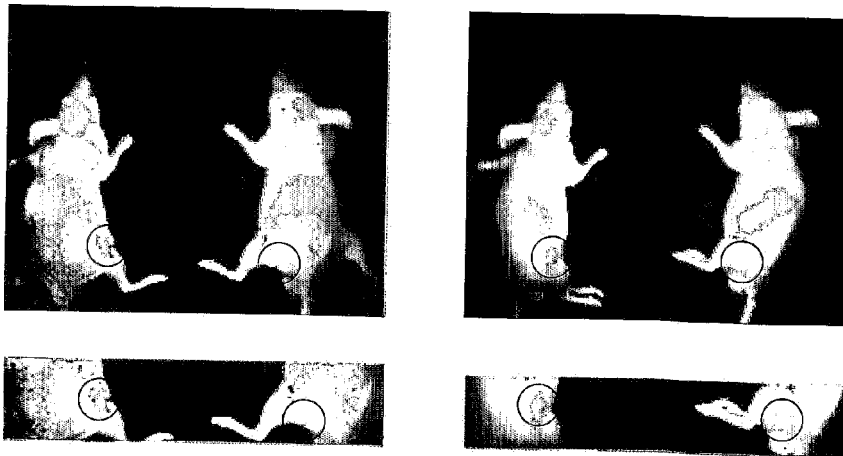


Fig. 20

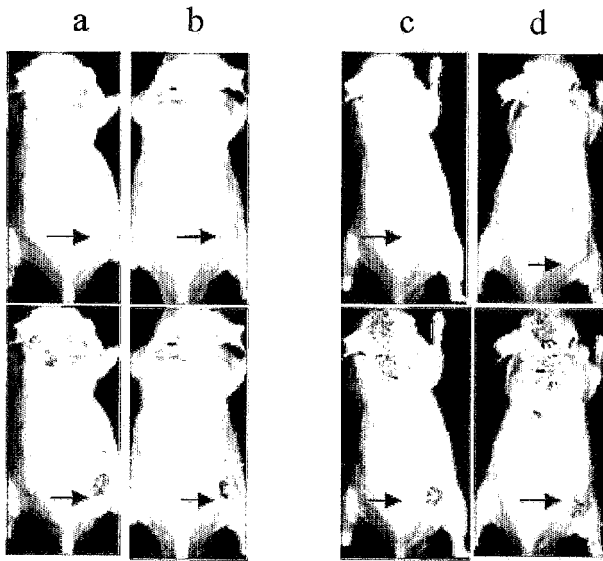


Fig. 21

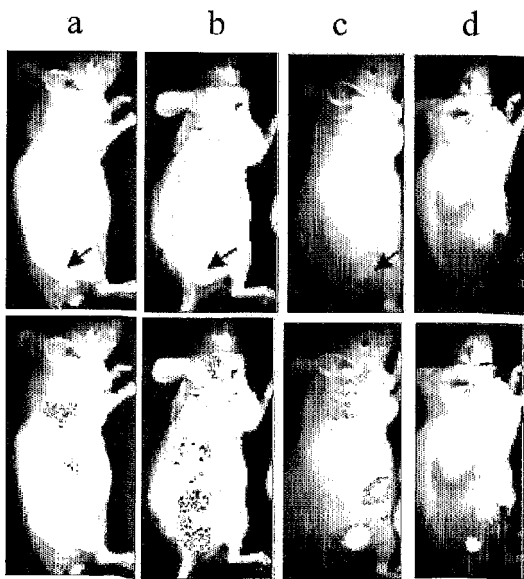
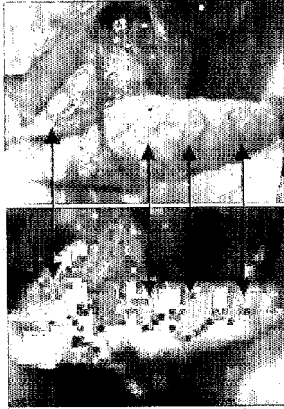


Fig. 22



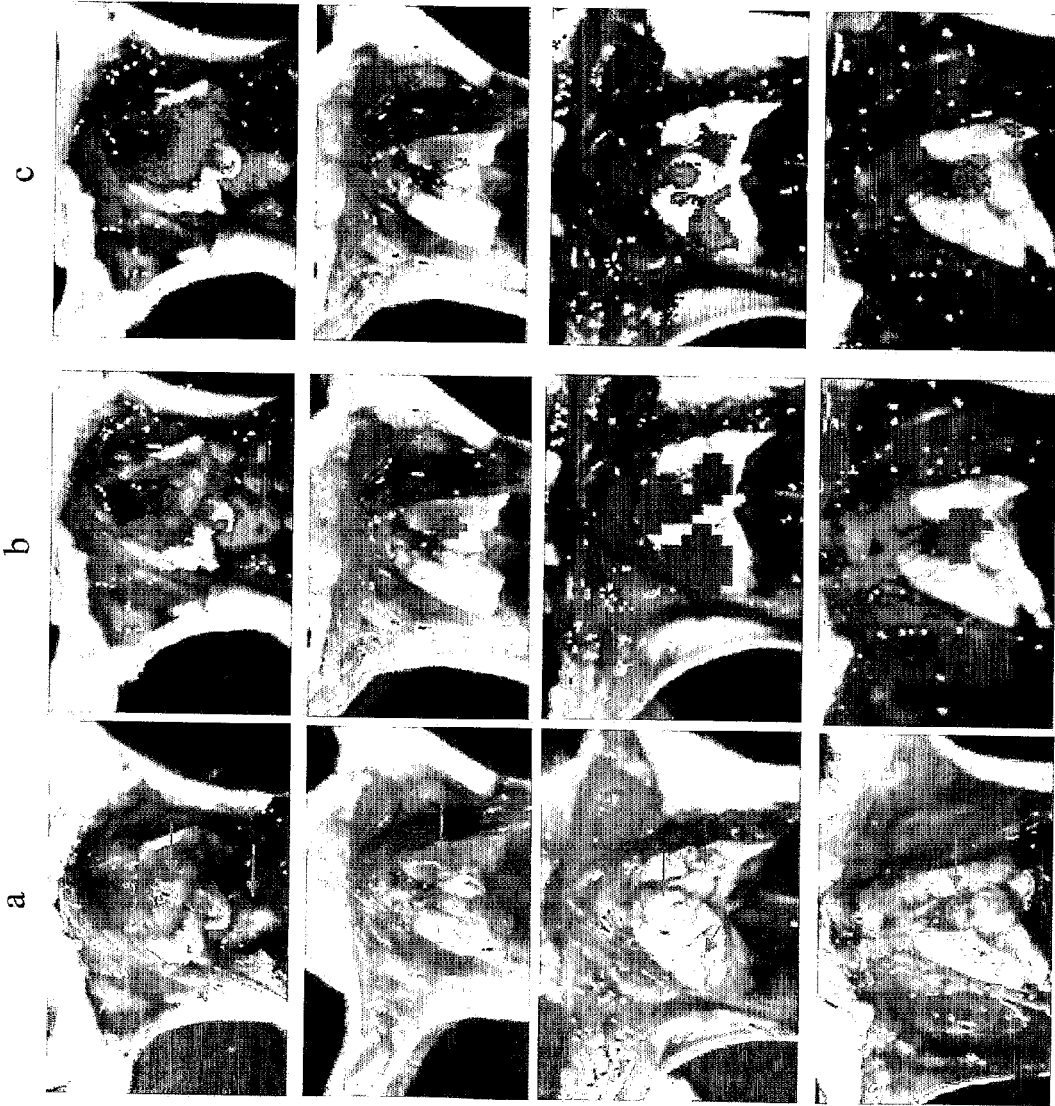


Fig. 23A

Fig. 23B

Fig. 23C

Fig. 23D

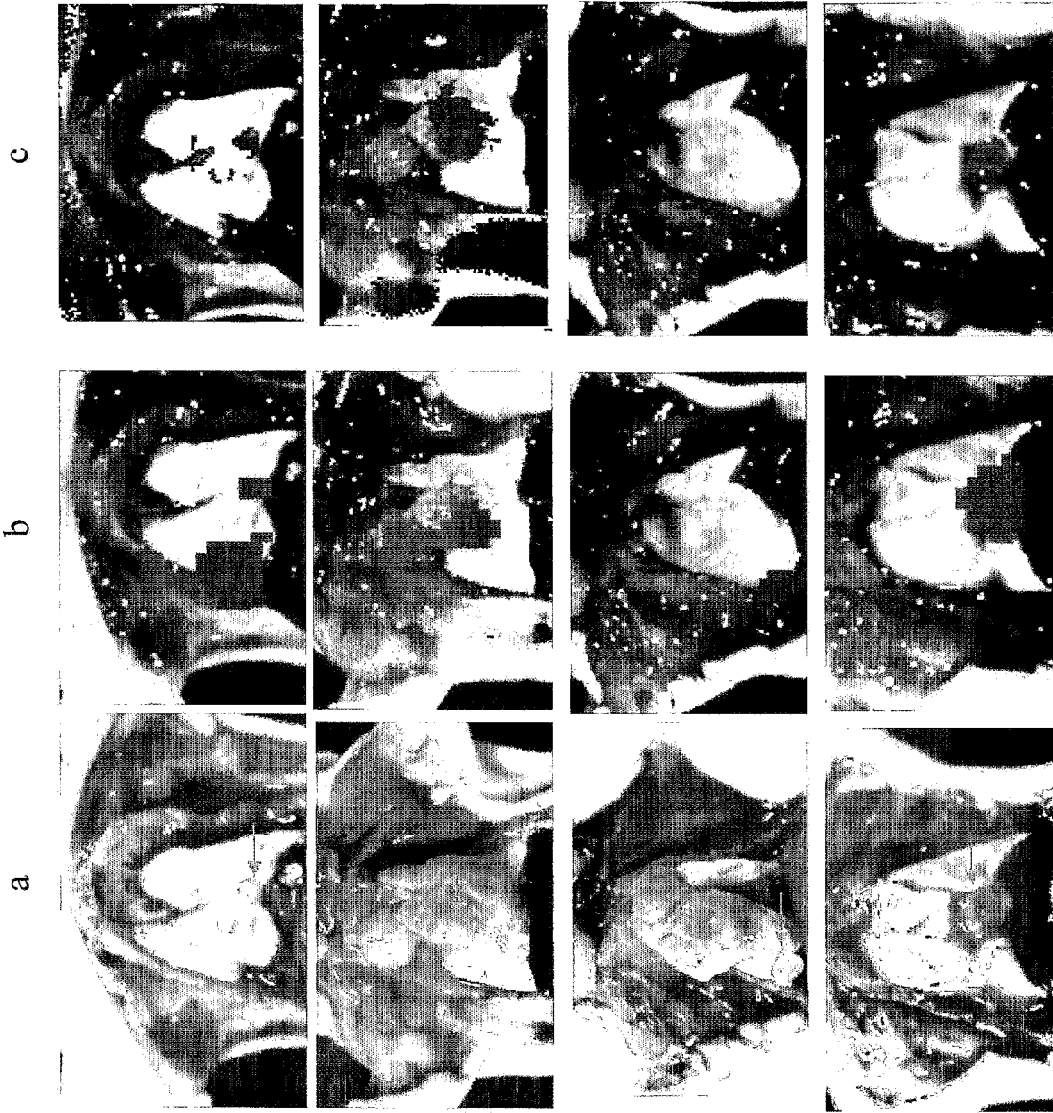


Fig. 23E

Fig. 23F

Fig. 23G

Fig. 23H

c



b



a



Fig. 23I

Fig. 24

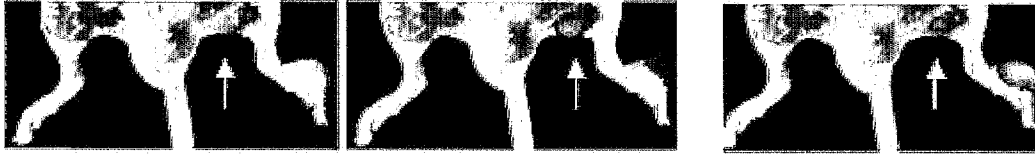


Fig. 25A

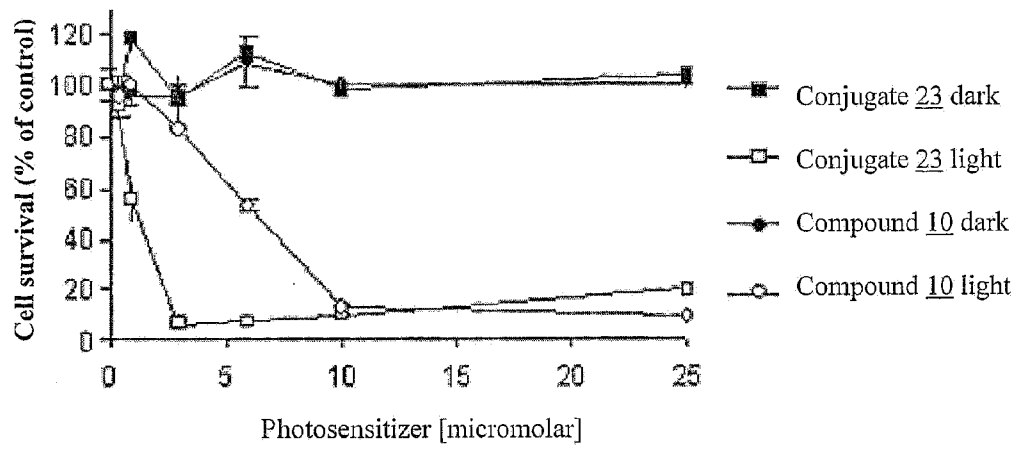


Fig. 25B

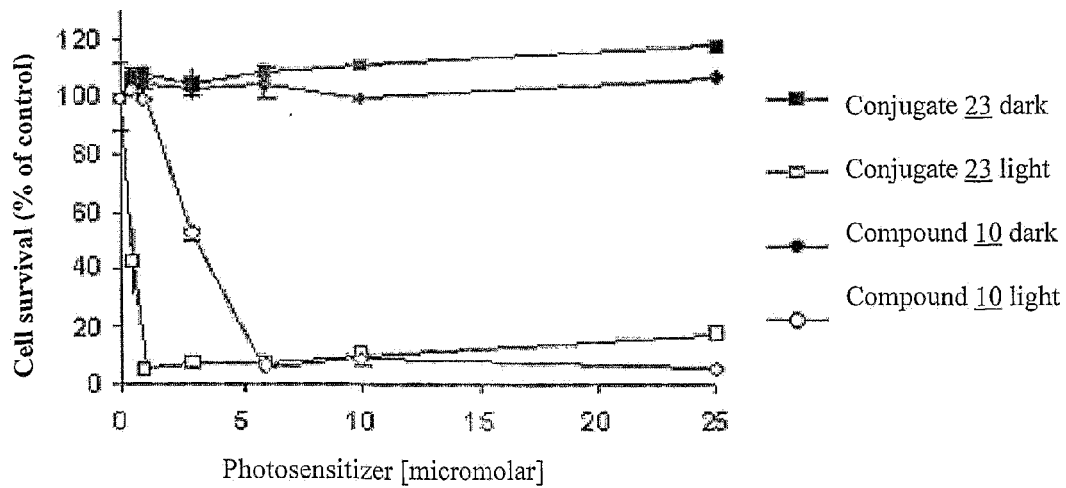


Fig. 25C

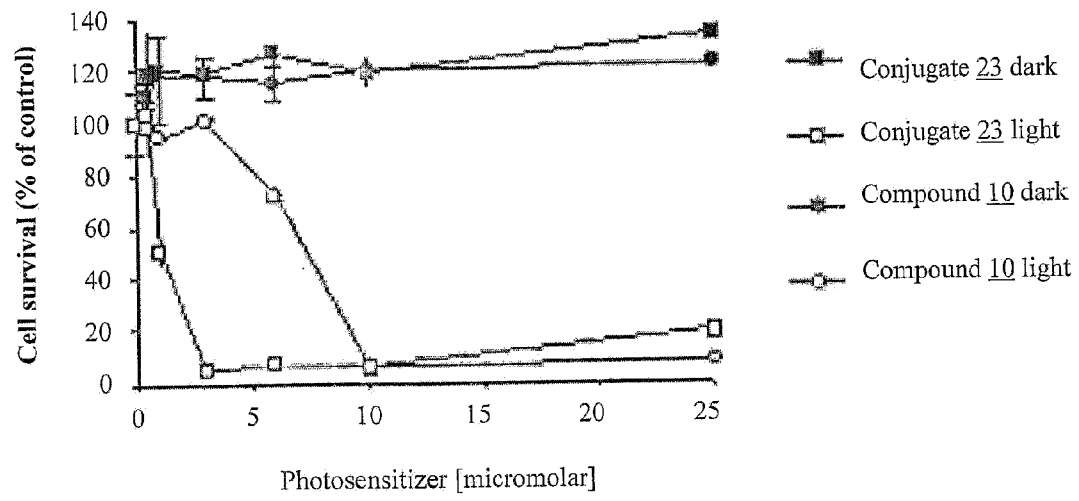


Fig. 26A

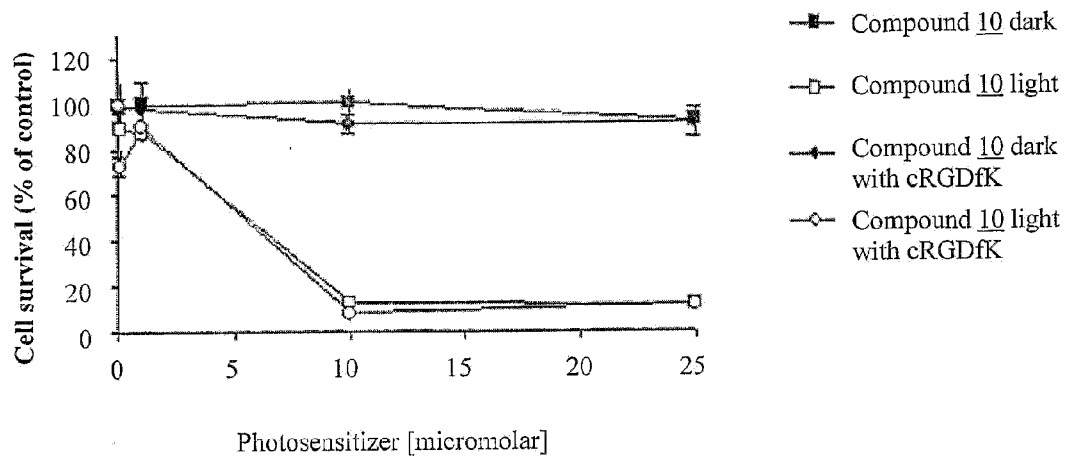


Fig. 26B

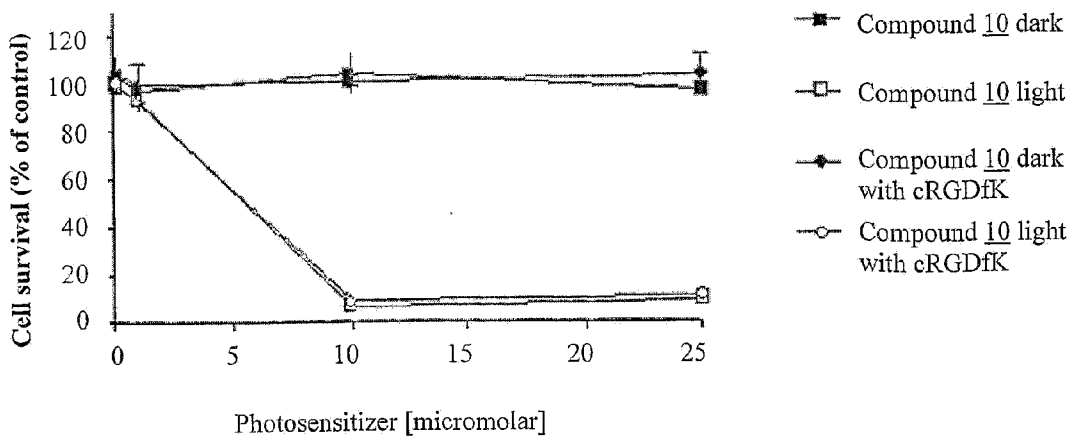


Fig. 26C

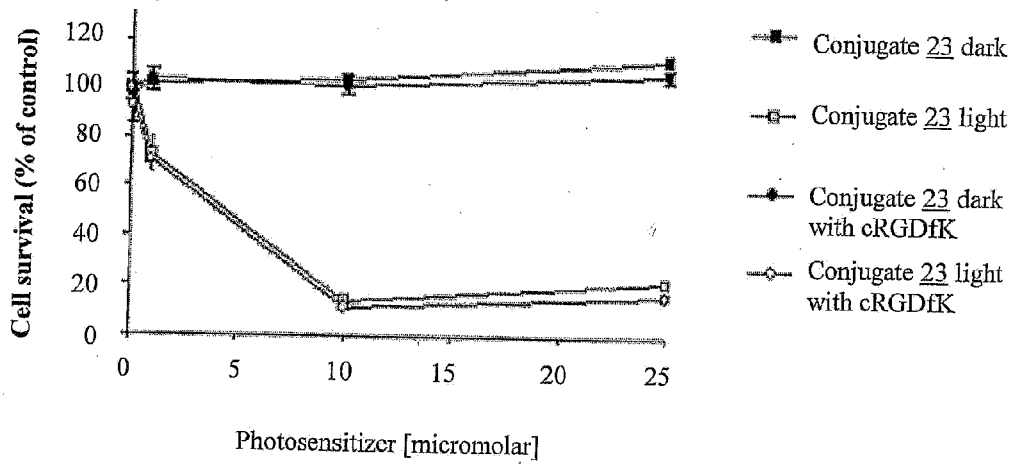


Fig. 26D

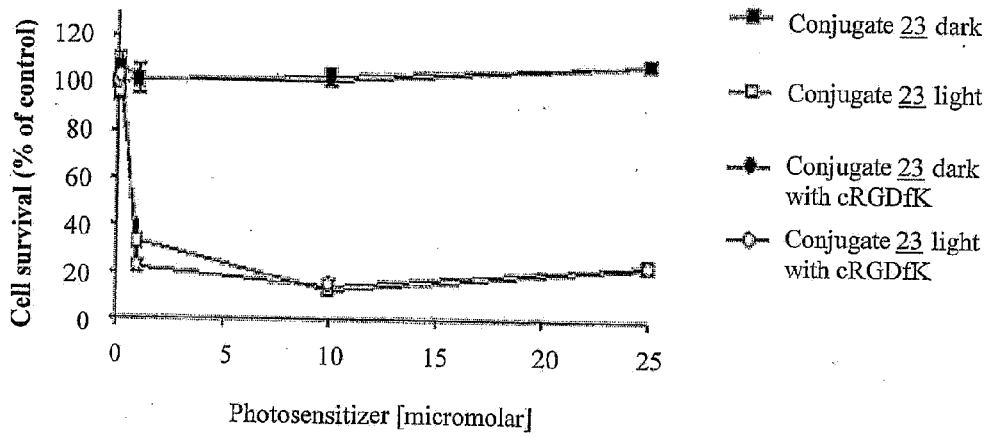


Fig. 27A

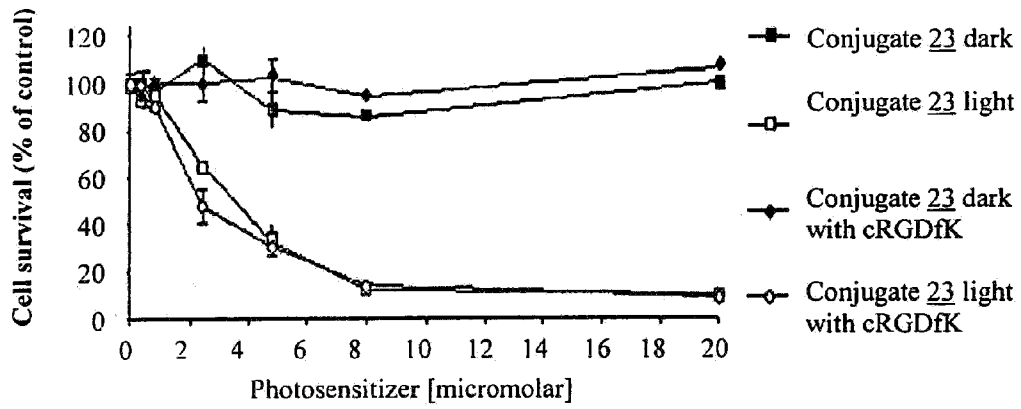


Fig. 27B

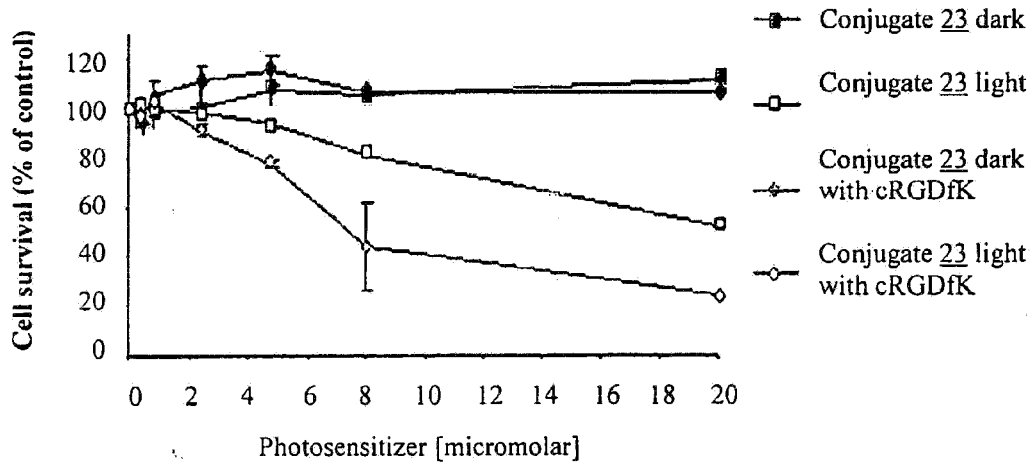


Fig. 28

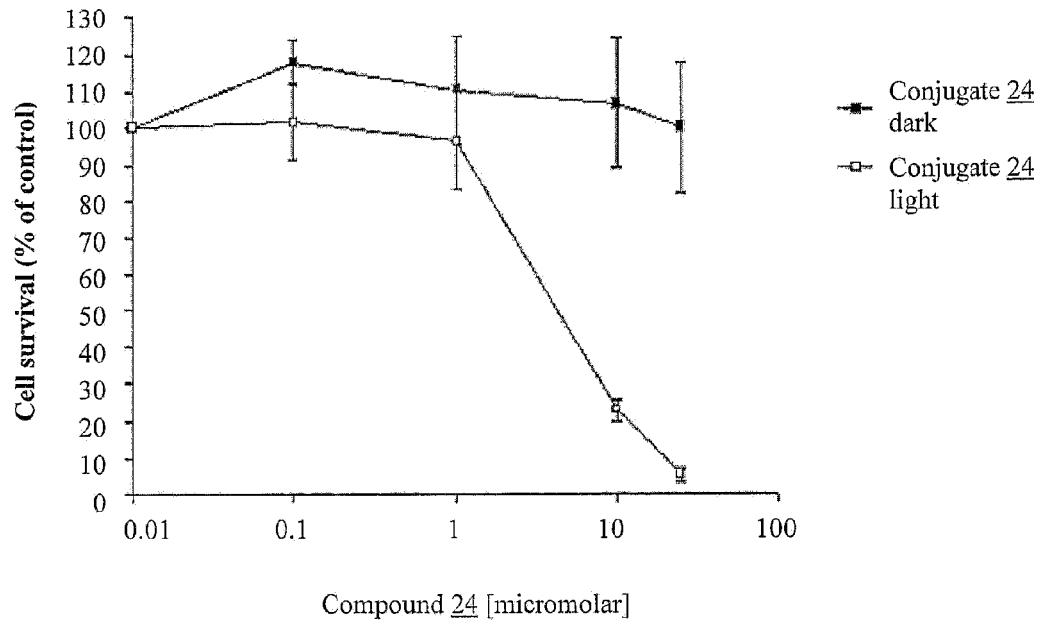


Fig. 29

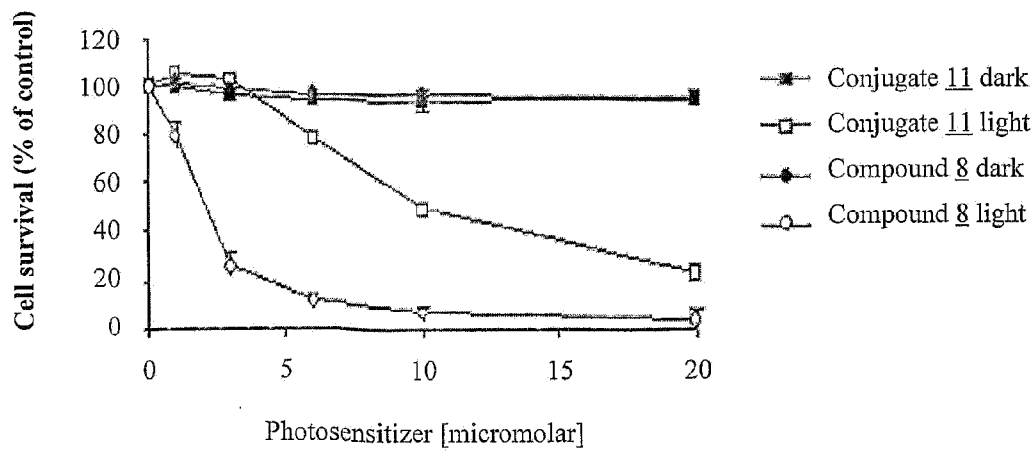


Fig. 30A

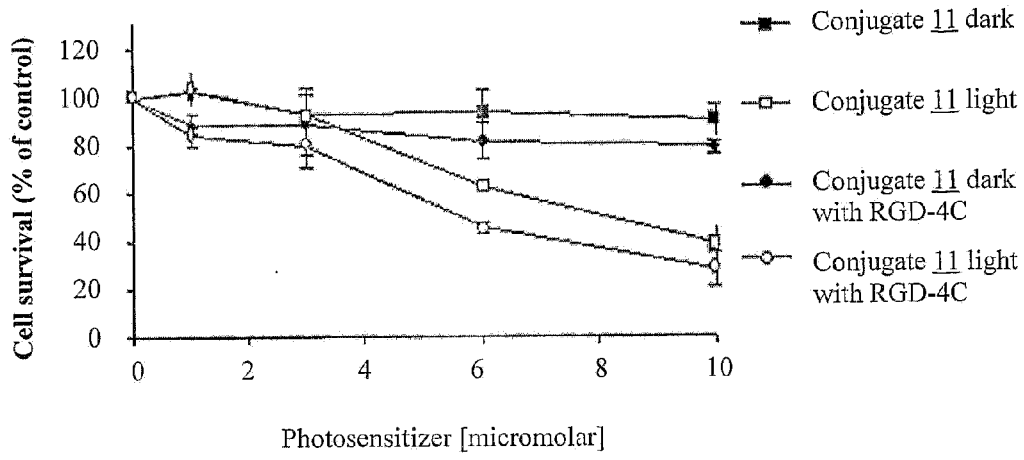
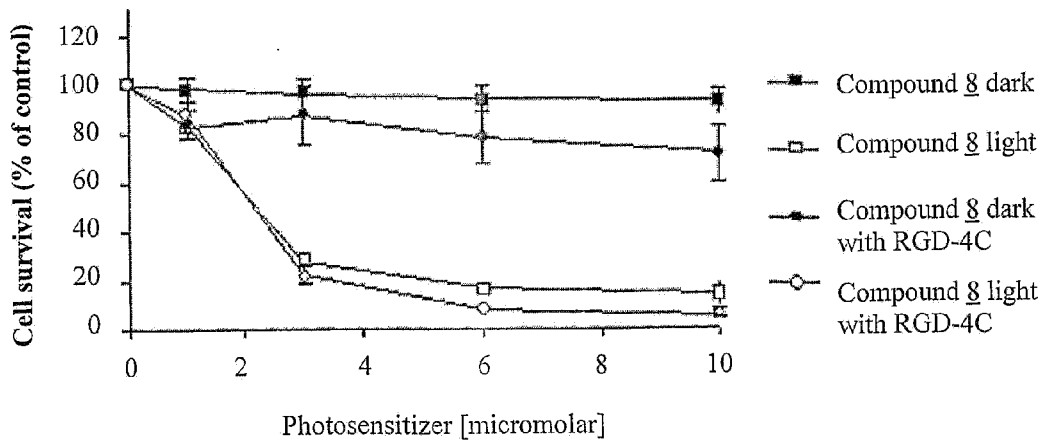


Fig. 30B



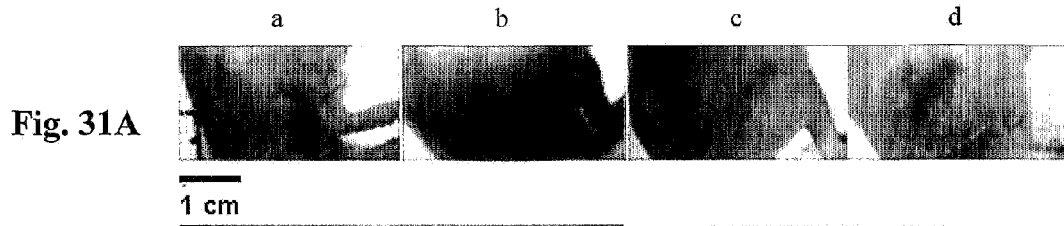


Fig. 31A



Fig. 31B

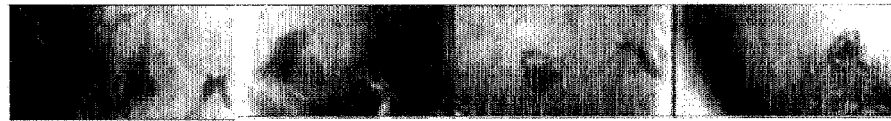


Fig. 31C



Fig. 31D

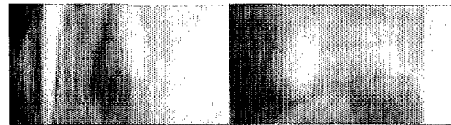


Fig. 31E

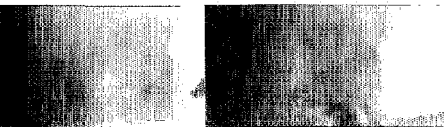


Fig. 32A

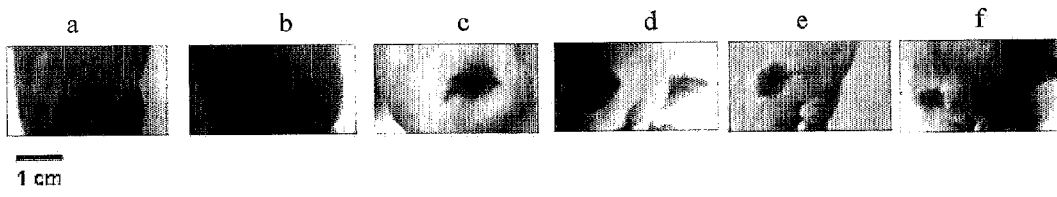


Fig. 32B

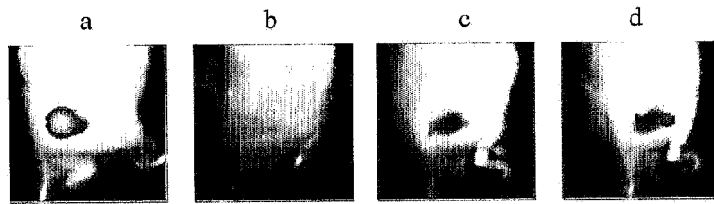


Fig. 32C

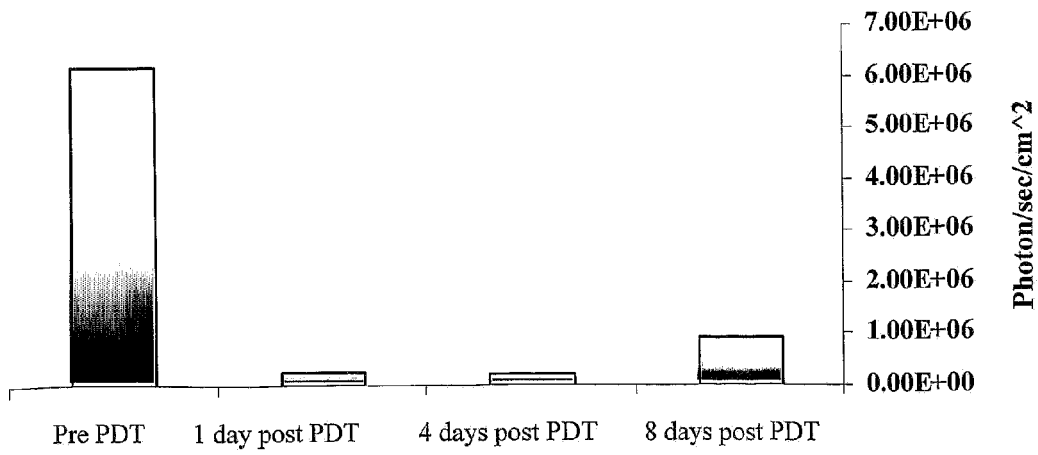


Fig. 32D

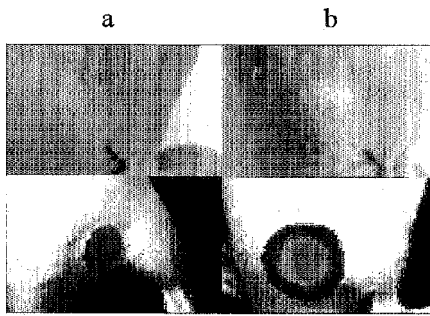


Fig. 32E

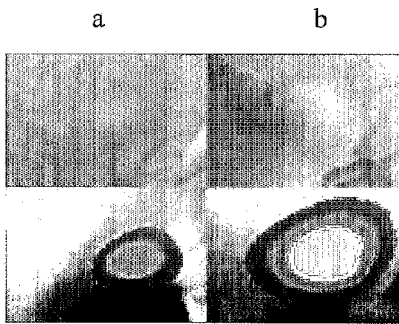


Fig. 32F

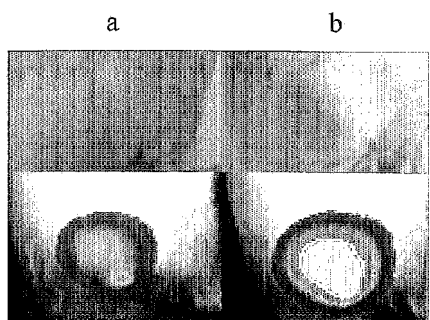


Fig. 33

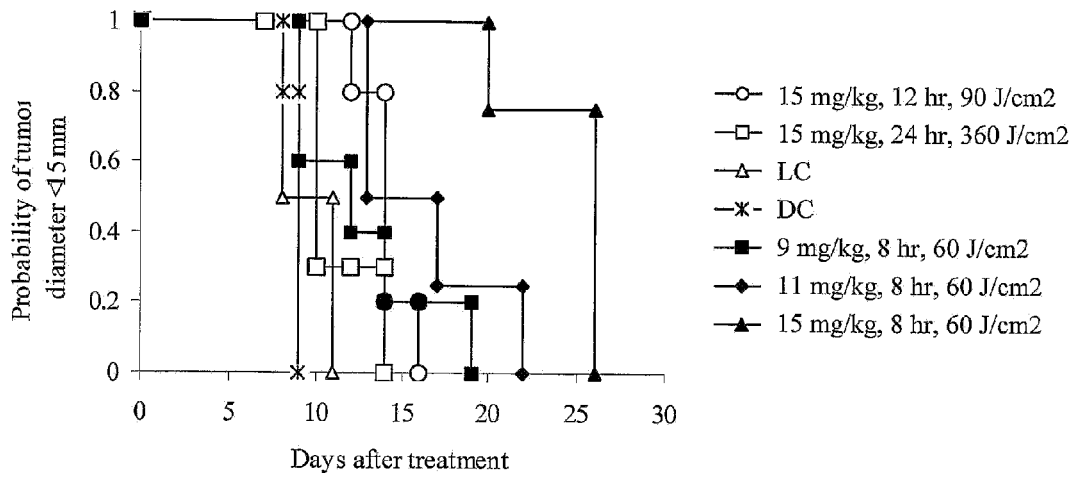


Fig. 34A

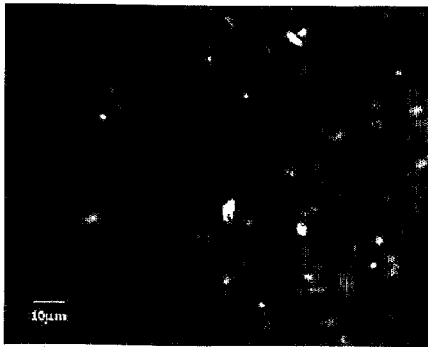


Fig. 34B

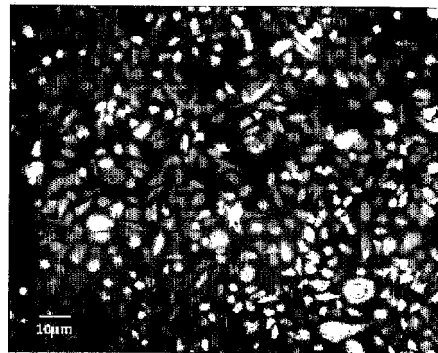


Fig. 35A

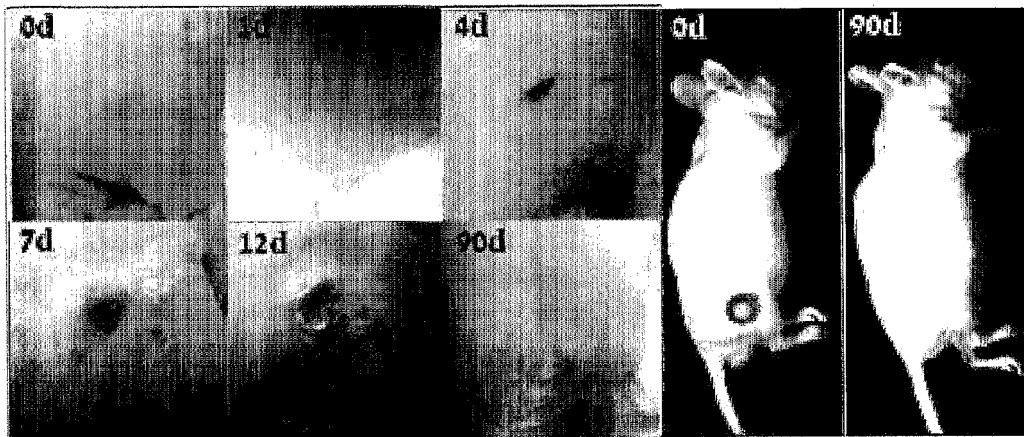


Fig. 35B

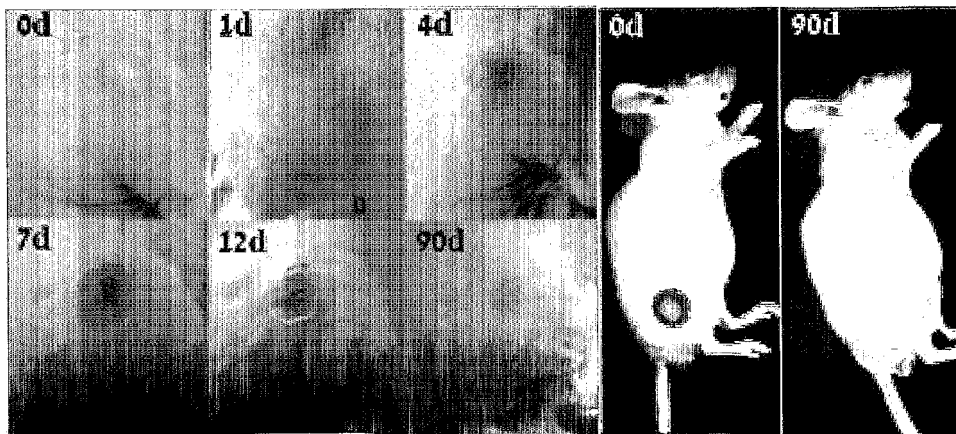


Fig. 36

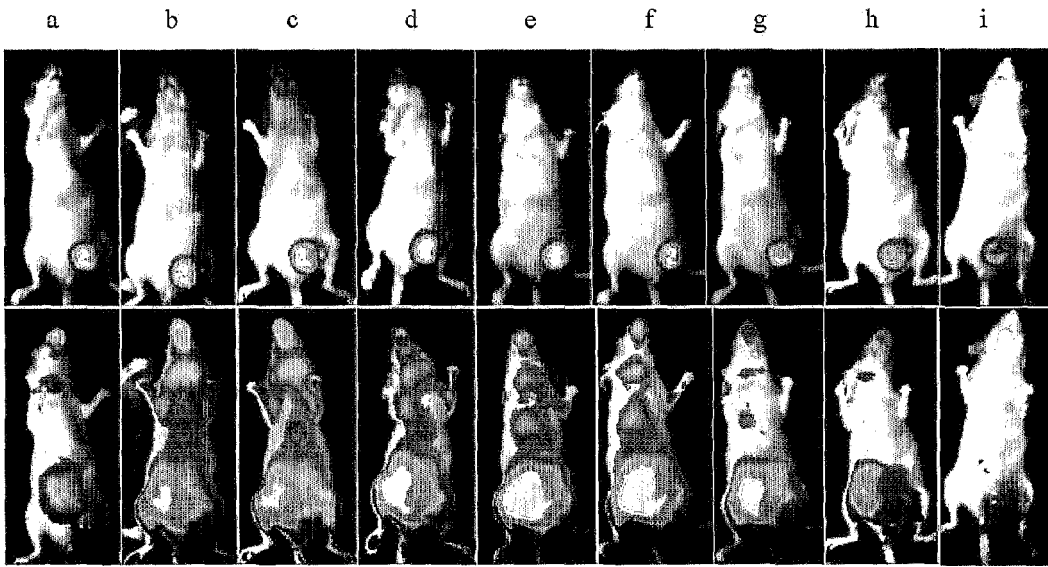


Fig. 37

